# ANALYTICAL APPLICATIONS OF ATOMIC SPECTROSCOPY,

# WITH PARTICULAR REFERENCE TO INDUCTIVELY COUPLED PLASMA

# EMISSION ANALYSIS OF COAL AND FLY ASH

A thesis submitted to the

UNIVERSITY OF CAPE TOWN

in fulfilment of the requirements for the degree of

MASTER OF SCIENCE

by

M A BRUNO POUGNET

---o0o---



Department of Analytical Science
University of Cape Town.

August 1983

## SUMMARY

This thesis outlines the analytical applications of atomic emission and absorption spectroscopy to a variety of materials. Special attention was directed to the analysis of coal and coal ashes.

A simple slurry sampling technique was developed and used to determine V, Ni, Co, Mo and Mn in the National Bureau of Standards Standard Reference Materials (NBS-SRM) coals 1632a and 1635 by furnace atomic absorption spectroscopy (FAAS). The percentage errors compared with certified values ranged from -1.6% to 16% for elemental concentrations from 19 to 44 ppm; however, as anticipated, the largest errors were obtained at lower levels. The relatively poor precisions obtained emphasize the importance of proper particle size characterization when using slurry injection of an inhomogeneous sample.

Coal and fly ash were analysed by inductively coupled plasma atomic emission spectroscopy (ICP-AES). Two dissolution methods were used. In one, coal and fly ash samples were dissolved in teflon-lined acid-digestion bombs. Fly ash samples were also dissolved by shaking with hydrofluoric acid at 70°C. Ca, Mg, Al, Si, Fe, Ti, Na, P, Mn and Ba were determined in the NBS-SRM coals 1632a and 1635, in fly ash 1633a and in coal and fly ash samples from different

locations and power stations in South Africa. Good agreement with reported values was obtained.

The determination of B, Be, Li, C, K and other trace elements by ICP-AES was investigated. Analytical methods were developed for the analysis of coal, fly ash and water samples. Boron was determined in the NBS standards and in 30 South African fly ash and coal samples. Results for B in the NBS standards compared well with published values while South African samples were found to contain 123 to 522 ppm B in fly ash, 95 - 118 ppm in boiler ash and 53 - 60 ppm in coal. The concentration of lithium measured in 32 fly ash samples from various locations in South Africa ranged from 65 to 402 ppm.

Fusion with sodium carbonate and a digestion bomb dissolution method were compared for the determination of boron in a South African boron-rich mineral (Kornerupine). Good agreement between the two techniques was obtained.

Eight elements were determined in 10 industrial water samples from a power plant. Ca, Mg, Si and B were determined by ICP-AES and V, Ni, Co and Mo by FAAS. The concentrations of some elements were found to vary with the pH of the sample. Boron was enriched in the samples presumably by leaching from coal ash within the plant since it was shown that up to 33% of the total B could be leached from fly ash samples by water.

006AAD

Boron and lithium were determined directly in sea water by ICP-AES and good agreement with published values was obtained.

ICP-AES was also shown to be useful for the analysis of metallurgical samples. Four brass samples and a special alloy were analysed.

Various problems encountered during the course of the work and interferences in ICP-AES analysis are discussed. Some recommendations concerning method development and routine analysis by this technique are suggested.

# A C K N O W L E D G M E N T S

I would like to express my gratitude to:

Associate Professor M J ORREN, for his support and assistance during the course of this work.

My parents and Elke for their constant support during the past years.

Professor H M N H IRVING for his help and all the staff members who have made the time spent in this Department a memorable one, especially Rob for his encouragement at official discussions (beer sampling) and Lana for preparing so many cups of coffee!

Colin Clarke for keeping the ICP spectrometer in "working order".

Janet Longman for typing the work.

The Council for Scientific and Industrial Research (CSIR) for financial support which made this work possible.

-----o0o-----

Science is a wonderful thing if one does not have to earn one's living at it. One should earn one's living by work of which one is capable. Only when we do not have to be accountable to anybody can we find joy in scientific endeavor.

Albert Einstein (1951)

# C O N T E N T S

---o0o---

# CHAPTER 1. INTRODUCTION

The main aim of this study was to investigate and develop methods for quantitative elemental analysis of coal, coal ash and fly ash samples using the techniques of furnace atomic absorption spectroscopy (FAAS) and inductively coupled plasma atomic emission spectroscopy (ICP-AES).

These energy-related samples provide interesting analytical problems due to their wide range of elemental concentrations. Interest in the elemental composition is broad and arises for several reasons. Huge tonnages of coal are used each year for electric power generation, in industry, and for producing liquid fuels, and a great deal of concern has been expressed about the presence of toxic elements released in the environment during these processes [1]. Some examples are Pb, Cd, Ni, Be, Bi, Hg, As and B. It has, therefore, become imperative to acquire more knowledge about the amounts of these elements present in coal, on their distribution, mode of occurrence and on their volatility during combustion and decomposition of coal. Much work has been done already in these fields and this is illustrated by the review edited by S Torrey [1].

Besides the obvious potential for environmental pollution, many metals function as poisons of costly catalysts used in certain coal liquefaction and gasification plants.

Another consideration is the use of ash from power plants for building materials or at least constitutents of these materials, for example, the use of fly ash additions to mortar and concrete and in brick making. Design of equipment

for coal burning plants is associated with the type of coal used and with the properties of the ash produced. Finally the possibilities of recovering certain elements from coal refuse materials such as fly ash and slag should not be neglected, an example being the extraction of aluminium from fly ash [11]. The properties of these materials are largely governed by the main constituents, viz oxides of aluminium and silicon.

The development of reliable, rapid analytical methods is becoming increasingly important and many different techniques have been applied [1]. Instrumental methods have included atomic absorption spectroscopy, optical emission spectrometry, neutron- and photon-activation analysis, mass spectroscopy, atomic- and x-ray-fluorescence spectroscopy, visible and ultraviolet absorption spectroscopy and other techniques such as voltammetry and potentiometry (ion-selective electrodes). ICP-AES is now a well-established technique and one of the most promising new analytical methods. Over the past few years, several methods for coal and ash analysis have been described in the literature. For example Mills and Belcher [2] have reviewed recent applications of atomic absorption, atomic fluorescence, atomic emission, optical emission and x-ray fluorescence spectrometry for the analysis of coal, coke, fly ash, coal ash and mineral matter. Emphasis was placed on the use of reference materials, calibration, sample preparation (grinding, ashing losses) and sample presentation.

In addition to investigating techniques for analyzing coal and related materials, method development and analysis of a wide range of other samples by ICP-AES was carried out,

including industrial water samples from a power plant, determination of Ca, Mg and P in minerals and in kidney stones and the analysis of brass and steel samples. The application of ICP-AES to a wide range of materials enabled development of the skills necessary to achieve accurate analytical results with this relatively new technique.

# CHAPTER 2. FURNACE ATOMIC ABSORPTION SPECTROSCOPY (FAAS)

## 2.1 Introduction

Atomic absorption spectroscopy (AAS) is currently one of the most widely used techniques for the analysis of coal, coal ash and fly ash for the reasons that AAS instrumentation is, perhaps, the most widely available and cheapest of atomic spectroscopic techniques and the sensitivity, especially by electrothermal or furnace atomization, is excellent for most of those elements which occur in coal and related materials at low levels.

Furnace atomization has three main advantages over flame AAS: increased sensitivity, the potential of **in situ** sample treatment in the furnace and the ability to accept small samples.

A major difference between flame and furnace AAS is that in the latter some matrix components are removed before atomization and the atomization takes place in an inert (usually argon) atmosphere. During atomization the gas stream through the atomiser (graphite tube) may be reduced or shut off so that the free atoms remain in the optical path for several tenths of a second. This is up to 1000 times longer than in the flame where, because of the gas flow rate, the atoms pass through the beam in a few milliseconds. Consequently, in the furnace a considerably larger number of atoms are stimulated to light absorption, thus allowing the use of very small sample volumes and high absolute sensitivity. The furnace atomizer offers sensitivites and

detection limits 100 to 1000 times better than the flame for most metals. Selective volatilization and so-called "matrix modification" within the furnace atomizer, together with the ability to analyse viscous or non-flammable liquids directly, are other important advantages.

Furnace atomic absorption atomization measurements have been widely used during the past decade for trace element analysis in the environmental, clinical and industrial fields. Much research and development has been directed towards overcoming the principal problems of background absorption and chemical interference effects [3]. The most important contributions include the improvement in the design of background correction systems, improved control of heating rate and the use of rapid heating systems, "matrix modification" and the introduction of pyrolytic or other tube coatings. Despite these developments, interference problems remain. Considerable attention is now being given to fundamental studies of electrothermal atomization, and other powerful techniques such as mass spectrometry are being coupled to furnace systems in order to study analyte vaporization characteristics [14]. The use of "platform" atomization [104] which ensures that atoms are released into a furnace environment at considerably increased temperatures, substantially or totally reduces interference effects. The potential for simultaneous multi-element analysis during electrothermal atomization could dramatically increase the analytical speed for trace element analysis. With the impressive recent advances in electronics and computer development, revolutionary change in terms of instrument design, performance and speed of analysis are expected to

occur.

FAAS methods involving indirect presentation of sample analytes, following dissolution (Chapter 5.1), conversion and preconcentration procedures, eg solvent extraction, constitute a large fraction of the published work. There has, however, been a considerable increase in the past few years in the utilization of electrothermal atomizers for the direct analysis of solid samples. The driving force is to eliminate the usually tedious steps necessary for complete dissolution of many complex matrices. Some examples are: determination of Cu, Ni and V in coal and petroleum coke [4]; determination of Cd, Pb, Ag, Th and Zn in silicate rocks [5]; determination of Ag, Bi and Cd in sulfide ores [6]; and other trace metals in polymers [7] and biological samples [8, 9, 10, 12]. The technique involves either dispensing the solid samples inside one end of the graphite tube by using a small spoon, or by using a tool similar to a syringe pipette which dispenses the sample through the graphite tube sample introduction hole [102].

## 2.2 INSTRUMENTATION AND OPTIMIZATION OF INSTRUMENTAL PARAMETERS

The atomic absorption measurements were made with a Perkin-Elmer Model HGA-500 furnace atomizer and the Perkin-Elmer model 5000 atomic absorption spectrometer, equipped with a background correction system designed to correct automatically for non-atomic absorption. The system is operated entirely automatically and the deuterium arc is used

over the ultraviolet range 190 to 350 nm while a tungsten halide lamp covers the remaining range of 350 - 900 nm.

The Perkin-Elmer model 56 chart recorder was used to study and record signal peaks.

Pyrolytically coated graphite tubes (Perkin-Elmer) were employed throughout the work. These exhibit longer useful lifetimes and, frequently, improved analytical performances. This arises because the diffusion of liquids and gases into the relatively porous graphite is greatly reduced, thus decreasing the possibility of samples soaking into the furnace, reducing the possibility of carbide formation, and minimising the loss by diffusion of atomic species through the walls of the tubes.

A feature of the HGA-500 furnace atomizer is temperature-controlled "maximum power" atomization. For atomization, a fast rate of heating is required to obtain the maximum ground state atom concentration as quickly as possible. To attain maximum sensitivity, it is essential that the atomization time is considerably shorter than the residence period of the atoms in the graphite tube. Maximum power heating permits the graphite tube to be heated with maximum available power (ie maximum speed) up to the preset atomization temperature. To prevent temperature overshoot, the temperature of the graphite tube is monitored by an optical sensor. Temperature-controlled maximum power atomization offers the following advantages:

a) lower effective atomization temperature, thus longer tube life;

b) higher sensitivity for refractory elements, eg vanadium;

c) the possibility of separating the specific signal for the element from that of the non-specific matrix signal, eg smoke from certain solid samples.

Maximum power mode was used for those elements showing increased sensitivites with this method.

Argon gas ("SpecArg", Air Products, South Africa (Pty) Ltd) was used for the internal and external sheating gas flow of the furnace.

Perkin-Elmer hollow cathode lamps were used unless otherwise indicated, and were run at the manufacturer's recommended operating currents.

**Optimization of HGA parameters:**

After setting up the spectrophotometer, involving alignment of the hollow cathode lamp, proper choice of the elements' spectral line, slit width (band-pass), lamp current and mode of analysis (eg "peak height" or "peak area") the HGA is aligned to obtain maximum light passage through the graphite tube.

With the HGA, individual parameters for different elements must be considered for each type of matrix. The most important parameters are the settings used during the "DRYING", "CHARRING (ashing)" and "ATOMIZATION" steps. The so-called standard conditions recommended by the manufacturer provide a guideline for initial set-up. Standard solutions, samples and blank solutions were used to determine the

following parameters:

a) Drying step

The purpose of the drying step is to evaporate low boiling liquids from the sample. The drying temperature is estimated on the basis of the boiling point of the solvent, or other liquid component present and a temperature slightly higher than this is normally used. The drying time is largely dependent upon sample volume and, for a typical aqueous solution, the drying time for a 20 µl sample is about 20 seconds. Proper drying of the samples was visually monitored to ensure that a steady expulsion of solvent occurs and no vigorous boiling or spattering, which leads to loss of the sample.

b) Charring step

Thermal pretreatment before atomization is usually necessary in order to remove any other absorbing components of the sample matrix. A sufficiently long charring time and a high enough temperature must be used to volatilize as completely as possible any interfering, eg "smoke"-producing sample matrix but the charring time must be short enough and the temperature low enough to ensure no loss of the analyte during that step. Selection of the maximum temperature is done by analysing the sample following charring at different temperatures to obtain a graph of absorbance values versus charring temperatures as in figure 2.1. For this sample it

is seen that a temperature of about 600°C is suitable for the determination of zinc.

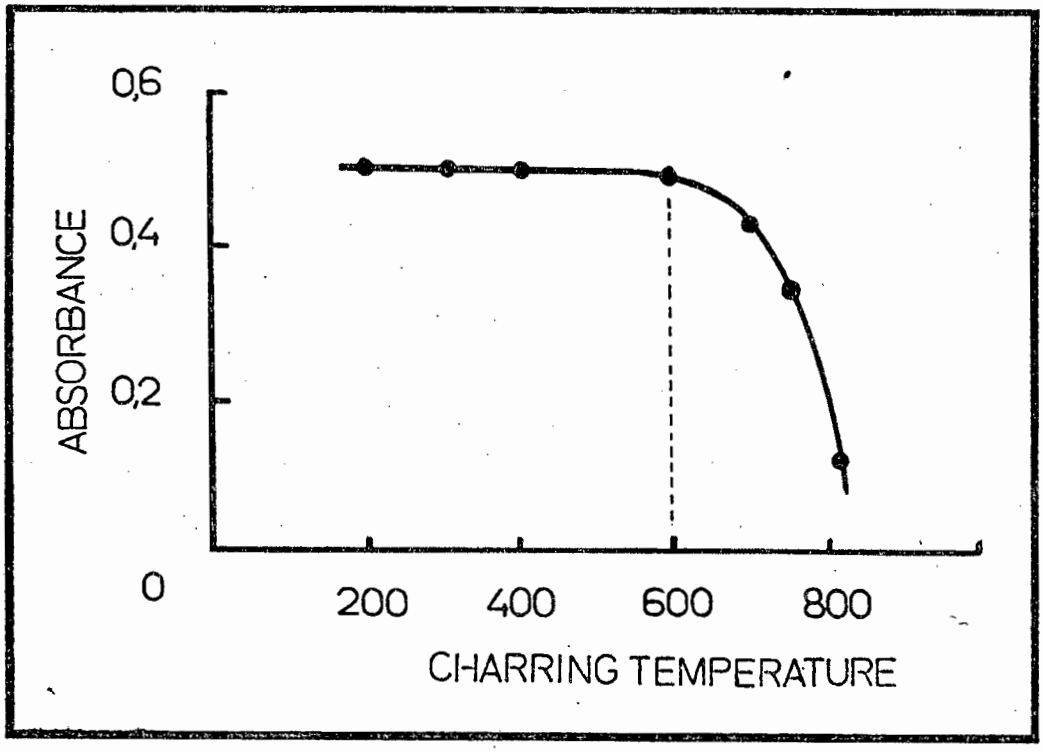


Figure 2.1 Optimum charring temperature for an aqueous solution of zinc.

In the case of complex samples both standard solutions and sample solutions are investigated and the best compromise temperature is selected.

c) Atomization step

To obtain high sensitivity and attain maximum graphite tube life, the atomization time is generally selected to be as short as possible whilst still providing complete atomization. Recorder tracings of the atomization peaks at optimum temperatures indicate the time required before the

atomization signal returns to the baseline. A plot of absorbance versus atomization temperature is then used to obtain the optimum temperature. As seen in figure 2.2, the optimum temperature will be the lowest temperature giving the maximum signal, in this case, about 1800 °C.

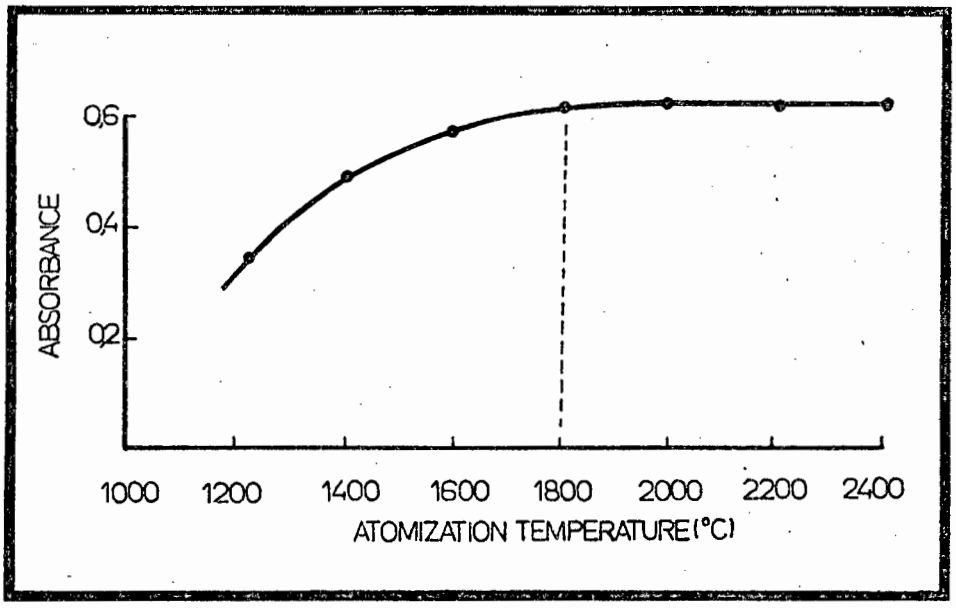


**Figure 2.2** Optimum atomization temperature for an aqueous solution of zinc.

Depending on the difference in volatility between the matrix and the analyte, "ramp" atomization, where the temperature is slowly increased over a few seconds to the final atomization temperature, can be used. This mode may permit volatilization of the analyte before the matrix, should the analyte be more volatile than the matrix. If the matrix is less volatile or has similar volatility to the analyte, then by using a stepped programme from charring to atomization, both the analyte and the matrix may be atomized simultaneously, making the use of the background corrector imperative.

Figure 2.3 shows chart recorder traces using three modes of operation for the analysis of powdered coal using ramp atomization. Figure 2.3(A) shows the smoke evolution at 1500°C (*) just at the beginning of the charring step and before atomization with evolution starting at about 2300°C. This was obtained with the background corrector off. Figure 2.3 (B) was obtained with the background corrector on. The use of the "BG" mode (ie looking at the correction applied by the corrector only) is illustrated in Figure 2.3 (c). (Note: the peaks are not "quantitative" since the weights of the three coal samples used were not identical but, nevertheless, as similar as possible).

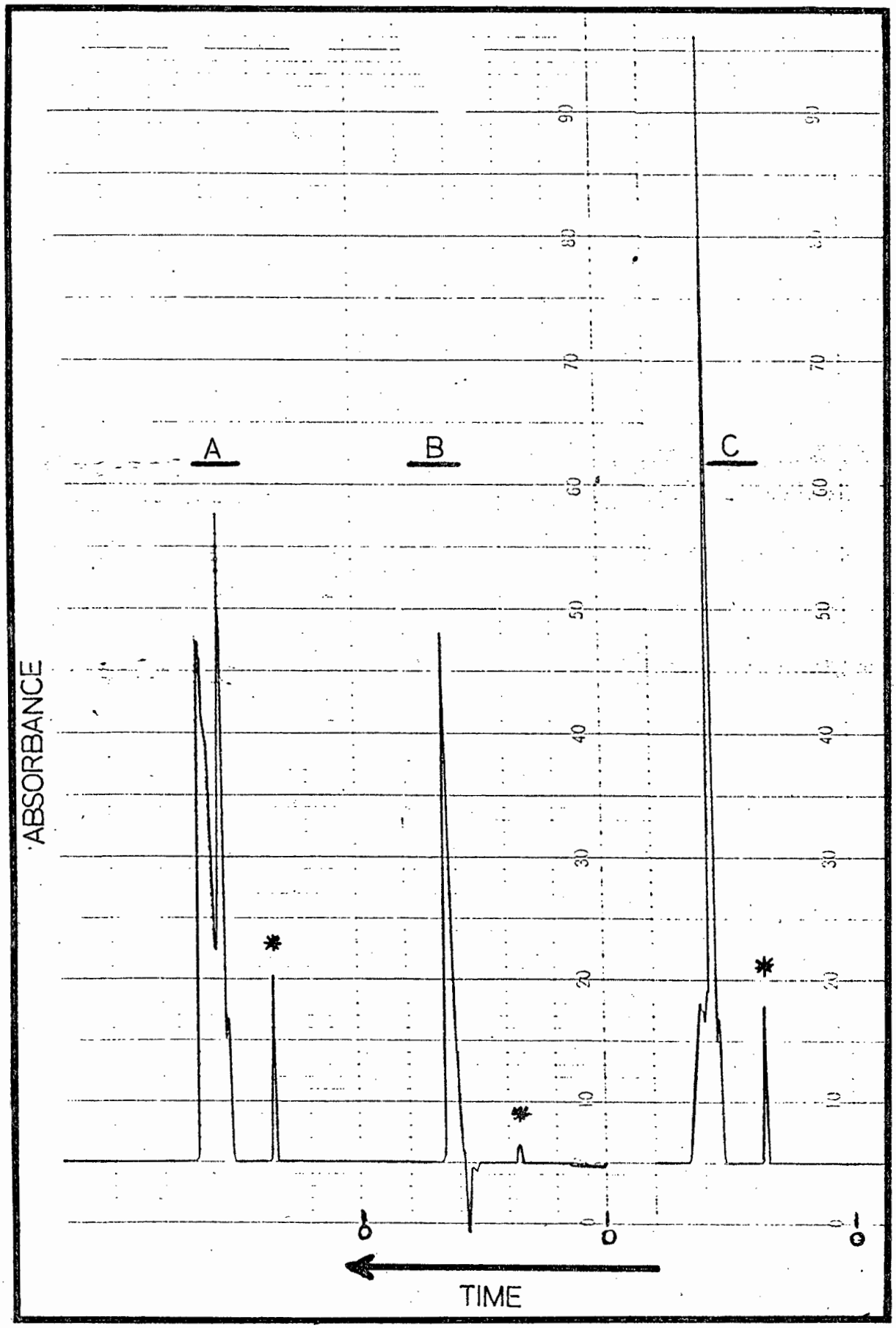


Figure 2.3 Chart recorder trace using (A) AA, (B) AABG, (C) BG modes.

# CHAPTER 3. TRACE METAL ANALYSIS OF COAL BY FAAS USING A SLURRY INJECTION TECHNIQUE.

## 3.1 INTRODUCTION

The stability of colloids in water can be increased if the particles are coated with a high molecular weight lyophilic species such as gelatin. While we are not concerned here with colloids but with larger particles, the possibility of suspension stabilization by organic substances has been reported. Different methods of preparing slurries for flame AAS analysis of solids have been described.

The first study on the direct flame spectroscopic analysis of solid samples appears to be that of Gilbert [15] who obtained flame emission spectra of a soil sample by aspirating a suspension of dried, sieved soil in 1:1 isopropanol-glycerol solvent directly into a burner.

Kashiki and Oshima [16] prepared slurries in methanol (0.01 - 0.05% m/m). The powders were kept in suspension by a "dispersion blade" using an electromagnetic vibrator. The powder dispersion unit was used to determine cobalt and molybdenum in alumina catalyst by flame AAS.

Willis [17] investigated the introduction of suspensions into the flame. Slurries of geological and mineral samples were prepared in water after grinding and sieving. Magnetic stirrers were used to keep the particles in suspension while aspirating. The use of an ultrasonic generator proved very efficient. However, with some materials it caused part of

the specimen to form colloidal solution. It was also found to heat the samples. A stream of air bubbles was also found to keep the particles in suspension. Addition of wetting agents such as sodium polyacrylate or "Calgon" for silicate materials and sodium sulfide for sulfide ores was found to slow the rate of settling of suspensions.

O'Reilly and Hicks [18] described a method for the determination of major, minor and trace level elements in powdered coal by aspiration of aqueous slurries into the flame for AAS analysis. It was found necessary to use 0.1 to 0.5% Triton X-100 (alkyl phenoxy polyethoxy ethanol) a surface active polymer to assist in wetting and dispersing the fine coal powder. Other organic liquids such as 1:1 isopropanol/water, methanol and methyl isobutyl ketone were found to "wet" and disperse the coal powders very quickly.

When this study began, no work was known to have been published on the analysis of coal using the slurry technique with furnace AAS. It was only after completion of the work presented here that a review (April 1982) on analytical methods [19] revealed the work of Fuller, Hutton and Preston, 1981 [20] who compared flame, electrothermal and ICP atomic techniques for the direct analysis of slurries. In their work, ores and rocks were ground to obtain very fine powders and slurries were prepared by suspending 1 g of sample in 100 to 1000 ml of a solution containing sodium hexametaphosphate, "Viscalex HV30" (Allied Colloid Ltd, Bradford), "NOPCO NPZ" (Diamond Shamrock Process Chemicals Ltd, Leeds) with ammonia to adjust the pH to between 6 and 7. The effect of particle size on atomization efficiency was investigated. Cr and V were determined by flame and flameless AAS and V and Zr by

ICP-AES. Two older papers published by Fuller [21, 22] made use of a similar suspension technique for the analysis of trace elements in titanium (IV) oxide pigments and rock samples by AAS.

Mills and Belcher, 1981 [2], quoted O'Reilly and Hicks [23] who determined Be in coal: "slurrying of gram quantities was used to reduce sampling error for Be determination". This work was apparently presented at a conference in Honolulu (1979), but not subsequently published.

Ebdon and Pearce [24] published in August 1982 their work on the direct determination of arsenic in coal by FAAS using a slurry technique. Coal (0.5 - 1 g) ground to less than 45 um was dispersed in 10 ml of a solution containing 10 g $l^{-1}$ of concentrated nitric acid and 100 ml $l^{-1}$ of ethanol using a magnetic stirrer in a sealed polypropylene bottle. After 5 minutes stirring aliquots of the suspension (5 - 20 µl) using a micro-pipette were dispensed in the furnace while continuously stirring.

## 3.2 Method development and procedure

Note: All reagents and standard solutions used in this work are listed in Appendix 1.

Standard solutions and coal slurries were dispensed into the graphite tube through the sampling port, using a 20 µl plastic tipped micro-pipette (Gilson Pipetman, France). Teflon coated magnetic stirrer bars were used.

The National Bureau of Standards Standard Reference Material (NBS-SRM) coals 1632a and 1635 were used for this investigation. Standards were dried and kept under vacuum as recommended by NBS. No further treatments were applied before weighing and preparation of the slurries.

When this investigation was made, no facilities for grinding and sieving small amounts of sample were available. The authors quoted above have stressed that it is necessary to use well ground powders (-325 mesh) for flame AAS analysis. It was decided to investigate slurry preparations using the NBS-SRM materials. The NBS-SRM 1632a and 1635 were ground to pass through 250 μm (No 60) and 230 μm (No 65) sieves respectively [25].

Work began by checking the sensitivites and instrumental parameters for the elements of interest (V, Mo, Co, Ni and Mu) using a range of aqueous standard solutions of the analytes. From the certified elemental concentrations [25] of the NBS-SRM samples, concentrations of the slurries were calculated to give reasonable absorbance values within the linear portions of calibration curves so that a standard addition method could be used.

Several substances were used in an effort to prepare stable slurries by weighing 10 to 20 mg aliquots of dried coal samples in glass boiling tubes and then adding 10 ml of the various substances below. A vortex mixer was initially used to suspend the particles but since the tube had to be held by hand while pipetting, it was later found more convenient to use a magnetic stirrer. All the substances investigated viz, 1:1 v/v isopropanol-water, methanol, glycerol-methanol, 2%

(w/v) gelatin solution and various concentrations of Triton X-100 (TX-100) were found to wet and disperse the coal particles efficiently. This is probably a result of the hydrophobic organic nature of coal. It was found very difficult to disperse coal powders in pure water since the power would float and tend to clump and even vigorous stirring did not produce satisfactory slurries. Use of an ultrasonic bath to keep the particles in suspension was also tried. However, it was again found inconvenient to hold the small tubes in the bath while pipetting. The 2% gelatin solution, prepared by dissolving gelatin powder in warm water and cooling, was found to be the best suspension stabilizer. A problem encountered with slurries containing high concentrations of TX-100 was that the drop spread laterally within the graphite tube immediately after it was introduced and, when heated, loss of sample occurred through the sample introduction hole. Sample deposited at the ends of the tube leads to inaccurate readings since atomization is not efficient at the cooler ends of the tube. Pyrolytically coated graphite tubes were used and it seems that the coating encourages wetting at the surface of the graphite. A compromise was reached between obtaining more stable slurries containing high concentrations of TX-100 and those using lower concentrations where spreading was minimized or avoided. The 2% gelatin solution did not cause spreading but the solution has to be prepared daily since aqueous gelatin solutions decompose within a few days. A 1% w/v TX-100 stock solution was prepared. This solution, stable for weeks, was also used as a wetting agent for samples, and standards in routine ICP-AES analysis (Chapter 5).

The procedure used for analysis of trace elements in coal was as follows:

10 and 20 mg of dried coal samples were weighed in small glass flat bottom tubes (24 mm diameter and 75 mm high). 1 drop of 1% w/v TX-100 solution was added to wet the coal followed by 10 ml of 0.005% TX-100 solution using a 5 ml pipette (Gilson, Pipetman, P5000).

The above procedure was found to be critical and must be followed exactly for proper wetting of the coal particles.

Samples of finely ground fly ash (NBS-SRM 1633a) and river sediment (NBS-SRM 1645) were also successfully suspended by this method.

It was observed that particles tended to adhere to the Teflon-coated magnetic stirrer bars when stirred for long periods of time. This may be due to magnetic material being attracted to the bar and/or due to the grinding effect between the stirring bar and the bottom of the glass tube since particles adhere to the teflon coating. The magnetic stirrer bars were soaked in 5% v/v $HNO_3$ or in 3% w/v EDTA solution to remove any adsorbed trace elements. Cleaning of teflon material was also achieved in an ultrasonic bath containing 5% v/v Contrad solution (a powerful detergent, Hickman and Kleber (Pty) Ltd, South Africa).

Another problem was encountered with the plastic tips of the micropipette. Small amounts of liquid (slurry) were found to be retained by these : washing with water between injections was found to be effective.

Standard solutions were prepared and the method of standard additions was used to calculate the analyte concentration in the slurries. 20 µl of slurry was dried in the furnace, the drying programme then interrupted and, after cooling, 20 µl of standard solution containing various known amounts of analyte was added. A programmable calculator was used to fit the peak height values, using regression analysis, following correction for the blank values (20 µl water containing the same amount of TX-100 as the slurries).

Recorder tracings of the standard addition peaks are illustrated in figures 3.1 and 3.2. The standard addition technique is illustrated in figure 3.3.

Figure 3.1 shows two additions of nickel standard (0.02 and 0.04 ppm) to a coal slurry containing 0.01 g NBS-SRM 1632a per 10 ml. Two separate standard additions of vanadium to two slurries are shown in figure 3.2, both contained 0.01 g NBS-SRM 1632a per 10 ml.

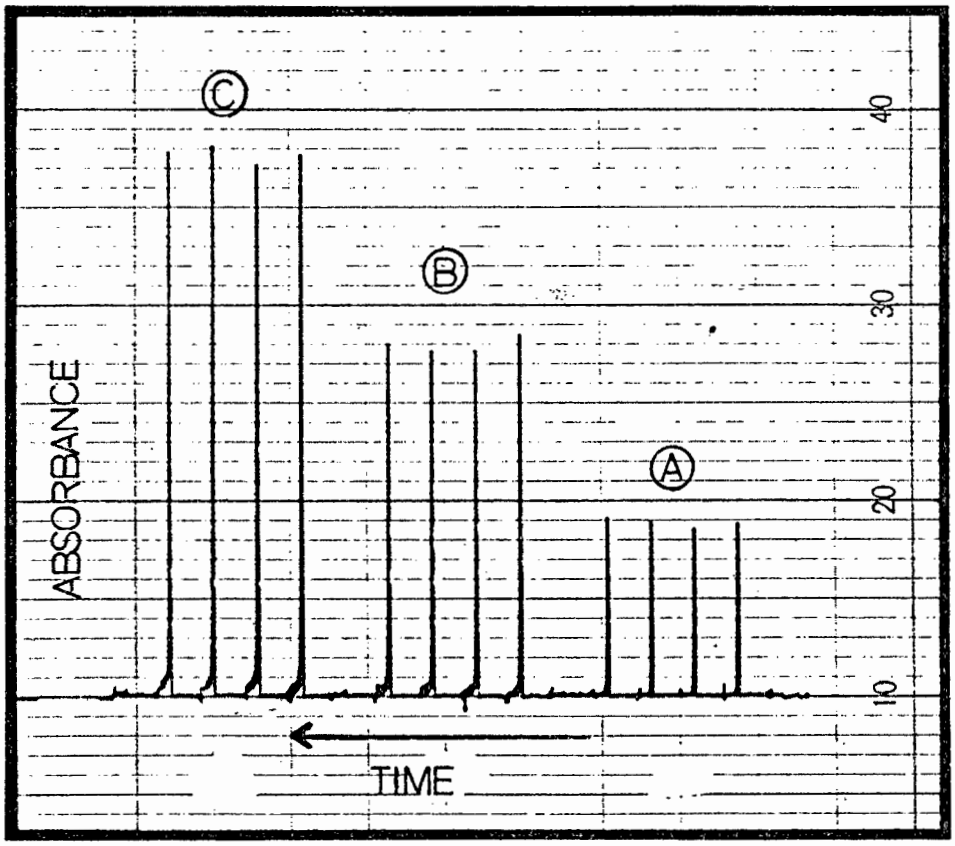


Figure 3.1 Determination of Nickel
A Sample
B Sample + 0.02 ppm Ni
C Sample + 0.04 ppm Ni

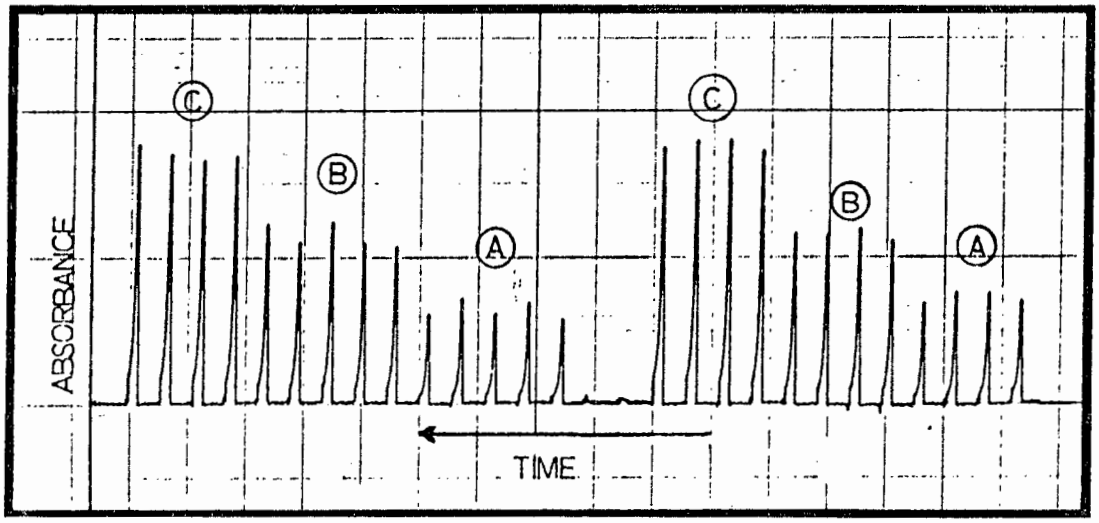


Figure 3.2 Determination of vanadium
A Sample
B Sample + 0.04 ppm V
C Sample + 0.08 ppm V

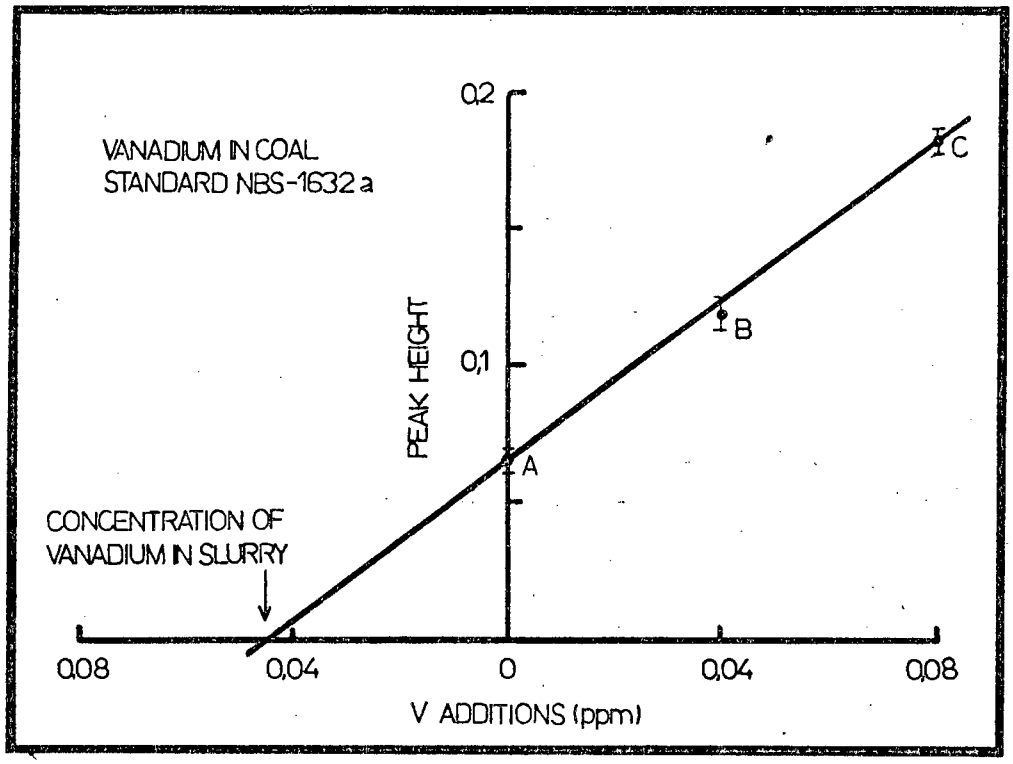


**Figure 3.3** Standard addition method; determination of vanadium.
A 20 µl slurry - blank
B 20 µl slurry + 20 µl 0.04 ppm V - blank
C 20 µl slurry + 20 µl 0.08 ppm V - blank
(Each point is the mean of four readings).

The instrumental parameters are listed in table 3.1. The background corrector system was used throughout the work and peak height readings were measured. The hollow cathode lamps and background corrector lamp were warmed up for at least 20 mins before measurements started.

Table 3.1 Instrumental parameters.

| Spectrophotometer | | | | | |
|---|---|---|---|---|---|
| Mode of operation: | AABG, PEAK HT, ABS, (1) REC ABS | | | | |
| Element | V | Ni | Co | Mo | Mn |
| Wavelength (nm) | 318.4 | 232.0 | 240.7 | 313.3 | 279.5 |
| Slit width (nm) | 0.7 | 0.2 | 0.2 | 0.2 | 0.7 |
| Lamp current (mA)* | 19 | 22 | 29 | 27 | 11 |
| **HGA** | | | | | |
| | V | Ni | Co | Mo | Mn |
| **Drying** | | | | | |
| Temp (°C) | 110 | 110 | 110 | 110 | 110 |
| Ramping time (sec) | 16 | 16 | 16 | 16 | 16 |
| Hold time (sec) | 30 | 30 | 30 | 30 | 30 |
| **Charring** | | | | | |
| Temp | 1000 | 800 | 1000 | 1600 | 1000 |
| Ramping time | 5 | 5 | 5 | 5 | 5 |
| Hold time | 15 | 15 | 15 | 15 | 20 |
| **Atomizing** | | | | | |
| Temp | 2700 | 2400 | 2400 | 2700 | 2700 |
| Ramping time | 0 | 0 | 1 | 0 | 1 |
| Hold time | 5 | 6 | 6 | 5 | 6 |
| **Internal Argon flow rate during atomization (ml $min^{-1}$)** | 10 | 10 | 10 | 10 | 200 |

* These were adjusted to meet the power balance requirements of the background correction system.

The Internal Argon flow rates during drying and charring were kept at 300 ml $min^{-1}$.

A cleaning step of 3 sec at atomization temperature was added.

Background correction is critical for direct solid analysis especially for complex samples like coal which tend to produce "smoke" during atomization. This is illustrated in figure 2.3 and if not properly corrected for yields a positive systematic error. Reducing the sample size of coal inside the furnace tends to reduce background absorption to a greater degree than the analyte signal. With the slurry technique, very small amounts of solid are present and with proper ashing parameters (high enough temperature and sufficient time to get rid of most of the volatiles) no problems were encountered, except with manganese where higher background absorptions were obtained. The internal gas flow was increased (compared with other elements) to try and decreased the residence time of the background-producing "smoke".

The "maximum power" mode of atomization (Chapter 2.2) was used for vanadium, nickel and molybdenum. With these elements, the sensitivities were found to be greatly enhanced, for example figure 3.4 shows the calibration curves (Peak height, absorbance versus vanadium concentration) obtained with both modes of atomization for the determination of vanadium. A one second ramp time before atomization was used for the normal mode. The sensitivity is doubled in the case of vanadium. This is because vigorous atomization conditions minimize interferences which otherwise reduce the signal.

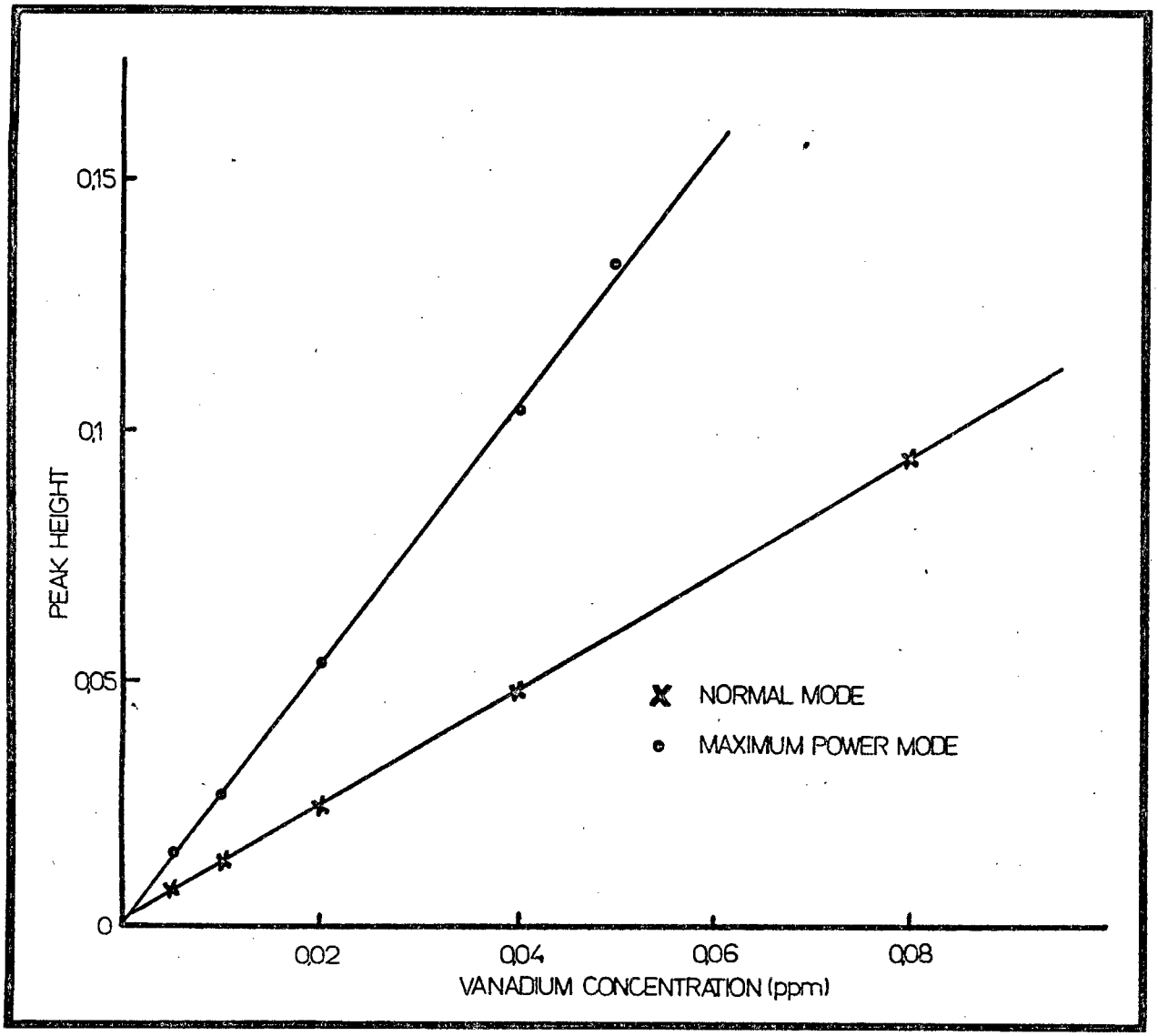


Figure 3.4 Calibration curves for vanadium determination.

## 3.3 RESULTS AND DISCUSSION

The analytical data are listed in table 3.2. Each element in the coal samples was determined by two separate standard addition methods (preparation of slurry and standard

solutions). A minimum of two additions and a maximum of 15 total readings of peak heights were used for each determination. Vanadium was also measured in NBS-SRM 1632a, 1635, 1645 (river sediment) and a fly ash sample, PFA 4, from a power station (Taaibos Power Station, South Africa) using a calibration curve constructed from standard solutions containing the same amounts of TX-100 as the slurries. The results are shown in table 3.3. Concentration values available for the samples analysed are listed in table 3.4 for comparison.

TABLE 3.2. Analytical data; standard addition method.

| | m | n | N | C | Conc (ppm) | Mean | SD | % RSD |
|---|---|---|---|---|---|---|---|---|
| NBS-SRM 1632a | | | | | | | | |
| V | 0.01 | 2 | 12 | 0.9913 | 47.25 | | | |
| | 0.01 | 2 | 13 | 0.9884 | 44.71 | 44.88 | 2.28 | 5.08 |
| | 0.01 | 2 | 13 | 0.9932 | 42.69 | | | |
| Ni | 0.01 | 2 | 12 | 0.9968 | 19.64 | 19.11 | 0.76 | 3.98 |
| | 0.01 | 2 | 12 | 0.9969 | 18.57 | | | |
| Mo | 0.02 | 2 | 15 | 0.9958 | 2.02 | 2.13 | 0.16 | 7.51 |
| | 0.02 | 3 | 9 | 0.9966 | 2.24 | | | |
| Mn | 0.01 | 2 | 11 | 0.9985 | 27.11 | 30.55 | 4.86 | 15.91 |
| | 0.01 | 2 | 10 | 0.9926 | 33.98 | | | |
| NBS-SRM 1635 | | | | | | | | |
| Ni | 0.02 | 2 | 9 | 0.9958 | 2.57 | 2.18 | 0.55 | 25.23 |
| | 0.02 | 2 | 9 | 0.9814 | 1.79 | | | |
| Co | 0.02 | 3 | 12 | 0.9915 | 0.90 | 1.02 | 0.16 | 15.69 |
| | 0.02 | 3 | 11 | 0.9927 | 1.13 | | | |
| Mn | 0.01 | 2 | 12 | 0.9939 | 24.97 | 24.76 | 0.30 | 1.21 |
| | 0.01 | 2 | 10 | 0.9915 | 24.55 | | | |

M : Mass of sample per 10 ml slurry (g)
n : Number of standard additions
N : Total number of readings
C : Coefficient of determination for curve fitting

Table 3.3 Determination of vanadium by calibration curve

| Sample | M | N | Conc. (ppm) | Mean (ppm) |
|---|---|---|---|---|
| NBS-SRM 1632a | 0.01 | 6 | 44.47 ± 2.6 | 43.01 |
| | 0.01 | 3 | 42.22 ± 3.9 | |
| | 0.01 | 3 | 42.34 ± 3.9 | |
| NBS-SRM 1635 | 0.03 | 6 | 4.06 ± 0.5 | 3.84 |
| | 0.03 | 5 | 3.62 ± 0.7 | |
| NBS-SRM 1645 | 0.01 | 3 | 28.00 ± 4.0 | 26.50 |
| | 0.02 | 3 | 25.00 ± 2.0 | |
| PFA 4 | 0.01 | 7 | 117.9 ± 5.5 | 119.70 |
| | 0.01 | 5 | 121.5 ± 4.3 | |

M : as above
N : number of readings

The same calibration curve was used for all the samples (c = 0.9932).

Table 3.4 Trace elements in NBS standards

| Sample | Reported Values *(ppm) 1. | 2. | 3. |
|---|---|---|---|
| **NBS-SRM 1632a** | | | |
| V | 44.0 ± 3.0 | 43.0 | 44 |
| Ni | 19.4 ± 1.0 | 19.0 | 23 |
| Mo | - | 2.0 | <4 |
| Mn | 28.0 ± 2.0 | - | 31 ± 2 |
| **NBS-SRM 1635** | | | |
| V | 5.20 ± 0.50 | 4.9 ± 0.2 | 4.5 |
| Ni | 1.74 ± 0.10 | 1.5 | 1.4 |
| Co | (0.65) | 1.1 ± 0.1 | 0.67 |
| Mn | 21.40 ± 1.50 | - | 23 ± 1 |
| **NBS-SRM 1645** | | | |
| V | 23.50 ± 6.90 | - | - |
| **PFA 4** | | | |
| V | - | 140 | - |

* 1. NBS certificate, "informational" value in parentheses [25].

2. XRF spectrometry, Department of Geochemistry, University of Cape Town.

3. Gladney [54].

In general, values obtained by the slurry technique show reasonable agreement with other data available. However, the reproducibility is poor, especially at low elemental concentrations, for example Ni and Co in NBS-SRM 1635. This is associated with the inhomogeneous nature of the samples and large particle size distribution. The results obtained by using an aqueous calibration curve are comparable to those obtained by the standard addition method. The reprodu-

cibility is also similar, showing that the errors arise from preparation of an inhomogeneous sample.

The calibration curve method has the advantage of being faster. However, since it is subject to errors arising from matrix interferences, these must be checked for each element and especially for those samples containing high concentrations of other elements, eg fly ash samples. Once a calibration curve is prepared, several samples (typically 3) can be analysed before recalibration is necessary. With solid sampling techniques, residues tend to accumulate in the graphite tube, causing changes in the surface of the tube, ie the contact between the sample to the tube surface, and decreases sensitivity for the next determination. Proper ashing and cleaning steps are important to minimize this effect, for example, oxygen ashing can be used to burn off carbon residues [102]. In this work, the small amounts of samples used did not cause any serious problems.

This method of analysis of coal is rapid and simple but at present it is not as accurate and precise as conventional methods.

Refinement of the method for trace element analysis in coal and related samples is possible by proper sampling and control of the particle size distribution.

# CHAPTER 4. INDUCTIVELY COUPLED PLASMA ATOMIC EMISSION SPECTROSCOPY (ICP-AES)

## 4.1 Introduction

A plasma is usually defined as a gaseous mixture in which a significant fraction of the atomic or molecular species present are in the form of ions. The plasma employed for emission analysis is usually generated in argon and/or nitrogen. When a sample is injected into this medium thermally induced atomization occurs since plasma temperatures may be as high as 10000 K. A typical plasma source is illustrated in figure 4.1.

Until recently, only the electric arc and the electric spark were employed in emission spectroscopy. During the last decade, however, argon or nitrogen plasma sources have been developed that combine many of the best features of flame sources with the attributes of the classical arc and spark.

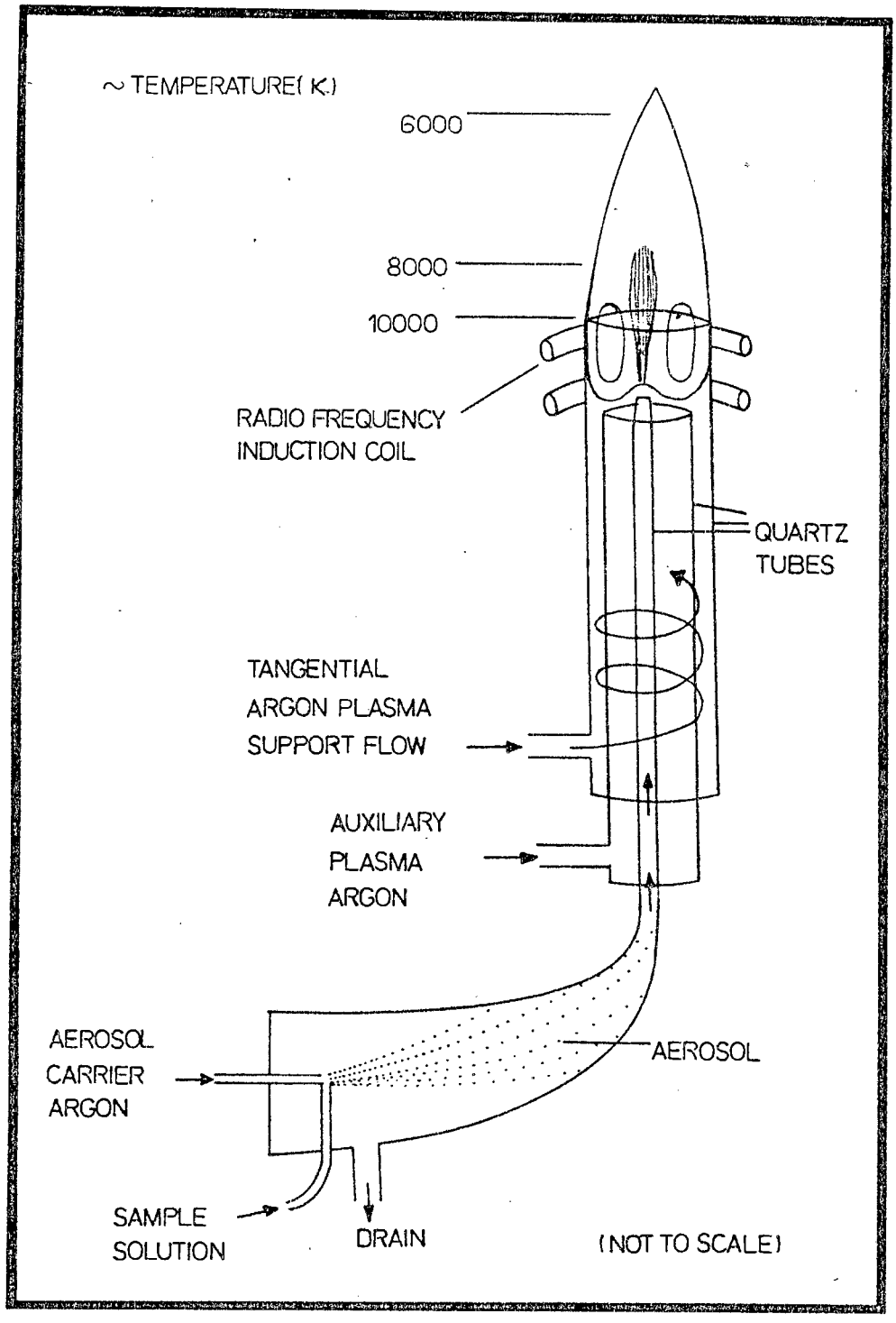


**Figure 4.1** ICP Source.

Fassel [35] in his review has attributed the slow acceptance of ICP-AES as a viable analytical technique to:

1. The emergence from the research laboratory at the same time that AAS was gaining wide acceptance.
2. Decline in the use of AES as a general laboratory tool during the period of approx 1965 to 1973.

3. "Fictional claims" on disadvantages of observing free atoms in emission.

4. Lack of commercial facilities.

However, the need for determining more and more elements in more and more samples at lower and lower concentrations, the multielement capability of AES and the emergence of ICP's as remarkably successful vaporization-atomization-excitation-ionization cells for analytical spectroscopy and the greater availability of commercial facilities have made ICP-AES more acceptable. The advances of electronics and computer technology have also contributed greatly to the design of modern instruments. It is believed that about 800 instruments were being used world wide in 1981.

ICP-AES has many advantages but many problems still remain. The instruments are generally much more expensive than atomic absorption spectrometers and the running costs are high due to their large consumption of high purity argon or nitrogen (typically 20 l Ar $min^{-1}$).

Advantages of ICP-AES systems include:

1. Applicability to most elements except argon and/or nitrogen. The greatest analytical capability of ICP-AES is that refractory elements such as boron, titanium, tantalum, tungsten and zirconium can be determined very easily at low levels. These elements can be determined well by AAS only at high concentration levels.

2. Simultaneous or rapid sequential multi-element

determination capability at the major, minor and trace concentration levels without changing experimental conditions.

In contrast to arc, spark and flame, the temperature cross-section of the plasma is relatively uniform; as a consequence, self-absorption and self-reversal effects are seldom encountered. Linear calibration curves over several orders of magnitude may be obtained.

3. Capability of providing rapid analysis, therefore amenable to process control. If the sample is ready for aerosol formation, two or three minutes are required for the simultaneous determination of up to 30 to 40 elements and approximately 30 seconds per element for sequential scanning spectrometers.

4. Detection limits are comparable to flame AAS and other spectrometric techniques.

5. Acceptable precision and accuracy.

6. Applicable to the analysis of solids, liquids and gases with minimal preliminary sample preparation or manipulation.

Many devices have been constructed for introducing solids into flame (Chapter 3) and plasmas either by the use of "atomization cells" or in the form of slurries through nebulizers [36, 37, 38]. Novel nebulizers have been designed for the analysis of viscous samples or samples containing high dissolved solids. Amongst others are the Babington type nebulizer [39], the "V" type nebulizer [40] and the ultrasonic nebulizer [41].

Gases can be analyzed directly and hydride generation has been used for those elements forming volatile hydrides like Pb, As, Ge, Se, Bi and Sb [67, 98, 99], although difficulties remain. Liquid samples are prepared by similar methods to those used for AAS (see Chapter 5).

7. Applicable to the analysis of microlitre samples.

Although ICP-AES has been claimed to be free from inter-element effects many problems with interferences occur (Chapter 11). Interferences may be grouped under two major classes : spectral and nonspectral.

Spectral interferences include:

(i) Line coincidences (spectral overlap).

(ii) Continuum (eg, ion recombination continuum spectra).

(iii) Molecular band emission (eg, OH).

(iv) Stray light effects (ICP sources are very intense).

Their occurrence and severity depends on the quality of the spectrometer grating and optics, resolution and choice of analytical lines.

Nonspectral interferences arise through physical or chemical processes that affect the transport, atomization or excitation of the analyte species. They can be subdivided into element-specific and nonspecific interferences.

Element-specific or interelement interferences originate in the plasma and involve chemical and ionization effects. For

example, enhancement or depression of analyte signals caused by the presence of an easily ionizable concomitant.

Nonspecific interferences are related to the physical properties of the analyte and/or its sample matrix. These properties affect the rate of introduction of the analyte into the plasma, for example solution viscosity or rate of vaporization.

Some modern instruments provide the facilities for identification and correction of some problems. Interferences in the ICP have been discussed by many authors, eg [42]. Relevant problems are illustrated in the appropriate chapters of this work.

## 4.2 INSTRUMENTATION, ICP OPTIMIZATION AND METHOD DEVELOPMENT

The instrument used was an Instrumentation Laboratory (IL) Plasma-100 Spectrometer coupled to a line printer (IL) and a video printer (Axiom Ex-850). Its component systems are the radio frequency power supply, the sample introduction system, the optical system and the electronics and computer system. A schematic diagram of the instrument is shown in figure 4.2.

The operating conditions are given below and the monochromator system is shown in figure 4.3. The instrument has been described in more detail by Smith et al [76].

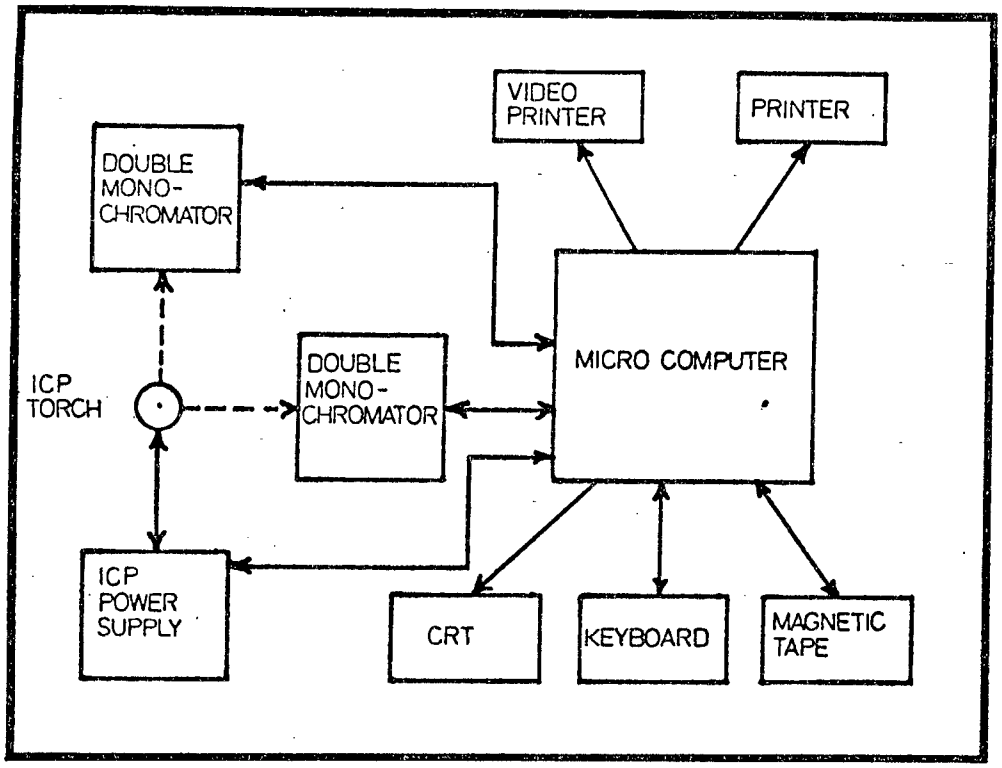


Figure 4.2 Block diagram of instrument.

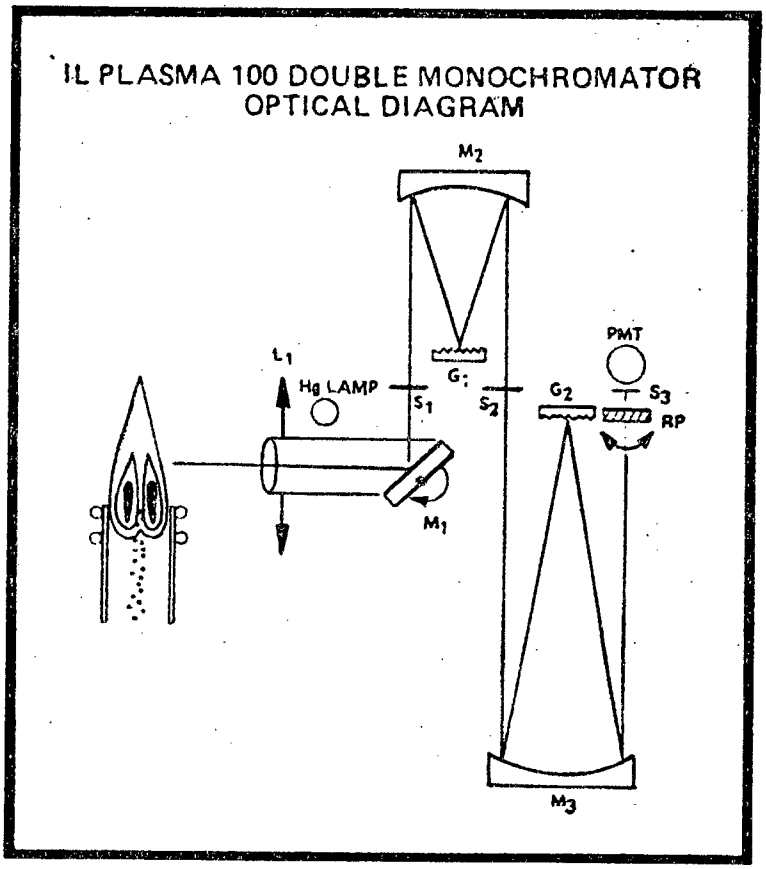


Figure 4.3 Monochromator system

## Operating Conditions

| | |
|---|---|
| RF power supply | 27.12 MHz, 950 - 1750 W, selectable in seven steps (0 to 6). |
| Optical system | (2 Double monochromators, channels A and B). |
| Primary monochromator | $\frac{1}{3}$ m Erbert-Fastie design |
| Premonochromator | $\frac{1}{6}$ m Erbert-Fastie design |
| Resolution | 0.02 nm |
| 1st Order | 190 - 365 nm |
| 2nd Order | 365 - 900 nm |
| Peak search window size | 0.033, 0.067, 0.1 nm (user selectable) |
| Computer system | Intel 8080A µP, FORTH language |
| Sample Introduction System | Polypropylene cross-flow nebulizer with synthetic saphire capillaries and concentric quartz tube torch. |
| Nebulizer driving pressure | 20 to 50 psi |
| Sample flow rate | peristaltic pump, 0.1 to 2.2 ml $min^{-1}$ |
| Plasma gas flow | 15 to 20 l $min^{-1}$ |
| Torch observation height | 0 to 40 mm above RF coil (2 mm increments). |

ICP Optimization

There are a number of instrumental parameters which affect the performance of an ICP:

(a) Torch power
(b) Nebulizer driving pressure
(c) Plasma gas flow
(d) Sample aspiration rate
(e) Wavelength selection
(f) Torch observation height.

These parameters are interdependent and changing one may well affect the optimal conditions for the others.

(a) The torch power must be held constant for all the elements in one programme, thus power must therefore be established at a compromise level for the sample matrix and all the elements of interest. Background to analyte intensity ratio tends to increase as power is increased, therefore best detection limits are obtained at low powers for simple aqueous matrices. However, at low powers, analyte atoms may not be efficiently excited and an enhancement effect due to secondary excitation caused by easily excited matrix constituents can occur.

Organic substances require more power than aqueous solutions. Very volatile solvents are difficult to use with an ICP. Power 6 is used for organics. The IL Plasma-100 has been operated at powers 4 and 5 with a xylene solution without any problem. The effects

of organic solvents in ICP-AES have been discussed by Boorn and Browner [62].

(b) The velocity of sample transport throughout the plasma is controlled by the nebulizer driving pressure. This parameter is set manually between 20 and 50 psi. The nebulizer driving pressure must be kept constant for an analytical programme. Elements with high excitation energies require a longer residence time in the plasma to achieve complete excitation, therefore lower driving pressures, typically 20 to 25 psi, are used. Elements with low excitation energies can be analyzed at pressure 35 to 40 psi. High pressures (>40 psi) are used for volatile organics and for samples with high dissolved solid concentrations to literally force the samples into the plasma.

(c) The plasma gas flow is divided between the primary and secondary flows by a fixed orifice system. The total flow is fixed at 15 l $min^{-1}$ for power levels 0 to 3 and at 20 l $min^{-1}$ for power levels 4 to 6. The higher gas flow is necessary at high power levels to raise the plasma discharge above the end of the sample introduction tube otherwise this may melt. Increased gas flow also cools the discharge slightly and reduces the amount of entrained air consequently spectral interference from emission lines by hydroxyl bands, cyanogen bands and other possible spectral interferences from air in the discharge is reduced.

(d) Increased sample aspiration rate reduces the temperature of the plasma discharge. Elements with

low excitation energies like alkali metals may have improved performance at higher aspiration rates while elements with high excitation energies may perform best at lower aspiration rates. Normally an aspiration rate of 1 ml/min is adequate for aqueous solutions. With organics, which nebulize more easily, sample aspiration rates can be decreased to 0.4 ml/min. When using high dissolved solid concentrations it was found best to use low aspiration rates to minimize the risk of blocking the cross flow nebulizer. The aspiration rate is kept constant for an analytical programme.

(e) The choice of wavelength affects the optimal conditions of the other parameters and should be taken into consideration when selecting optimal conditions.

(f) The torch observation height of the plasma discharge for each element within a programme can be varied from 0 to 40 mm above the coil in 2 mm increments. The region of highest temperature provides the greatest excitation but also highest background intensities due to emission from argon and other plasma constituents. The optimal signal to noise ratio is obtained at a different height for each element depending on other conditions. Elements with high excitation potentials are best observed lower in the torch.

It is vital in method development to be aware of the critical nature and interdependence of the above instrumental parameters.

Method Development

Various electronic and software parameters are available in the IL Plasma-100 for optimization and refinements in method development. The graphic facilities are especially useful in that this feature allows the analyst to identify interferences and different routines can then be used for corrections. The ICP parameters and graphics are illustrated by video printouts in **appendix 2.** Several interferences are shown and the symbols used are explained.

A systematic approach for method development is essential and, prior to sample preparation, a study of the capability of the instrument to analyse the element at a desired level is necessary, ie the sensitivity, an estimate of detection limit, the upper concentration level and the linearity of the calibration curve must all be investigated for each spectral line.

The choice of a spectral line is based on information obtained from the literature and by using line coincidence tables, eg those of Boumans [43] and possible interferences from other elements present in the samples must also be considered.

Usually background interferences and overlapping of spectral lines are easily seen while spectral interference brought about by total "burying" of the interfering element peak under the analyte peak is not apparent. Discrepancies between concentrations obtained by using several spectral lines indicate some source of interference. These are checked by adding varying amounts of high purity concomitants

to standard solutions of the analyte or, alternatively, by using the device developed (see chapter 4.4).
There are several factors to be considered in selecting the best of the available analyte wavelengths for the determination of an element in a particular sample matrix.

The parameters described below ("spectral characteristics") are used to compare the usefulness of spectral lines:

1. Detection limit ($C_L$)

   It is defined as the concentration of the element that produces an analytical signal equal to two or three times the standard deviation of the background signal ( $\sigma_B$). For this work 3 $\sigma_B$ is used in compliance with IUPAC recommendations [44].

$$C_L = \frac{3\ \sigma_B}{S_{ICP}}$$

   where, the sensitivity, $S_{ICP}$ = slope of the linear calibration curve or

$$\frac{I_A - I_B}{C_A}$$

   $I_A$ = Intensity of the highest standard

   $I_B$ = Intensity of the blank or background

   $C_A$ = concentration of the highest standard, usually in ppm.

   $\sigma_B$, $I_A$ and $I_B$ are calculated from a minimum of ten readings.

   A most useful approach in AES [44, 45] is to introduce the background signal into the above equation:

$$C_L = \frac{3\ \sigma_B \times I_B}{I_B \quad S_{ICP}}$$

$$= \frac{3\ \sigma_B \times I_B}{I_B \quad I_N} \times C_A$$

where $I_N$ = net signal intensity

$= I_A - I_B$

$I_N/I_B$ is the signal to background ratio.
It has been found that under normal conditions, $\sigma_B$ is approximately constant and is equal to about 1% of the background signal. Therefore, $\sigma_B$ can be approximated by 0.01 $I_B$ and $C_L$ can be estimated from

$$C_L = 0.03\ C_A \frac{I_B}{I_N}$$

$$= \frac{0.03\ I_B}{S_{ICP}}$$

Winge, Peterson and Fassel [45] have estimated detection limits of 70 elements using the latter equation. Detection limits calculated by this equation were shown to agree moderately well with those calculated in the conventional manner.

It seems to be a tendency by many authors to report $C_L$ values which have been calculated using large integration times (exceeding 10 sec) and excessively large numbers of readings (over 20 replicates) thereby obtaining an unrealistically low $C_L$ which is the best achievable limit with the instrument. In this work $C_L$

values reported are calculated using more practical data ie, shorter integration times which are used for practical analytical work. Although the $C_L$ values might be larger, they represent much more typical analytical situations.

Background intensities are those intensities measured while aspirating the blank at the analytical wavelength. "Blank interferences" are discussed by Boumans and Bosveld [77].

2. Background Equivalent Concentration (BEC)

The BEC is defined as the concentration of analyte which gives an intensity equal to the intensity of the plasma background at the analyte wavelength.

$$BEC = \frac{I_B}{I_A} C_A$$

3. Interference Equivalent Concentration (IEC)

It is defined as the apparent analyte concentration that is observed for a defined concentration of an interfering component of the analyte wavelength.

$$IEC = \frac{I_I}{I_A} C_A$$

$I_I$ = intensity of interferent.

4. Upper Concentration Limit (UCL)

It is the maximinum concentration (in ppm) that can be aspirated without the signal intensity exceeding

the dynamic range of the instrument (ie 25000 "counts" per 25 ms). This value can be estimated by extrapolating the intensity value obtained for a known concentration of the analyte, ie

$$UCL \simeq \frac{25000 \times 10^3 \times C_A \times t}{25 \times I_A}$$

where t is the integration time (sec).

Note: The linearity of the calibration curve up to UCL must be verified.

Some spectral characteristics for 41 lines are given in appendix 3. These results were part of an investigation for trace element analysis of coal and fly ash. The compromise instrumental parameters, kept constant for all elements, were (aqueous standards) : Power 3, 1 ml/min sample flow rate, 30 psi nebulizer driver pressure, 30 sec washing time ("pump delay"), 5 sec integration time. The viewing heights were optimized for each element. $C_L$ values were based on ten blank (water) readings. The % RSD values obtained for an analyte concentration of $C_A$ were based on five readings. The $C_L$ values obtained compared well with reported values. On average 0.24% RSD is obtained for five consecutive readings at levels of 10 and 100 ppm analyte in aqueous solutions. The % RSD of the blank readings varied from 0.1 to 1 (av. 0.41%) with only a few values larger than one.

## 4.3 Interference Investigation

The preparation of test solutions containing both the analyte and the possible interferent (also different acid concentrations) is a very tedious procedure requiring the preparation of large numbers of standard solutions. To facilitate this task, a device was constructed for mixing two solutions prior to nebulization into the ICP torch. Once the interference is identified, the necessary correction steps can be taken and in the case of spectral interference, a correction factor must be determined accurately.

A schematic diagram illustrating the components is shown in figure 4.4.

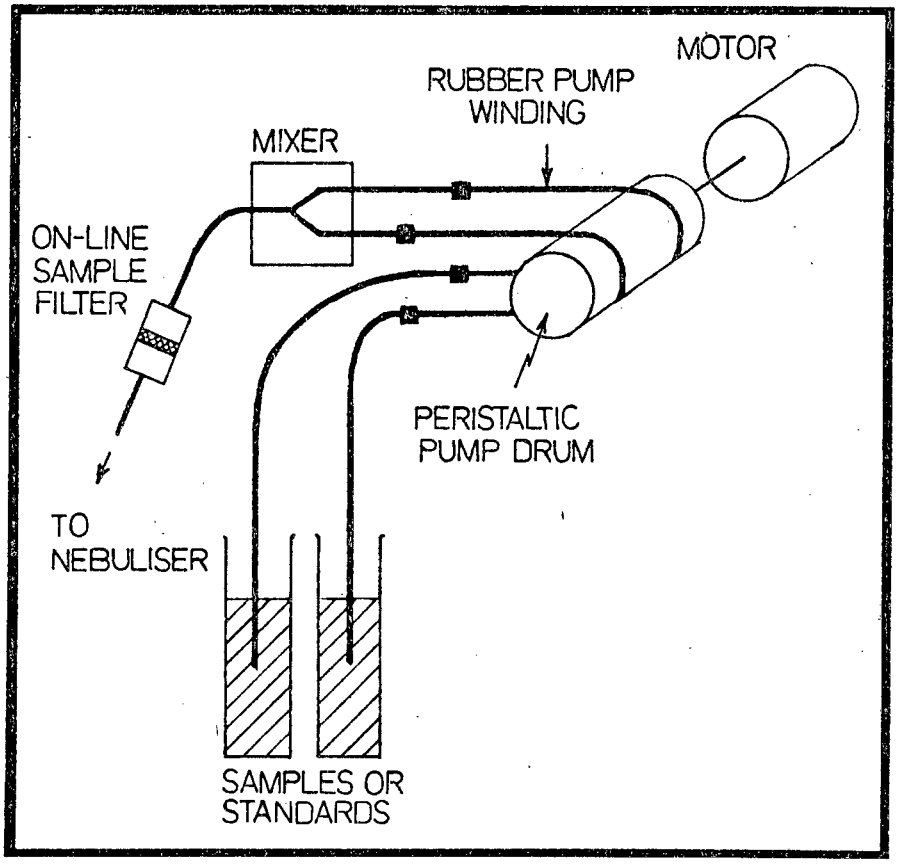


Figure 4.4 Operation of the mixing device

The peristaltic pump drum and the sample filter form part of the instrument and the drum has space for two rubber windings.

Different designs and sizes of mixing chambers (mixer) were tried and the one described below was found to perform best. However, mixing of two solutions was not "quantitative", ie the flow rates were not the same from both windings, but the difference is small enough to allow qualitative work.

The device also allows the standard addition technique to be used without prior spiking of samples, however, a correction for non-quantitative mixing (which is nevertheless constant during an analysis) must be applied. The advantages of using this device are:

(i) Rapid analyses, since little preparation is required;

(ii) There is no waste of standard solutions or samples especially when very small volumes are available;

(iii) A possibility of fast multielement standard addition.

Details of the mixer appear in figure 4.5.

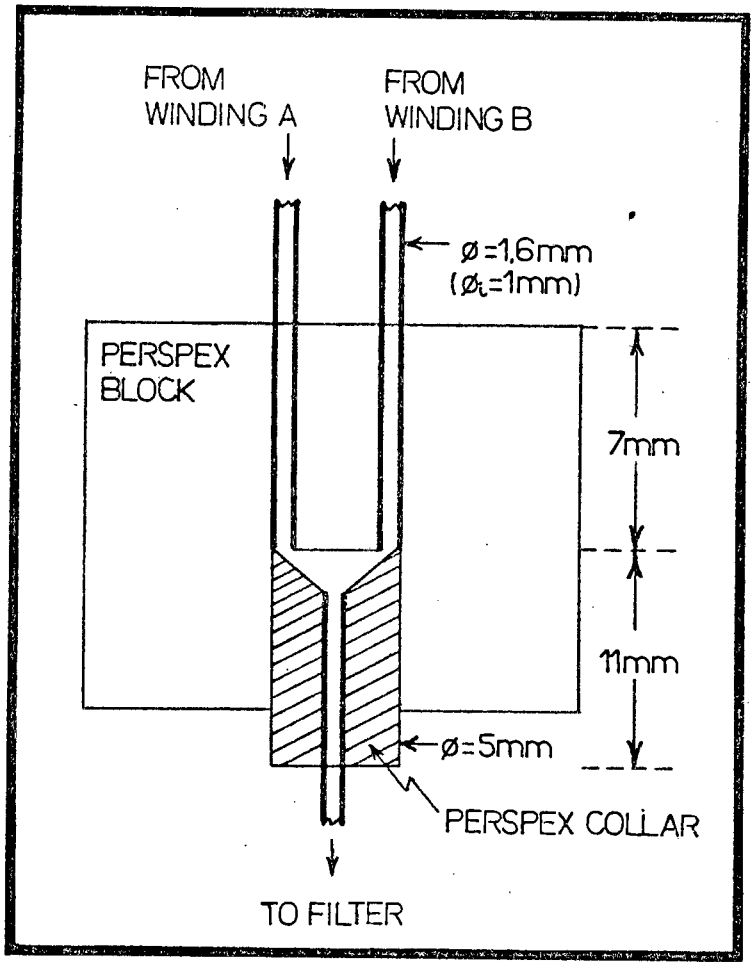


Figure 4.5 Diagram of mixing unit.

## 4.4 Determination of carbon by ICP-AES

The determination of total carbon in a sample is often required. For example, the amount of carbon in steels has a marked effect on the properties of the steel. Common methods use the evolution of carbon dioxide and absorption in a suitable material, eg soda lime, followed by the measurement of the increase in weight of the absorbent.

Carbon emission is observed from the ICP source and has potential for carbon determination in some samples. Since the carbon is lost when dissolving a sample by most normal procedures (acid attacks), one way of determining carbon by ICP-AES would be to use a carbon dioxide generator (similar to the hydride generator) where the sample is decomposed in a closed vessel and the evolved carbon dioxide then aspirated, into the plasma.

The sensitivities and detection limits of three carbon emission lines were investigated. A standard solution was prepared by dissolving 1 g of oxalic acid (Analytical Reagent) in 100 ml of water. The theoretical concentration of carbon in the standard was 1904 ppm. This solution was used to calculate the $I_N/I_B$ and $C_L$ values listed in table 4.1. Carbon was found to have maximum emission at 14 mm torch viewing height, Power 3 and 30 psi nebulizer driving pressure. The sample flow rate was 1 ml $min^{-1}$.

Table 4.1 Carbon spectral characteristics

| Spectral line (nm) | $S_{ICP}$ $(ppm)^{-1}$ | $I_N/I_B$ | $C_L$ (ppm) |
|---|---|---|---|
| 193.09 | 160 | 8.9 | 1.6 |
| 247.86 | 279 | 4.6 | 2.1 |
| 199.36 | 0.4 | 0.2 | 120 |

The $I_N/I_B$ values are very low due to high blank (water) intensities obtained. On dismantling the torch-nebulizer system for cleaning, many graphite particles were found inside the torch system and even inside the sample capillary. These arise from the slow destruction of the graphite igniter tip used to initiate the plasma. It is possible that these

particles may cause high backgrounds.

A test solution was prepared by dissolving 0.25 g succinic acid ($C_4H_6O_7$) in 100 ml of water and analysed using the first two spectral lines in table 4.1. Calibration was done with two solutions containing 1 and 0.5 g oxalic acid per 100 ml and a water blank. 1014 ppm C (0.8% RSD) was found which agrees satisfactorily with the theoretical value (1025 ppm).

Although little attention has been given to carbon determination by ICP-AES, the above results show that it is possible and should be considered as an additional tool for the analyst.

# CHAPTER 5. MAJOR ELEMENT ANALYSIS OF COAL AND FLY ASH BY ICP-AES

The elements in coal and fly ash can be divided into two groups: the major elements (Si, Al, Fe, Mg, Ca, Na, K, Ti, P and S) and the minor or trace elements (usually $\leq$1000 ppm). A complete ash elemental analysis consists of the determination of $SiO_2$, $Al_2O_3$, $Fe_2O_3$, MgO, CaO, $Na_2O$, $K_2O$, $TiO_2$, $P_2O_5$ and $SO_3$ in order to calculate ash-quality parameters for the reasons mentioned in Chapter 1. (Concentrations are traditionally reported as "percent oxide").

General methods for sample preparation are described below and for this work two dissolution procedures by acid attack were used.

## 5.1 Sample preparation for coal, coal ash and fly ash analysis

Several methods for dissolution of these materials for analysis by spectroscopy have been developed. Mills and Belcher in their review [2] have listed four approaches: room temperature dissolution, pressure dissolution, combined dissolution/fusion and fusion re-solution presentation. Both dissolution by acid attack and fusion techniques have been widely used for AAS analysis of coal and ashes. Similar methods are used for ICP-AES analysis [46, 47].

### 1. Dissolution using acids

Nitric ($HNO_3$), perchloric ($HClO_4$) and hydrochloric (HCl) acids or combinations of these (eg aqua regia) are used

to oxidize the organic (carbonaceous) matter, especially in coal, and dissolution of the siliceous material is accomplished by hydrofluoric acid (HF) according to the reaction [26] :

$$SiO_2 + 6HF \longrightarrow H_2[SiF_6] + 2H_2O$$
$$\longrightarrow SiF_4 + 2HF$$

Other materials such as $Al_2O_3$ can also be attacked by HF [26] :

$$Al_2O_3 + 6HF \rightarrow 2AlF_3 + 3H_2O$$

The acid attacks are more efficiently accomplished at high temperatures but the losses of certain elements occur, for example As, B, Ti, Si [27], especially on evaporating to dryness. Hence the use of closed vessels (Teflon Lined Acid Digestion Pressure Bombs) at high temperatures where high pressures are obtained, have been developed and used [28, 29]. Attack by HF results in solutions with high fluoride concentrations and sometimes residues of sparingly soluble fluorides of Mg, Ca, Sr, Ba U and the rare earths are obtained [27]. Many elements can be determined directly in the fluoride media without the need for evaporation of the acid. A common procedure is to add an excess of boric acid ($H_3BO_3$) which complexes with fluoride to form fluoroboric acid according to the reaction:

$$4\,HF + H_3BO_3 \longrightarrow HBF_4 + 3H_2O$$

Presence of boric acid also helps to dissolve precipitated fluorides. The advantage of this procedure

is that solutions containing excess $H_3BO_3$ can be prepared and stored in glassware for some time, 2 hours according to Bernas [28], without any attack of the glassware by HF, or silicon leaching into the analyte solution.

Langmyhr and Sveen [70] and Langmyhr and Paus [71] have discussed the use of HF for the decomposition of inorganic siliceous materials. Langmyhr and Kringstad [72] also investigated the composition of precipitates formed by decomposition of silicate rocks in HF. They found Ca, Mg, Al, Fe and Na to be major constituents of the precipitates and Ti and Mn as minor constituents. They reported compounds such as $CaF_2$, $MgAlF_5.xH_2O$, $NaAlF_4 \cdot xH_2O$ and the probable formation of Fe(II) (Al,Fe(III)) $F_5 \cdot xH_2O$. They also noted that the amounts of precipitate increased with the basicity of the rock samples.

A frequent procedure for coal analysis is to ash the samples, prior to dissolution by acid attack or fusion, in order to remove the organic matter. Two procedures are available - high temperature (HTA) and low temperature ashing (LTA). Many studies have been done on the losses of elements from coal by high temperature ashing. However, the results are sometimes conflicting [2]. During this process, the ash concentrates the inorganic elements.

A few examples of sample preparation and analytical methods using acid attack are presented below. Methods similar to those used for mineral analysis (eg silicates) are also applicable to coal and ashes analysis.

**Sample preparation by dissolution using acids**

| Sample | Elements determined | Analytical technique used | Amounts of sample used | Acids used<br>AR = Aqua Regia<br>$FHNO_3$= Fuming $HNO_3$ | Method description<br>PV = pressure vessel | References |
|---|---|---|---|---|---|---|
| Silicates | Si, Fe, Al, Ti, V, Ca, Mg, Na, K | Flame AAS | 50 mg<br>300 mg for V | 0.5 ml AR + 3 ml HF (48%) | PV, 30-49 mins at 110°C. Add 2.8 g $H_3BO_3$ | [28] |
| Coal | Be, Cd, Ca, Co, Cu, Li, Mg, Mn, Ni, K | Flame AAS | 50 mg | 6 ml $FHNO_3$ (90%) + 3 ml HF (48%) | PV, 2.5 hr at 150°C Add HF, 15 mins at 150°C. Add 2.8 g $H_3BO_3$ | [29] |
| Fly ash | Si, Al, Fr, Ca, Mg, K, Na, Ti, Cu, Mn, Zn, Be, Ba, Co, Cd, Cr, Ni, Pb, Sr | Flame and FAAS | 1 g | 10 ml HF (48%) | Shake, 6 hr at room temperature. Add 80 ml saturated $H_3BO_3$ solution | [30] |
| Coal,<br>Coal ash<br>Fly-ash | Pb | FAAS | 200 mg<br>30 mg<br>30 mg | 3 ml 14 M $HNO_3$ + 4 ml 30 M HF | PV, 6 hr at 230°C | [31] |
| Silicate rocks | Trace and major elements | ICP-AES | 0.5 g | 4 ml $HClO_4$ (60% v/v) + 15 ml HF (40% v/v) | Pt crucible, evaporate, cool, add 4 ml $HClO_4$ + 15 ml $H_2O$, warm | [32] |
| Coal ash | Ca, Mg, Na, K, Fe | Flame AAS | 0.1 g | 3 ml $HClO_4$ + 10 ml HF | Pt crucible, heat to release HF | [33] |
| Alumino-silicate | Al, Ca, Fe, K, Mg, Mn, Na, Si, Ti, Co, Cr, Cu, Li, Ni, Pb, Sr, V, Zn | Flame AAS | 100 mg | 1 ml AR + 6 ml conc. HF | PV, 30 mins at 100°C Add 5.6 g $H_3BO_3$ | [34] |
| Silicates | Si, Fe, Mn, Al, Mg, K, Ti, Ca, Na | ICP-AES | 50 mg | 1 ml HCl + 0.5 ml HF | Teflon vessel, >4 hr at room temperature. Add 6 ml 4% (w/v) $H_3BO_3$ soln | [103] |

## 2. Fusion Methods

A large variety of fluxes have been used for the fusion of ashes and silicates. Fusion is usually carried out in platinum or platinum-gold alloy vessels at high temperatures (eg 1000°C) in furnaces, or over flames. Borate based fluxes include lithium tetraborate ($Li_2B_4O_7$) and lithium metaborate ($LiBO_2$). Other fluxes which have been used are sodium or potassium carbonate and mixtures such as $H_3BO_3$ + $Li_2CO_3$.

Fluxes such as NaOH, KOH and LiOH can also be used. Because of the relatively low melting points of these hydroxides, fusions can be carried out at much lower temperatures than with carbonates or borates, typically 450 - 500°C. These fusions can be done in nickel or silver crucibles since these materials are hardly attacked by hydroxide melts.

Since large flux to sample ratios are used (2:1 to 10:1), high purity materials are essential for trace work. High flux to sample ratios also yield samples containing large concentrations of dissolved salt which often cause problems in conventional nebulizers.

Some examples of fusion methods used for ICP-AES analysis are listed below. More details of dissolution and fusion procedures appear in Bock [27].

**Sample preparation using fusion methods.**

| Sample | Elements determined | Amounts of sample | Flux used | Method description | References |
|---|---|---|---|---|---|
| Coal ash | Si, Al, Fe, Ti, P, Ca, Mg, Na, K | 0.2 g | 2 g $LiBO_2$ | Pt crucible, heat at 950°C in muffle furnace for 25 mins. Dissolve melt in 4% $HNO_3$ | [49] |
| Coal ash | Si, Al, Fe, Mg, Ca, Na, K, Ti, Ba, Mn | 0.1 g | 1 g $Li_2B_4O_7$ + 0.05 g CsI (non wetting agent) | Automatic fusion device. Pt - 5% Au crucible. Heat on air-propane flame ( 1200°C) for 6 mins. Dissolve in 15% HCl. | [48] |
| Fly ash & silicates | B | 100 - 400 mg | 2 g $Na_2CO_3$ | Pt crucible, heat for 15 mins at 850°C and for 15 mins at 950°C. Dissolve in hot water. Neutralize with $HClO_4$. | [50] |
| Silicate rocks | Si, Al, Fe, Mg, Ca, Na, K, Ti, P, Mn | 0.5 g | 2 g $LiBO_2$ | Pt crucible, fuse on Mekerburner for 30 mins. Dissolve in 50% $HNO_3$. | [32] |
| Coal | Al, Ca, Fe, K, Mg, Na, Si, Cd, Cr, Co, Cu, Mn, Ni, Pb, V, Zn | 3 g | 1.5 g $Li_2B_4O_7$ | Pt crucible, heat for 1 hr at 1000°C. Dissolve in 5% HCl. | [78] (AAS analysis) |

## 5.2 Method development and procedure

### Samples

The NBS-SRM fly ash 1633a, coals 1632a and 1635 were kept and dried under vacuum as recommended by NBS. Two coal samples from South Africa Vierfontein Collieries (C2) and Natal Anthracite (C12) were received as coarse powders and about 45 gram amounts were crushed in an agate 'Siebtechnik' mill for 5 minutes (2 mins followed by 3 mins after a few minutes "cooling").

Fly ash samples from the Taaibos Power Station, South Africa, (PFA4) and (PFA5), and one sample from a SASOL I plant (FA2) were used as received without any grinding.

A coal ash sample (CA1) from the SASOL I plant was first dried at 80°C for several hours, crushed in a jawcrusher and this was followed by 2 minutes grinding in a 100 cc carbon steel swingmill.

### ICP parameters and sample preparation

Some of the spectral lines used for this work have been used by other authors [32, 48, 49] for major element analysis of similar samples (different instruments were used) and no interferences were reported.

The lines were checked for linearity with several standard solutions and concomitants (eg Si, Al, Ca, Fe) were used to check for any background and spectral interferences. A few spectral lines were investigated for each element and the

"best" ones were selected for analysis using optimization procedures detailed above.

In the case of Al and Si, two lines were used for comparison. Figures 5.1 to 5.5 show some of the peaks obtained by aspirating standard solutions and samples.

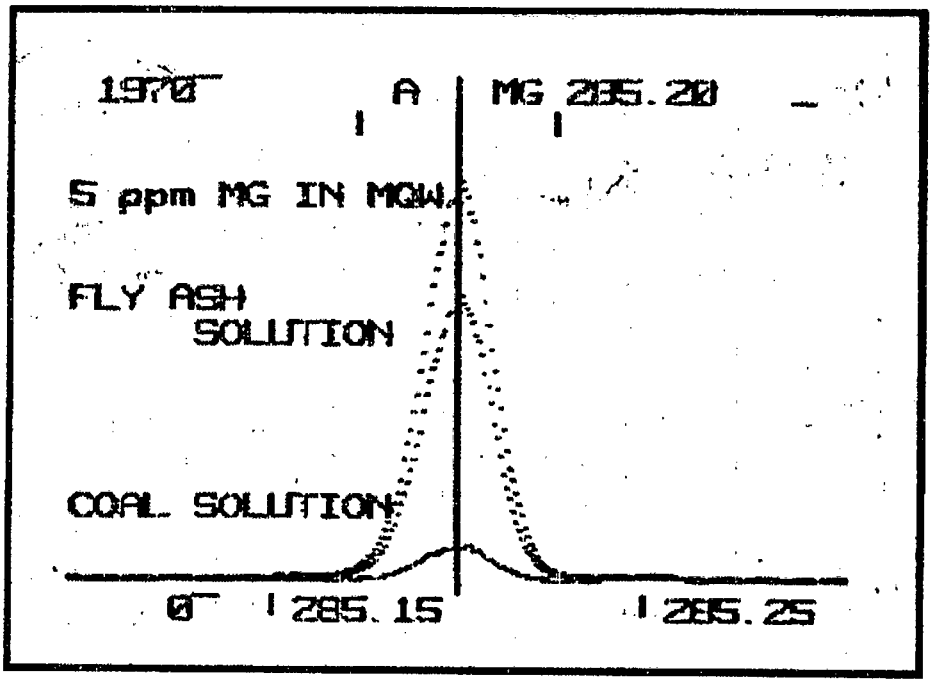


Figure 5.1 Magnesium emission

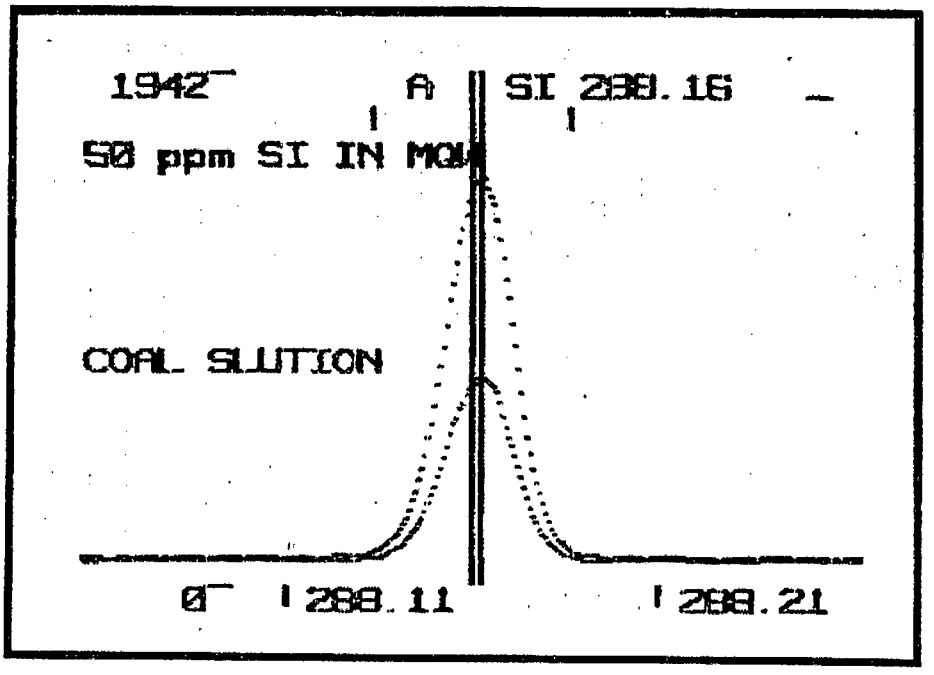


Figure 5.2 Silicon emission.

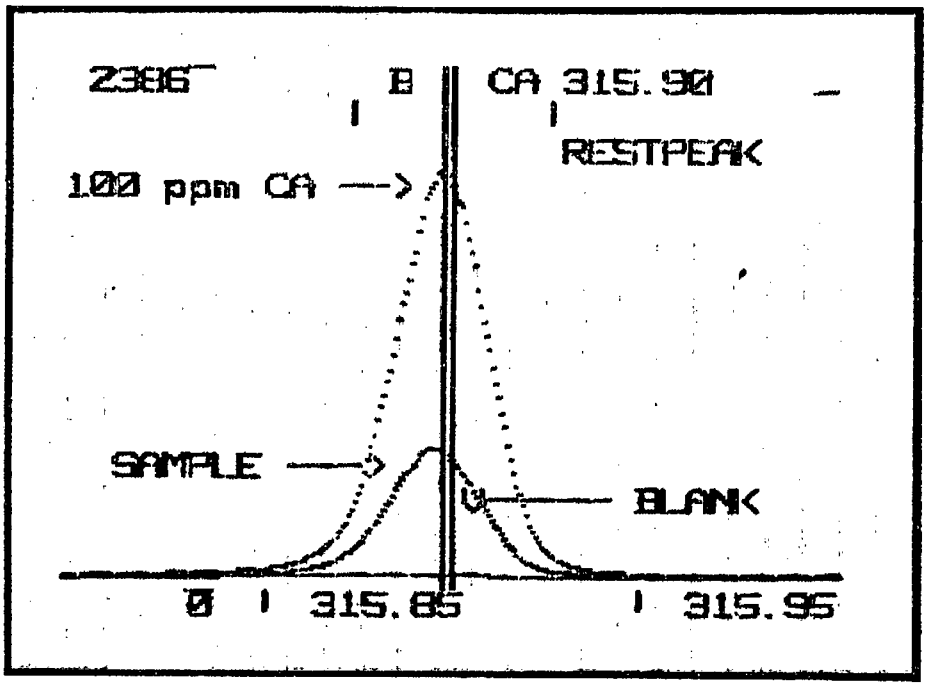


Figure 5.3 Calcium emission.

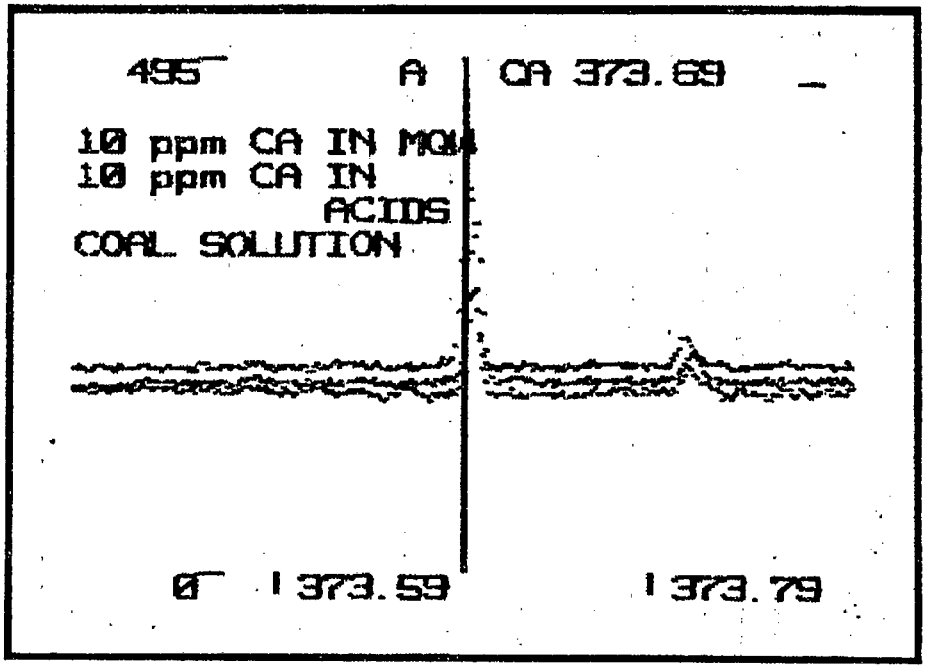


Figure 5.4 Calcium emission
(background (BKG) shift)

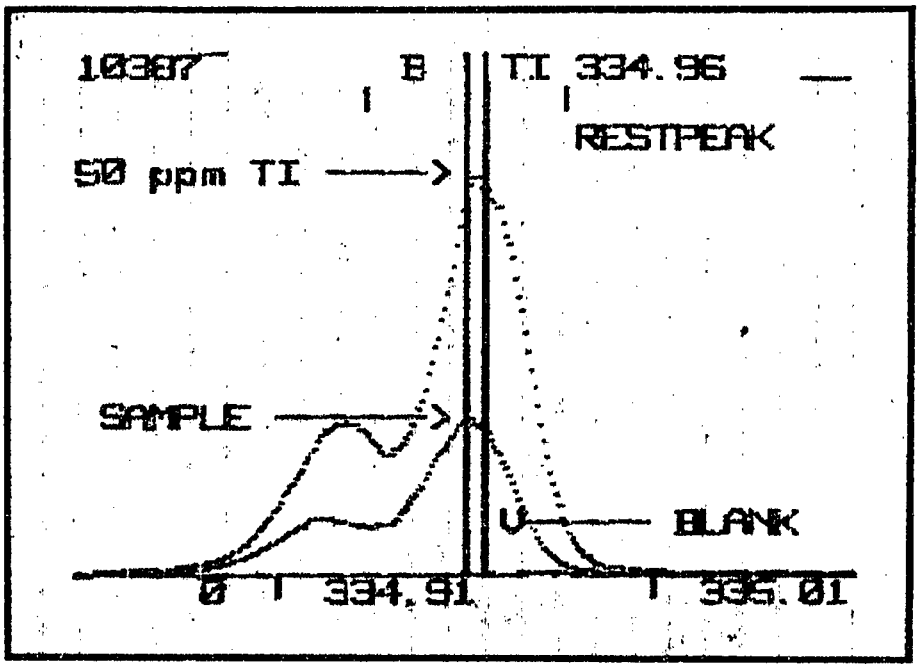


Figure 5.5 Titanium emission.

Figure 5.4 shows a small background shift at the Ca 373.69 nm line which can be corrected by using the IL-100 background correction routine on one side of the peak. A scan at the titanium 334.94 nm line is shown in figure 5.5. The line is part of a doublet which cannot be resolved but the lower peak is small enough not to provide any serious non-linearity, no correction was applied and the small window was used (0.033 nm). The sodium line at 589.00 nm is shown in figure 6 (Appendix 2) despite its low sensitivy the small window was used without any noticeable effect on the sensivity. The background correction positions are shown in the figure. It was found that at high concentrations no background correction was necessary.

After calibration with several standard solutions (usually 4 or 5 equally spaced between the blank and highest standard) only the highest standards and the blanks were used for

recalibration after checking the linearity of the calibration curves.

High dissolved boric acid concentrations (see below) affected the background intensity and precision of analysis, and concentrations above 6% (w/v) tended to block the nebulizer after long aspiration times. (Deposits form between the argon flow orifice and the sample capillary inside the nebulizer). Samples and standards were aspirated for 40 seconds ("pump-delay", PDLY) at 2.2 ml/min before readings were recorded at the programme's sample flow rate. Between analysis of two samples, water was aspirated at 2.2 ml/min for at least 30 seconds for adequate washout. All solutions aspirated contained about 0.05 % w/v Triton X-100 which improves nebulization efficiency.

Because of instrumental drift especially when aspirating high dissolved salt concentrations, recalibration was necessary after the analysis of 4 to 5 samples.

Botto [48] has described the use of water-saturated argon for sample nebulization in a cross-flow nebulizer. This system was shown to prevent blocking of the cross-flow nebulizer and thus reducing drift.

The two methods (A and B) used for dissolution with their instrumental parameters are described below:

Method A

The samples were dissolved in Parr acid digestion bombs (catalogue No 4745) using a mixture of nitric and hydrofluoric acids. The bomb and its characteristics are illustrated in figure 5.6. It is composed of stainless steel casing, with a screw-on cap, and a Teflon cup and lid.

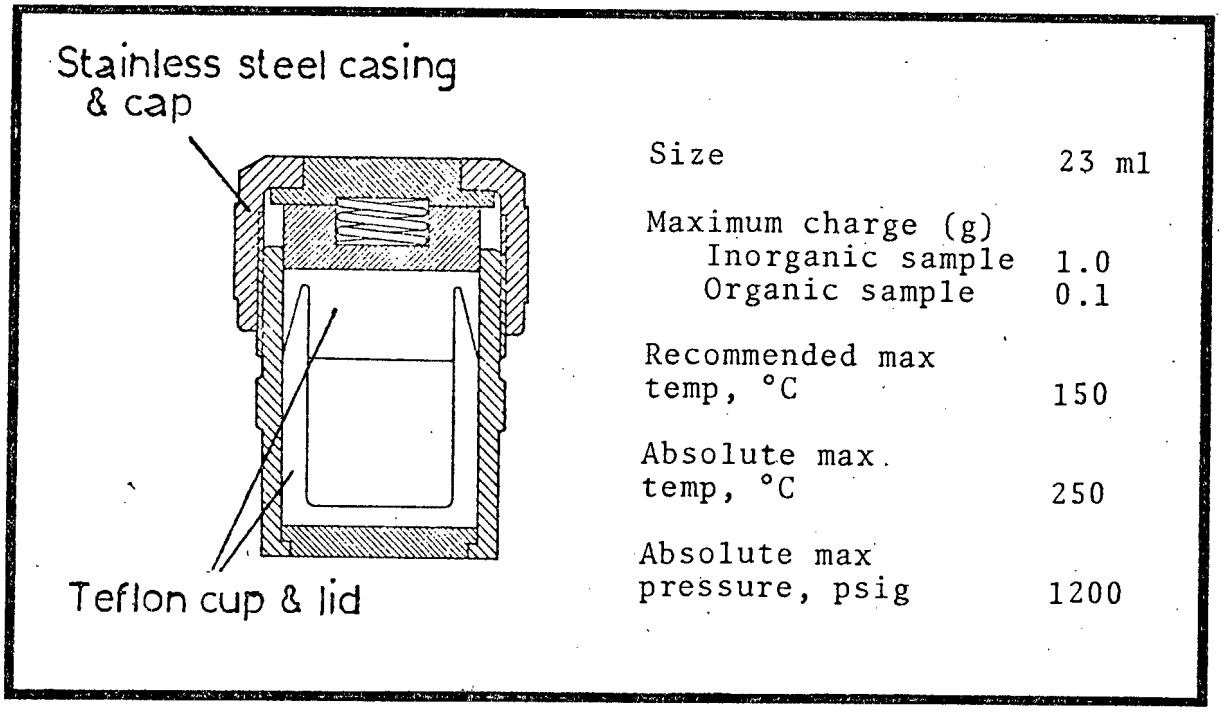


**Figure 5.6** Parr acid digestion bomb.

After trying different amounts of samples and acids, temperature and time of heating to obtain complete or maximum dissolution of the samples, the following procedure was adopted for the analysis of both coal and fly ash samples. The same procedure was used for both types of samples for convenience in preparing standard solutions and obtaining optimum conditions for ICP analysis.

After several dissolutions a certain amount of corrosion was seen on the inside walls of the bombs. Although the bombs

were not used within their maximum capacities and limits, deformation of the teflon cups occurred at the sealing areas resulting in leakage. It is likely that high internal pressures were attained, especially when using fuming nitric acid attack on coal samples. Low recoveries for certain elements, especially Si, was noted in those instances indicating that leakage had occurred. The teflon cups were inspected regularly and replaced whenever deformation was noted.

Sample preparation:

About 0.05 g dried samples were weighed directly in the PTFE cups. 3 ml fuming $HNO_3$ were added slowly, followed by 3 ml 40% HF after proper wetting of the samples by the $HNO_3$. The bombs were sealed and heated to about 130°C in an oven for 3 hours. After cooling, 2.3 g of solid boric acid were added to the cups with stirring. The contents were transferred to volumetric flasks for dilution and shaking to dissolve the boric acid and insoluble fluorides. All samples and standards were stored in plastic bottles.

Blanks containing identical amounts of HF, $HNO_3$ and $H_3BO_3$ as the samples were also prepared in the bombs. In the case of coal samples, clear orange liquids were always obtained. Fly ash samples always yielded small amounts of black residue and these samples were filtered before analysis.

The instrumental parameters used are shown in table 5.1. Al and Si were determined together. The standard solutions for calibration contained both elements. The other elements were

determined separately using optimum conditions for each of them.

TABLE 5.1 Method A, Instrumental parameters.

| Elements | Spectral line (nm) | Torch Power | Nebulizer pressure (psi) | Obs height (mm) | Sample flow rate (ml/min) |
|---|---|---|---|---|---|
| Ca | 315.89 | 5 | 40 | 24 | 1.2 |
| Mg | 285.21 | 5 | 40 | 22 | 1.2 |
| Ti | 334.94 | 5 | 40 | 22 | 1.2 |
| Al | 308.22 | 4 | 30 | 16 | 0.8 |
| Si | 288.16 | 4 | 30 | 18 | 0.8 |
| Mn | 257.61 | 5 | 40 | 22 | 1.2 |
| Ba | 493.36 | 5 | 40 | 22 | 1.2 |
| Fe | 259.94 | 5 | 40 | 20 | 1.2 |

Different elements in the samples were determined several times (separate dissolution and standard solution preparations), the same instrumental parameters were used each time and each prepared sample was analysed twice for each element, each analysis of two readings for 3 seconds duration. The results are mean values of all the separate determinations. The samples analysed by this method are NBS- SRM 1632a, 1635, 1633a, samples C2, C12, PFA4, PFA5.

Method B

A similar method to that described by Silberman and Fisher [30] was used for the dissolution of fly ash and coal ash samples.

About 0.5 g aliquots of the samples were transferred to 250 ml polypropylene volumetric flasks and 10 ml of water added to wet the samples. 10 ml 48% HF were added from plastic tipped pipettes; the flasks were sealed and shaken overnight (about 15 hours) at low speed, with the flasks half immersed in a water bath kept at 70 $\pm$ 2°C. After cooling, 70 ml of saturated (at room temperature) aqueous boric acid solution as added, followed by about 4 more hours of shaking in the water bath. After cooling, the solutions were transferred to 200 ml volumetric flasks and diluted to the mark with water. Further dilutions were required for the determination of Fe, Al and Si. Black residues were obtained and these were filtered off. All solutions were stored in plastic bottles.

The instrumental parameters are shown in table 5.2. It was found more convenient to use 6 analytical programmes combining elements as follows:

| | | | |
|---|---|---|---|
| 1 | Ca, Mg, Ti | 4 | Fe |
| 2 | Al, Si | 5 | Na |
| 3 | Mn, Ba | 6 | P |

Table 5.2 Method B, Instrumental Parameters

| Elements | Spectral line (nm) | Torch Power | Nebulizer pressure (psi) | Obs height (mm) | Sample flow rate (ml/min) |
|---|---|---|---|---|---|
| Ca | 315.89 | 4 | 30 | 16 | 1.2 |
| Mg | 285.21 | 4 | 30 | 18 | 1.2 |
| Ti | 334.94 | 4 | 30 | 18 | 1.2 |
| Al | 396.15 | 3 | 25 | 14 | 1.0 |
| | 308.22 | 3 | 25 | 14 | 1.0 |
| Si | 288.16 | 3 | 25 | 14 | 1.0 |
| | 251.61 | 3 | 35 | 16 | 1.0 |
| Mn | 257.61 | 4 | 30 | 18 | 1.2 |
| Ba | 493.41 | 4 | 30 | 16 | 1.2 |
| Fe | 259.94 | 4 | 30 | 16 | 1.2 |
| Na | 589.00 | 0 | 40 | 6 | 1.5 |
| P | 213.62 | 5 | 25 | 14 | 1.5 |

Calibration of the spectrometer was done using mixed standards containing exactly the same final amounts of acids as the samples. For Si and Al two spectral lines for each element were used for comparison; there was no noticeable difference between the two sets of data. Results for Si and Al determination by this method in the NBS-SRM 1633a is a mean of the two sets of results obtained using both lines. Each determination is a mean value of six separate 5 seconds integration time readings. Three separate analyses (sample dissolutions and standard preparations) were done for the NBS-SRM 1633a sample and two for the other samples.

Estimated detection limits for the elements determined by this method are listed in table 5.3.

The samples analysed by this method are NBS-SRM 1633a, PFA 4, FA2, CA1.

Table 5.3 Method B, Detection Limits.

| Element | Line Spectrum | Wavelength (nm) | $C_L$ (ppm) |
|---|---|---|---|
| Ca | II | 315.89 | 0.04 |
| Mg | I | 285.21 | 0.005 |
| Mn | II | 257.61 | 0.005 |
| Ti | II | 334.94 | 0.02 |
| Si | I | 288.16 | 0.08 |
| Si | I | 251.61 | 0.09 |
| Al | I | 396.15 | 0.08 |
| Al | I | 308.22 | 0.06 |
| Fe | II | 259.94 | 0.02 |
| Ba | II | 493.41 | 0.009 |
| Na | I | 589.00 | 0.5 |
| P | I | 213.62 | 0.2 |

## 5.3 Results and discussion

The analytical results are summarized in tables 5.4 to 5.12. Data available for these samples are also included for comparison. A comparison of the results obtained by the two methods for the analysis of fly ash samples (NBS-SRM 1633a and PFA 4) in tables 5.11 and 5.12 show good agreement with each other and with reported values except for Mn whose value is lower in the NBS-SRM 1633a with Method A. NBS-SRM 1632a also shows a lower value for Mn by Method A while the agreement of NBS-SRM 1635 by method A and of NBS-SRM 1633a by method B seems better. This cannot be readily explained. It could be due to a low recovery for this element by method A although manganese is not expected to form any insoluble species under those conditions. In their studies of residues from a similar dissolution procedure as method B,

Silberman and Fisher [30] did not report the presence of high concentrations of Mn. They quoted the work of Davison et al [105] who identified the elements present in residues after dissolution of coal fly ash in a bomb by a mixture of aqua regia and HF at 110°C for 2 hours, followed by the addition of boric acid. No manganese was reported. Although interferences were carefully checked, an unidentified background shift could be responsible for such differences since no background correction was used for the determinations. This requires further investigation.

A large difference exists between the P concentration measured in the NBS-SRM 1633a compared with the value reported by Gladney [54]; 0.24% P and 1.5% P respectively (table 5.11). Failey et al [69] reported a value of about 0.2%. The latter analysis was done by neutron capture prompt x-ray activation analysis. Brenner et al [75] used ICP-AES to analyse major elements in NBS standards after fusion with $LiBO_2$. Their data reported as % oxides were transformed to % elements in table 5.11. They obtained a value of 0.2% P which is in close agreement with the measured concentration. The value quoted in reference [54] is believed to be a printing error; it should read 1500 ppm, not 15 000 ppm.

Silberman and Fisher [30] reported undissolved residues from their dissolution procedure. In their method, up to 1 g of fly ash was dissolved in 10 ml 48% HF in polypropylene volumetric flasks by shaking overnight at room temperature. 80 ml saturated boric acid solution were then added and the flasks shaken for a further 4 hours. Undissolved residues were analysed by instrumental neutron activation analysis

(INAA). The dissolved samples were analyzed by flame and flameless AAS. Results reported for 19 elements including Si, Al, Fe, Ca, Mg, Na, Ti, Mn and Ba in NBS-SRM 1633 (An old fly ash standard, not available any more) were in good agreement with reported values except that Mg and Ba concentrations were lower. Based on the INAA data, better than 95% recovery was observed for all the elements except Ba and Ti, for which the residue contained 12% and 5.9% respectively, of the total elemental contents. The Ti values measured in this work are in good agreement with reported values in NBS-SRM 1633a by methods A and B. Ba values determined by both methods are in good agreement but not enough data is available for proper comparison.

The percentage of residue obtained in dissolving fly ash samples by the two methods were not measured. However, 1 g of NBS-SRM 1633a was shaken overnight with 10 ml 48% HF at room temperature and 5.1% residue was obtained. This is expected to contain insoluble or sparingly soluble fluorides since no boric acid was added. The coal ash sample CA1 yielded 22.2% residue. Silberman and Fisher measured 3.43 and 3.47% of undissolved residues from the NBS-SRM 1633 by their method. It is expected that the amounts of residue will be dependent on the compositions of the ashes which is in turn dependent on the types of coal used and the combustion conditions. It is interesting to note that Silberman and Fisher reported a correlation between the relative masses of undissolved residue and the carbon contents of different fly ash samples. The carbon content of the residues from the NBS-SRM 1633 was 82 $\pm$ 1%. The black residues obtained by the

two dissolution methods is thus most probably unburnt carbon. Unpublished work by Orren and Bacon (1982) supports this conclusion.

In general the data obtained in this work show good agreement with other reported data. A comparison of the elemental concentration in South African fly ash samples PFA 4, PFA 5 and FA 2 indicates very small differences. The coal ash CA1 also shows similar elemental concentrations as the fly ash samples.

The % relative standard deviations for three independent analyses differ from element to element, depending upon the elemental concentrations. Generally they are comparable to deviations of reported data where different analytical techniques are used.

In conclusion, ICP-AES has proved to be a useful technique for the determination of major elements in coal and fly ash. The total analysis time is rather long due to the long sample preparation times.

TABLE 5.4. Method A, analytical data for NBS-SRM 1632a.

| Element | Values, this study | | | | Reported values [25] | | | [54] | | | [73] | | |
|---|---|---|---|---|---|---|---|---|---|---|---|---|---|
| | C | S | R* | N | C | S | R | C | S | R | C | S | R |
| Ca | 0.22% | 0.02 | 8.05 | 2 | 0.23% | 0.03 | 13.04 | 2300 ppm | 100 | 4.35 | 0.23% | 0.02 | 8.70 |
| Mg | 0.10% | 0.01 | 13.22 | 5 | (0.1%) | | | 600 - 1300 ppm | | | 0.13% | 0.03 | 23.08 |
| Ti | 0.16% | 0.01 | 7.14 | 6 | (0.18%) | | | 1650 ppm | 130 | 7.88 | 0.161% | 0.004 | 2.48 |
| Mn | 22.00 ppm | 4.47 | 20.33 | 5 | 28 ppm | 2 | 7.14 | 31 ppm | 2 | 6.45 | 32ppm | 3 | 9.38 |
| Ba | 110 ppm | 14.14 | 12.86 | 2 | - | | | 130 ppm | | | 122ppm | 11 | 9.02 |
| Fe | 1.10% | 0.09 | 8.12 | 6 | 1.11% | 0.02 | 1.8 | 1.13% | 0.03 | 2.65 | 1.16% | 0.03 | 2.59 |
| Al | 2.89% | 0.04 | 1.49 | 2 | (3.1%) | | | 2.97% | 0.04 | 1.35 | 2.94% | 0.13 | 4.42 |
| Si | 5.85% | 0.06 | 0.97 | 2 | - | | | 5.9% | 0.2 | 3.39 | 5.8% | 0.1 | 1.72 |

C : elemental concentrations
S : standard deviations
R : % relative standard deviations
N : number of determinations
* : R calculated from raw data
[25]: NBS values; information values in parenthesis

TABLE 5.5. Method A, analytical data for NBS-SRM 1635.

| Element | Values, this study | | | | Reported values | | | | | | | | |
|---|---|---|---|---|---|---|---|---|---|---|---|---|---|
| | | | | | [25] | | | [54] | | | [73] | | |
| | C | S | R* | N | C | S | R | C | S | R | C | S | R |
| Ca | 0.54% | 0.05 | 9.38 | 2 | - | | | 5600ppm | 200 | 3.57 | 0.55% | 0.02 | 3.64 |
| Mg | 0.092% | 0.01 | 11.06 | 3 | - | | | 980 ppm | | | 0.10% | 0.02 | 20.00 |
| Ti | 0.02% | 0.001 | 5.26 | 3 | (0.02%) | | | 210 ppm | 30 | 14.29 | 0.020% | 0.002 | 10.00 |
| Mn | 20 ppm | | | 3 | 21.4 ppm | 1.5 | 7.01 | 23 ppm | 1 | 4.35 | 22 ppm | 3 | 13.64 |
| Ba | 70 ppm | 14.14 | 20.20 | 2 | | | | 84 ppm | | | 70 ppm | 9 | 12.86 |
| Fe | 0.24% | 0.02 | 7.24 | 4 | 0.239% | 0.005 | 2.09 | 0.24% | 0.03 | 12.50 | 0.23% | 0.01 | 4.35 |
| Al | 0.29% | 0.02 | 5.39 | 3 | (0.32%) | | | 0.32% | 0.02 | 6.25 | 0.30% | 0.03 | 10.00 |
| Si | 0.53% | 0.01 | 2.28 | 3 | - | | | 0.64% | 0.13 | 20.31 | 0.52% | 0.02 | 3.85 |

TABLE 5.6 Method A, Analytical data for C2

| | Values, this study | | | | Reported Values [13] |
|---|---|---|---|---|---|
| | % Oxide | S | R | N | % Oxide |
| CaO | 1.03 | 0.25 | 2.40 | 2 | 1.12 |
| MgO | 0.20 | 0.03 | 15.09 | 4 | 0.17 |
| $TiO_2$ | 0.37 | 0.005 | 1.35 | 4 | 0.33 |
| FeO | 1.01 | 0.04 | 3.62 | 2 | 1.37 |
| $Al_2O_3$ | 7.84 | 0.27 | 3.41 | 3 | 7.91 |
| $SiO_2$ | 11.62 | 0.06 | 0.52 | 2 | 12.71 |

TABLE 5.7 Method A, Analytical data for C12

| | Values, this study | | | | Reported Values [13] |
|---|---|---|---|---|---|
| | % Oxide | S | R | N | % Oxide |
| CaO | 0.10 | 0.01 | 5.98 | 2 | 0.09 |
| MgO | 0.08 | 0.01 | 6.79 | 3 | 0.09 |
| $TiO_2$ | 0.14 | 0.01 | 5.59 | 3 | 0.15 |
| FeO | 0.52 | 0.01 | 2.07 | 3 | 0.53 |
| $Al_2O_3$ | 2.52 | 0.03 | 1.13 | 3 | 2.86 |
| $SiO_2$ | 4.71 | 0.25 | 5.40 | 2 | 5.11 |

TABLE 5.8. Method A, Analytical data for PFA 5.

| | Values, this study | | | | Reported Values [13] |
|---|---|---|---|---|---|
| | % Oxide | S | R | N | % Oxide |
| CaO | 5.17 | 0.09 | 1.82 | 2 | 5.60 |
| MgO | 1.42 | 0.05 | 3.38 | 2 | 1.40 |
| $TiO_2$ | 2.04 | 0.09 | 4.29 | 2 | 2.14 |
| MnO | 0.02 | 0.001 | 4.04 | 2 | 0.03 |
| $Fe_2O_3$ | 2.83 | 0.11 | 4.03 | 2 | 2.96 |
| $Al_2O_3$ | 32.30 | 0.99 | 3.05 | 2 | 34.49 |
| $SiO_2$ | 47.09 | 2.38 | 5.05 | 2 | 49.04 |

TABLE 5.9 Method B, Analytical data for FA2.

| Element | % or otherwise indicated | % oxide |
|---|---|---|
| Ca | 5.57 $\pm$ 0.01 | 7.79 |
| Mg | 0.92 $\pm$ 0.003 | 1.53 |
| Al | 12.68 $\pm$ 0.16 | 23.95 |
| Si | 22.90 $\pm$ 0.17 | 49.00 |
| Fe | 2.21 $\pm$ 0.02 | 3.16 |
| Ti | 0.61 $\pm$ 0.01 | 1.01 |
| Mn | 219.6 ppm $\pm$ 4.8 | 0.03 |
| Na | 0.75 $\pm$ 0.01 | 1.01 |
| P | 0.47 $\pm$ 0.01 | 1.08 |
| Ba | 0.159 $\pm$ 0.002 | |

TABLE 5.10. Method B, Analytical data for CA1.

| Element | % or otherwise indicated | % oxide |
|---|---|---|
| Ca | 4.88 ± 0.01 | 6.83 |
| Mg | 0.89 ± 0.003 | 1.47 |
| Al | 11.23 ± 0.16 | 21.21 |
| Si | 20.54 ± 0.24 | 43.94 |
| Fe | 3.29 ± 0.06 | 4.71 |
| Ti | 0.580 ± 0.011 | 0.98 |
| Mn | 242.4 ppm ± 6.4 | 0.03 |
| Na | 0.703 ± 0.007 | 0.95 |
| P | 0.30 ± 0.01 | 0.67 |
| Ba | 0.120 ± 0.002 | |

TABLE 5.11. Analytical data for NBS-SRM 1633a.

| Element | Values, this study | | | | | | | Reported values | | | | |
|---|---|---|---|---|---|---|---|---|---|---|---|---|
| | Method A | | | | Method B | | | [25] | | | [54] | [73] |
| | C | S | R | N | C | S | N | C | S | R | C | C (%) |
| Ca | 1.13% | 0.02 | 1.43 | 2 | 1.19% | 0.03 | 3 | 1.11% | 0.01 | 0.90 | 12900 ppm | 1.11 |
| Mg | 0.44% | 0.05 | 11.07 | 3 | 0.45% | 0.01 | 3 | 0.455% | 0.010 | 2.20 | | 0.46 |
| Ti | 0.80% | 0.05 | 5.84 | 3 | 0.75% | 0.01 | 3 | (0.8%) | | | 8400 ppm | 0.8 |
| Mn | 160 ppm | 10 | 6.25 | 3 | 188.7 ppm | 4.0 | 3 | (190 ppm) | | | 190 ppm | - |
| Ba | 0.12% | 0.001 | 0.57 | 2 | 0.124% | 0.008 | 3 | (0.15%) | | | - | - |
| Fe | 9.12% | 0.07 | 0.78 | 2 | 9.27% | 0.12 | 3 | 9.40% | 0.10 | 1.06 | 9.7% | 9.37 |
| Al | 13.95% | 0.03 | 0.22 | 2 | 14.02% | 0.12 | 3 | (14%) | | | 14.0% | 14.00 |
| Si | 22.69% | 0.27 | 1.21 | 2 | 22.60% | 0.23 | 3 | 22.8% | 0.8 | 3.51 | 22.2% | 22.81 |
| P | - | | | | 0.24% | 0.01 | 3 | - | | | 15000 ppm | 0.20 |
| Na | - | | | | 0.197% | 0.004 | 3 | 0.17% | 0.01 | 5.88 | 2100 ppm | - |

TABLE 5.12 Analytical data for PFA 4

| | VALUES, THIS STUDY | | | | | | | Reported values [13] |
|---|---|---|---|---|---|---|---|---|
| | Method A | | | | Method B | | | |
| | % Oxide | S | R | N | % oxide | S | N | % oxide |
| CaO | 5.46 | 0.29 | 5.23 | 3 | 5.73 | 0.02 | 2 | 5.59 |
| MgO | 1.41 | 0.04 | 2.67 | 3 | 1.31 | 0.01 | 2 | 1.33 |
| $TiO_2$ | 1.92 | 0.15 | 7.73 | 3 | 1.63 | 0.02 | 2 | 1.95 |
| MnO | 0.02 | 0.001 | 6.25 | 3 | 0.025 | 0.001 | 2 | 0.02 |
| Ba | 990 ppm | | | 1 | 1047 ppm | 19 | 2 | 1030 ppm |
| $Fe_2O_3$ | 2.86 | 0.06 | 1.95 | 3 | 2.84 | 0.07 | 2 | 2.94 |
| $Al_2O_3$ | 32.18 | 1.15 | 3.56 | 2 | 31.67 | 0.45 | 2 | 32.40 |
| $SiO_2$ | 50.21 | 0.15 | 0.29 | 2 | 45.61 | 0.27 | 2 | 51.14 |
| $P_2O_5$ | - | | | | 0.57 | 0.01 | 2 | 0.40 |
| $Na_2O$ | - | | | | 0.95 | 0.01 | 2 | 1.11 |

# CHAPTER 6. ANALYSIS OF METALLURGICAL SAMPLES BY ICP-AES

In metallurgical studies and applications of alloys, elemental ratios are the most critical parameters. The concentration of an alloying element will determine the chemical and physical properties of the alloy. Thus it is important to accurately analyse alloys for their major and minor components.

This part of the work describes the analysis of four brass samples and a "special steel" sample.

## 6.1 Brass analysis

The following analysis arose from metallurgical studies of four brass samples which showed different characteristics from those expected.

About 0.5 g of four brass samples (MC 306, MC 101, NFM 7030, 70/30), in the form of drillings, were dissolved in 5 ml concentrated nitric acid. No undissolved residues were obtained.

Three spectral lines for copper and zinc and one line for lead were chosen for the analysis. The instrumental parameters were optimized and interferences on each spectral line checked by aspirating standard solutions containing other elements present in the brass samples, ie Cu, Zn and Pb. No background interference was experienced. A 100 ppm Cu standard showed a small spectral interference on the 202.55 nm Zn spectral line due to Cu I emission at

202.434 nm. Each element was determined using three separate programmes. The parameters are shown in table 6.1. Each analysis using one spectral line is a mean of five readings, each of five seconds for copper and zinc, and 10 seconds for lead. The results obtained are shown in tables 6.2, 6.3 and 6.4.

TABLE 6.1. Instrumental parameters.

| Programme | Element | Spectral line (nm) | Sample flow rate (ml/min) | Observation height (mm) |
|---|---|---|---|---|
| 1 | Cu | 324.75 | 1 | 18 |
| | | 224.70 | - | 18 |
| | | 327.40 | - | 18 |
| 2 | Zn | 213.86 | - | 18 |
| | | 202.55 | - | 16 |
| | | 206.20 | - | 16 |
| 3 | Pb | 283.31 | 1.5 | 14 |

(The nebulizer driving pressure was kept at 30 psi and the torch power was 3).

Table 6.2 Copper determination.

| Sample | Spectral line (nm) | Measured conc (ppm) | SD | %RSD | Mean conc. corr. for sample masses (%) |
|---|---|---|---|---|---|
| MC306 | 324.75 | 61.00 | 0.221 | 0.36 | |
| | 224.70 | 61.33 | 0.223 | 0.36 | 60.52 ± 0.42 |
| | 327.40 | 61.42 | 0.279 | 0.45 | |
| MC101 | 324.75 | 62.56 | 0.139 | 0.22 | |
| | 224.70 | 62.64 | 0.242 | 0.38 | 62.77 ± 0.30 |
| | 327.40 | 62.72 | 0.106 | 0.16 | |
| NFM70/30 | 324.75 | 75.07 | 0.251 | 0.33 | |
| | 224.70 | 75.07 | 0.207 | 0.27 | 72.30 ± 0.39 |
| | 327.40 | 74.14 | 0.233 | 0.31 | |
| 70/30 | 324.75 | 71.96 | 0.319 | 0.44 | |
| | 224.70 | 71.95 | 0.202 | 0.28 | 71.80 ± 0.44 |
| | 327.40 | 71.93 | 0.219 | 0.30 | |

Table 6.3 Zinc determination.

| Sample | Spectral line (nm) | Measured conc (ppm) | SD | %RSD | Mean conc.* corr. for sample masses (%) |
|---|---|---|---|---|---|
| MC306 | 213.86 | 38.89 | 0.061 | 0.15 | |
| | 202.55 | 39.57 | 0.039 | 0.09 | 38.68 ± 0.07 |
| | 206.20 | 38.97 | 0.039 | 0.10 | |
| MC101 | 213.86 | 35.57 | 0.027 | 0.07 | |
| | 202.55 | 36.11 | 0.046 | 0.12 | 35.68 ± 0.09 |
| | 206.20 | 35.65 | 0.086 | 0.24 | |
| NFM70/30 | 213.66 | 29.75 | 0.039 | 0.13 | |
| | 202.55 | 30.51 | 0.043 | 0.14 | 28.75 ± 0.07 |
| | 206.20 | 29.71 | 0.055 | 0.18 | |
| 70/30 | 213.86 | 29.81 | 0.089 | 0.29 | |
| | 202.55 | 30.33 | 0.082 | 0.27 | 29.82 ± 0.10 |
| | 206.20 | 29.94 | 0.042 | 0.14 | |

* mean obtained using only results from the two spectral lines : 213.86 and 206.20 nm.

Table 6.4 Lead determination.

| Sample | Measured conc. | | | Conc. corr. for sample masses (%) |
|---|---|---|---|---|
| | ppm | SD | %RSD | |
| MC306 | 3.127 | 0.014 | 0.44 | 3.09 ± 0.01 |
| MC101 | 3.073 | 0.012 | 0.39 | 3.08 ± 0.03 |
| NFM 70/30 | ND | | | |
| 70/30 | ND | | | |

Good agreement between results obtained from the three copper lines is noted (table 6.2) definitely showing that there was no interference. In the case of zinc, agreement between results from the two lines 213.86 and 206.20 nm is excellent. However, an average increase of 0.6 ppm is obtained when using the 202.55 nm line. This was expected from the observation of a small peak when aspirating a copper solution at this wavelength.

Very little lead was present in samples NFM 70/30 and 70/30. No effort was made to quantify the concentrations since its significance was not important for this particular metallurgical study. The data was required to check the Cu to Zn ratios and compare them with the suppliers' specifications since microstructure analysis indicated some characteristics of a different composition to that specified. For example sample 306, supposed to contain 70% Cu and 30% Zn, was found to contain about 60% Cu and 40% Zn. Lead was determined to justify the presence of "dark spots" present in the microstructures. ICP-AES is thus found to be a useful technique for rapid analysis of brasses.

## 6.2 Steel analysis

An unknown "steel" was analysed for the elements listed below. Unlike brass samples which are easily dissolved, steels containing tungsten and other alloying elements are often difficult to dissolve. Several acids and mixtures of acids such as conc $HNO_3$, HCl, $HClO_4$ and $H_2O_2$ were tried without much success. The sample could not be heated in an open container (Teflon beaker) with HF since silicon is normally lost during this process. About 0.01 g of steel was dissolved in "Parr" bombs using a mixture of concentrated $HNO_3$ and 48% HF (2 ml 1:1). No residues were obtained after heating for 3 hours at 130°C.

Two mixed standards were prepared, the first one containing Ni, Co, Mo and V and the second containing Fe, Cr, Ti, Si, Mn and P. W was determined separately because of the problems involved in preparing a stable standard solution. When solutions of tungstates are made weakly acidic, polymeric anions are formed but from more strongly acid solutions, insoluble tungstic acid is obtained. A 1000 ppm stock solution was prepared as described in **appendix 1.**

The spectral lines used and the results obtained are listed in table 6.5. The values are mean of two separate analyses. With the samples as prepared above, very poor precision was obtained for silicon determination. The problem was traced to silicon being leached from the injector tube by hydrofluoric acid, thus leading to higher silicon concentrations. The addition of boric acid and TX-100 to both samples and standards eliminated the problem. The precision for five

determinations was 0.31%.

The main components of the alloy were established to be Co, Cr and W which explains the difficulties encountered in dissolving the sample. The total % was 99.84. A small amount of carbon and other minor and trace elements are usually present.

Table 6.5 Analytical results

| Element | Spectral line used (nm) | Concentration (%) |
|---|---|---|
| Ni | 232.00 | 1.79 |
| Co | 228.61 | 52.46 |
| Mo | 202.02 | 0.03 |
| V | 310.23 | 0.01 |
| Fe | 238.20 | 2.43 |
| Cr | 205.55 | 24.57 |
| Ti | 336.12 | 0.01 |
| W | 207.91 | 10.24 |
| Si | 288.16 | 7.8 |
| Mn | 293.93 | 0.37 |
| P | 213.62 | 0.13 |

In conclusion, ICP-AES is well suited for metallurgical samples, once the sample preparation procedure is established and the analytical programme developed. Multielement programmes can be used and the analysis is fast. A well characterized standard can be used for calibrating the instrument.

# CHAPTER 7. DETERMINATION OF BORON BY ICP-AES

Boron is an essential element in plant metabolism. However, many plants can only tolerate a very narrow range of boron concentrations in the soil [64]. Boron is concentrated in the ashes during combustion of coal. Leaching of this element from coal fly ash dumps by rain could pose a potential hazard to agriculture. Detailed studies of boron levels in environmental materials have in the past been hampered by the lack of fast, simple, sensitive and precise analytical techniques capable of determining boron concentrations at low levels. Methods for the determination of boron have been reviewed [65] and recently ICP-AES has been included [50, 66].

The procedure presented here is a typical example of a step-by-step method development for determining low concentrations of an element in a complex sample matrix.

Boron has one of the simplest of atomic spectra. It is a light element with a relatively high ionization potential and, therefore, exhibits only a few neutral atom lines in the excitation environment of the ICP. The following doublet lines are useful for boron determination:

| | |
|---|---|
| 249.77 nm<br>249.68 nm | 1 |
| 208.96 nm<br>208.89 nm | 2 |
| 182.64 nm<br>182.59 nm | 3 |

The third doublet cannot be used with the IL Plasma-100 since

it lies below the lower optical cut-off of the system. Both doublets 1 and 2 are well resolved and can be used for analysis. They are shown in figure 7.1. From the figure it is observed that the sensitivities decrease at lower wavelengths.

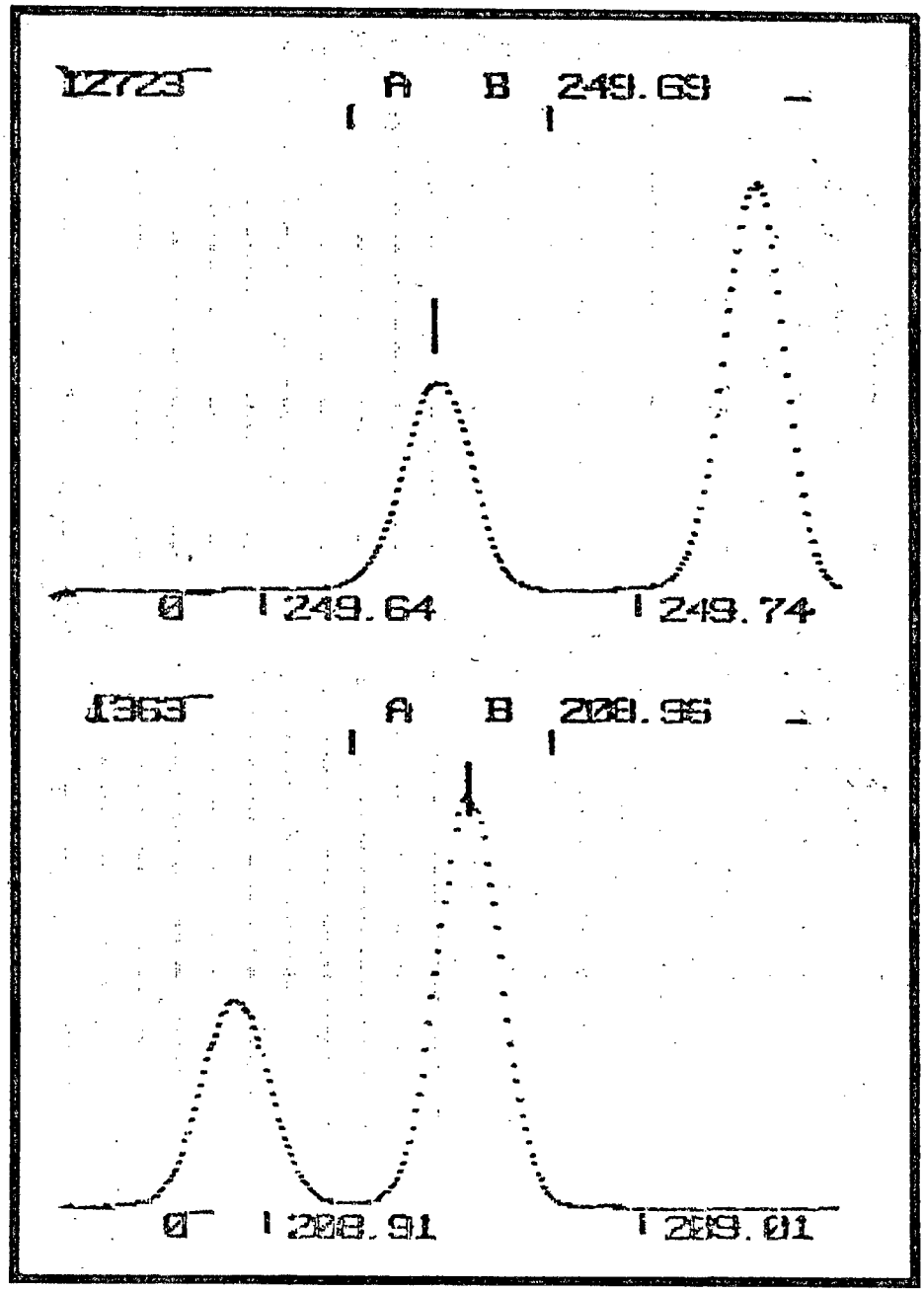


Figure 7.1 Boron doublets 1 and 2
(10 ppm B solution)

Optimum conditions were obtained for the four lines of the two doublets by using the RESTPEAK-PLOT routine to study the analyte peaks and intensities while adjusting different parameters, mainly the torch power and the nebulizer driving pressure. Optimization was done using an aqueous solution of boron, prepared by dissolving high purity boric acid (Aristar, BDH) in water. After changing a parameter, at least one minute stabilization time was allowed before obtaining a plot.

Figure 7.2 shows plots of the peak at 249.78 nm when the torch power (PWR) is changed, keeping the nebulizer driving pressure constant at 30 psi and a fixed observation height. A background shift is seen to occur. However, the line to background ratio increases more rapidly with increasing power.

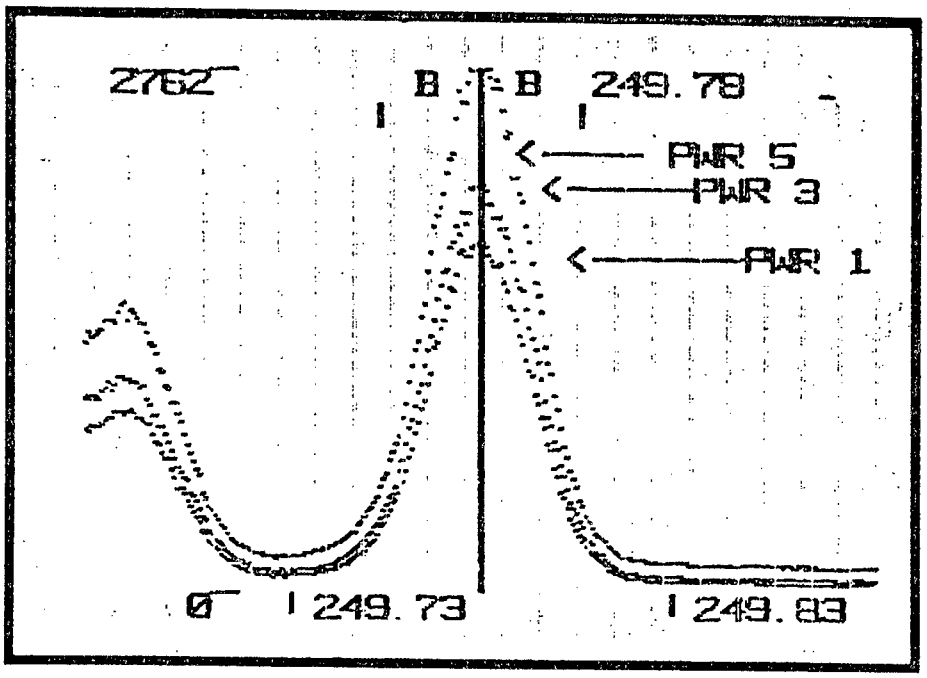


Figure 7.2 Effect of changing the torch power.

Figure 7.3 is a similar plot where the torch power is kept constant (3 PWR) and the nebulizer driving pressure is varied. Background shift is also observed but at 30 psi higher intensities are obtained.

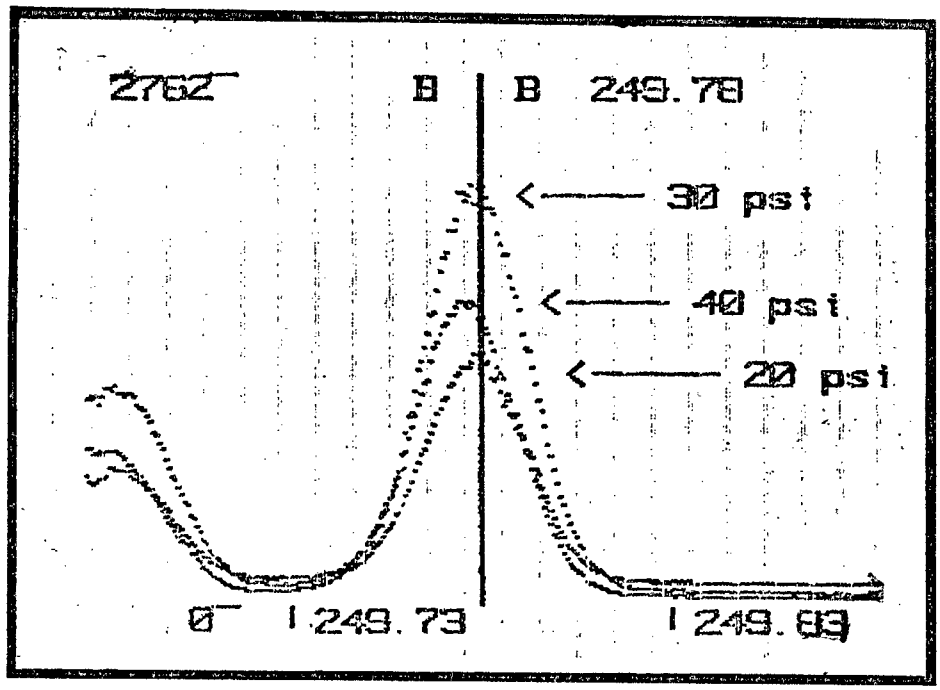


Figure 7.3 Effect of changing the nebulizer driving pressure

Figures 7.4 and 7.5 show TPLOTS when the torch power and nebulizer driving pressure are changed. Shifting of the optimum observation height when the pressure is increased is noted in figure 7.5. This occurs because high pressures cause the plasma "fire-ball" to rise in the torch.

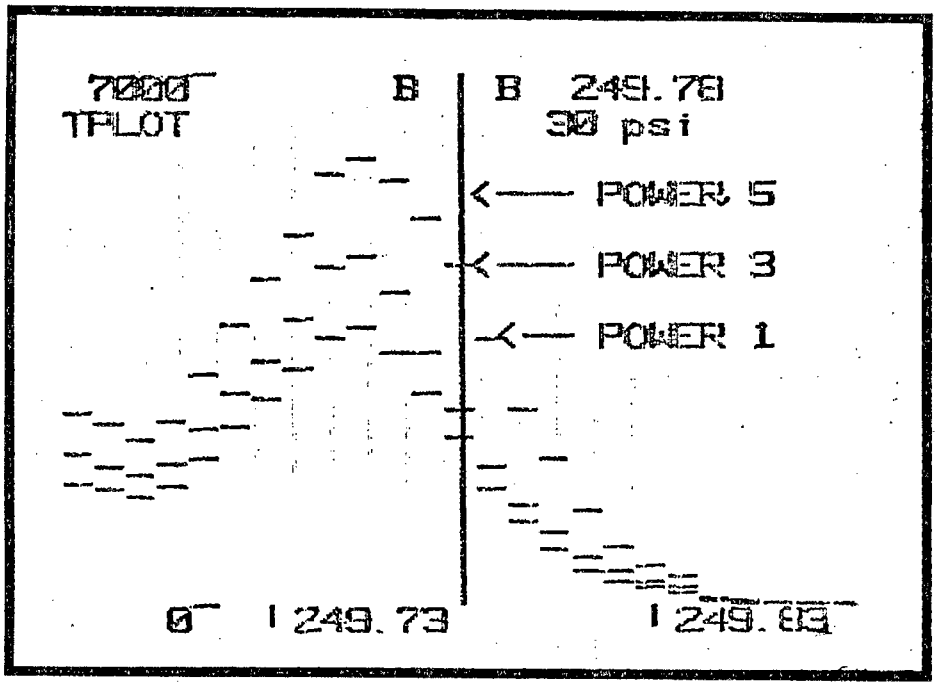


Figure 7.4 Effect of power changes on TPROFILE.

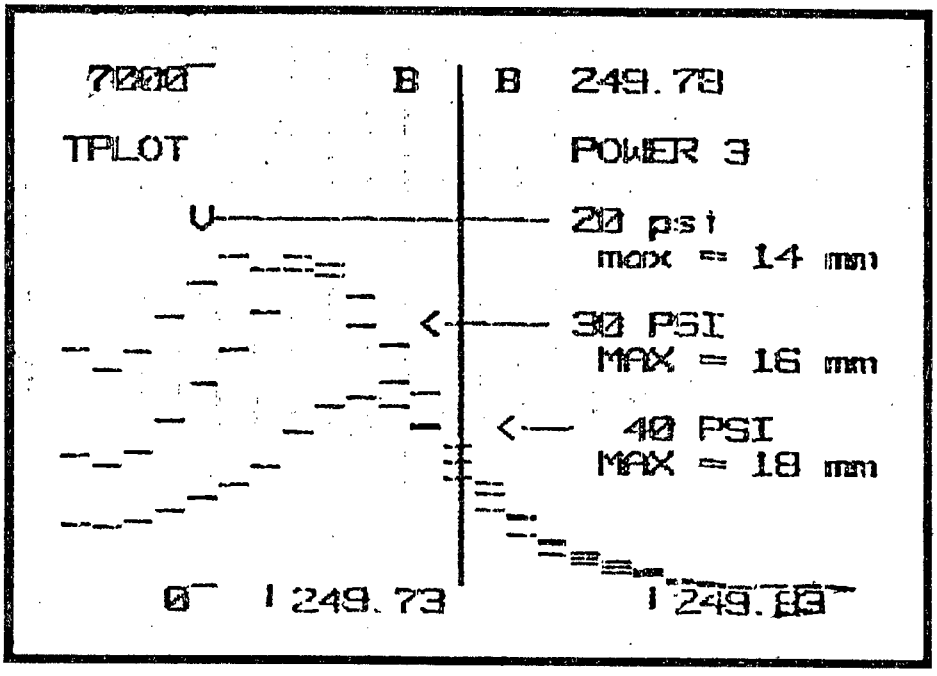


Figure 7.5 Effect of nebulizer pressure changes on TPROFILE

IPLOTS were obtained by varying the nebulizer pressure and the torch power to obtain optimum stability of the intensity signal leading to better analytical precision. Figure 7.6 shows that at 40 psi the signal is more stable. Similar trends were observed for the other doublet.

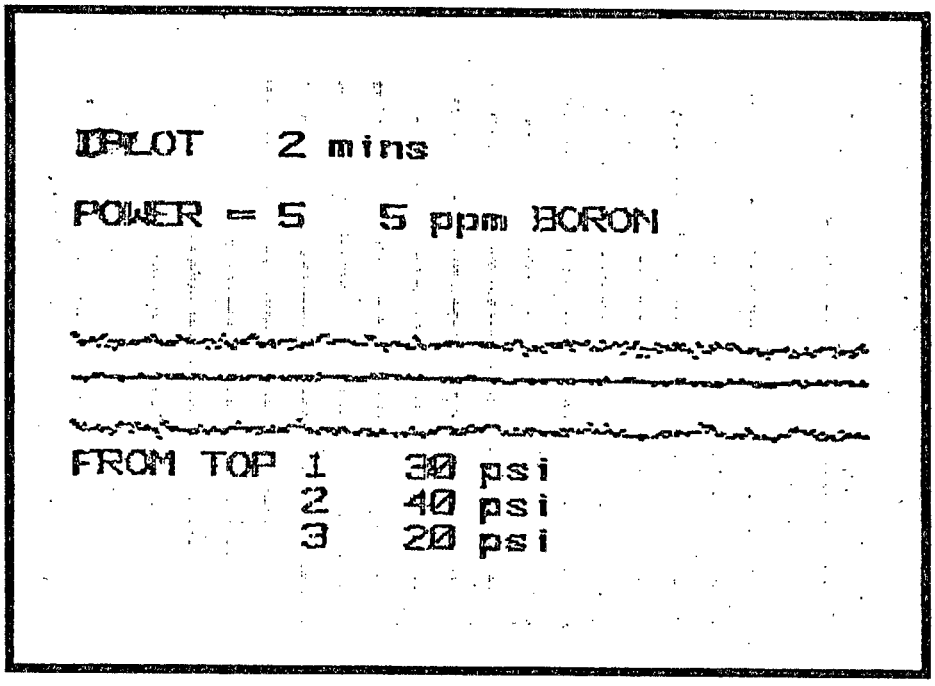


**Figure 7.6** Effect of nebulizer pressure on signal stability.

Considering all the above observations, the following parameters were considered to be optimum for the determination of boron in aqueous solutions:

| | |
|---|---|
| Power | = 5 |
| Nebulizer driving pressure | = 40 psi |
| Viewing height | = 12 mm |

A "multiline" programme was used to calculate spectral characteristics of the four lines. The instrument was

calibrated using a water blank and a 10 ppm boron standard (with 0.05% TX-100). The calculations were done using intensity values for 10 readings, each of five seconds.

The results are presented in table 7.1 below.

Some reported values by Winge et al (45) are also listed for comparison. Whilst the $C_L$ values show good agreement, the $I_N/I_B$ values obtained are lower than those reported. An experiment was done to measure the background intensity near the 249.77 nm line by shifting the window to about 0.1 nm on the high wavelength side of the boron peak and measuring the intensity when a water blank was aspirated. (Note: when water is not aspirated the background emission is affected due to entrainment of air and/or because the plasma is not "cooled").

The $I_N/I_B$ value was calculated to be 58.7 which is in closer agreement with the value reported. This difference is due to the high blank values obtained for boron. The $C_L$ and $I_N/I_B$ values will vary from one instrument to the next and with the instrumental parameters used. The type of sample analysed has a marked effect on those values especially in complicated matrices containing high concentrations of dissolved salts, eg boric acid and sodium chloride, due to loss in nebulization efficiency leading to noisy signals and poor precisions.

TABLE 7.1. Spectral characteristics of boron lines.

| Line (nm) | This work | | | Reported values [45] | |
|---|---|---|---|---|---|
| | $S_{ICP}$ ($ppm^{-1}$) | $C_L$ (ppm) | $I_N/I_B$ (10 ppm) | $C_L$ (ppm) | $I_N/I_B$ (10 ppm) |
| 249.77 | 113.2 | 0.005 | 40.8 | 0.0048 | 63.0 |
| 249.68 | 56.6 | 0.007 | 29.6 | 0.0057 | 53.0 |
| 208.96 | 12.4 | 0.009 | 25.9 | 0.010 | 30.0 |
| 208.89 | 6.3 | 0.012 | 14.1 | 0.012 | 25.0 |

After completing the work presented in chapter 5, high blank intensities were obtained at the boron wavelength. The problem was traced to memory effects in the nebulizer-torch system following the aspiration of high boric acid concentrations (up to 5% w/v). On removing the torch and nebulizer from the instrument, it was noticed that a white deposit had formed at the tip of the sample capillary tube of the torch. The whole nebulizer torch system was washed thoroughly with water and soaked in a 5% v/v Contrad solution for one day and subsequent analysis showed a reduction of the blank levels. A further soaking for 2 days helped to obtain an acceptable blank level. Aspirating a solution of hydrofluoric acid (5%) for about 15 mins in the hope of complexing the boric acid or any other form of the boron from the nebulizer or torch system had no effect on the blank level. The exact mechanism of this memory effect is not known. Memory effects in the ICP introduction system have been reported in the literature, for example Ti, Mo and W in certain media are adsorbed on the walls of the sample introduction system [63].

An experiment was carried out to study the stability of a concentration calibration curve used for ICP analysis. The multielement programme shown in figure 7.7 was used after 20 minutes of plasma stabilization. The instrument was calibrated with standard solutions containing 10 ppm of the analytes. The calibration procedure proceeded in the following order : measurement of the highest standard followed by the blank (water) and other standards. The washing time (PDLY) between calibration measurements was first set to 30 seconds. A 1 ppm standard was analysed just

after calibration and 20 analyses each of 3 readings for 3 seconds were done. The results obtained are illustrated in figure 7.8.

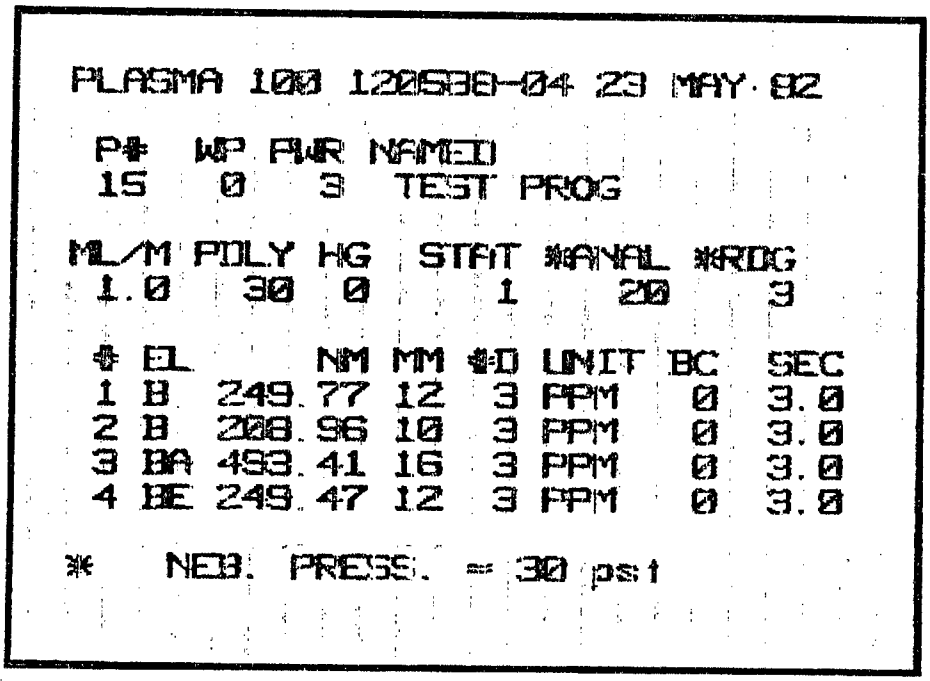


Figure 7.7 Test programme for concentration calibration curve stability.

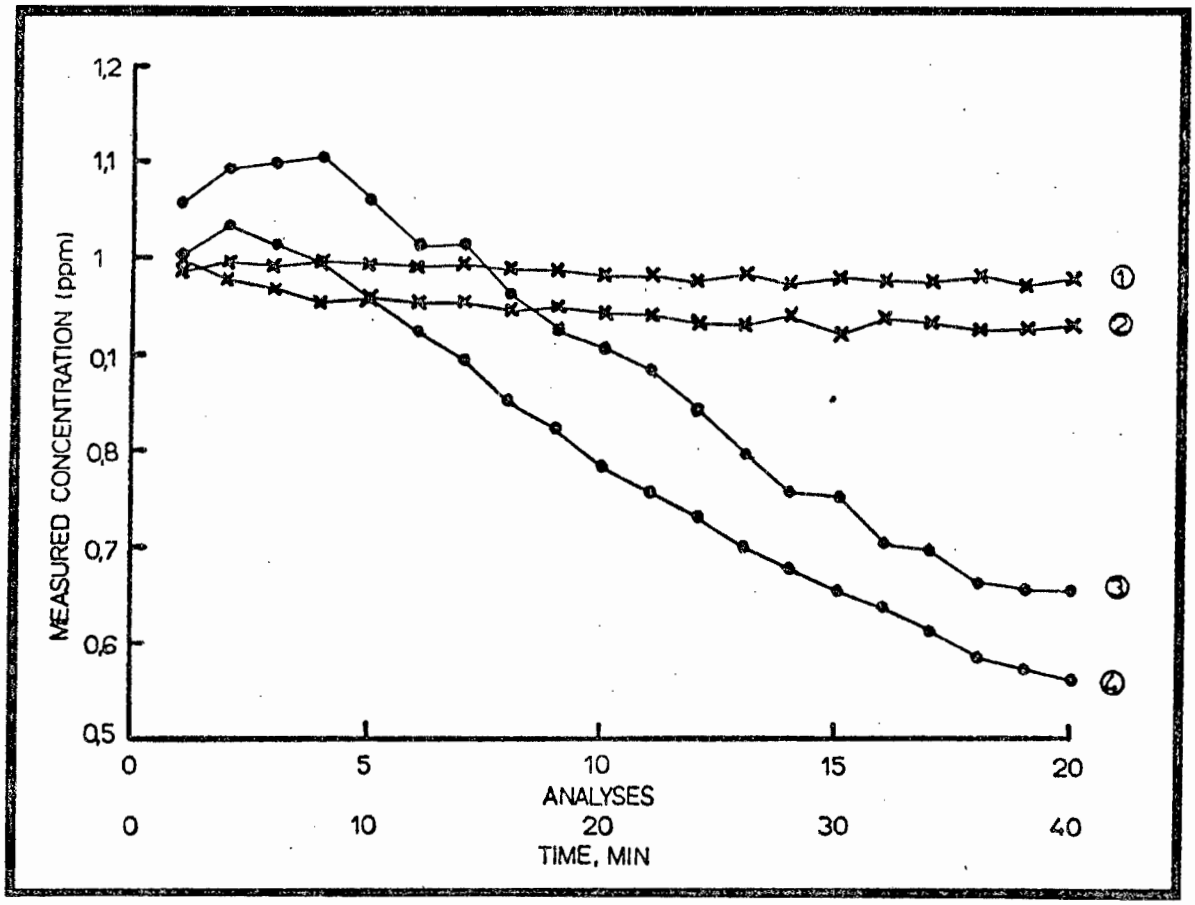


Figure 7.8. Stability of conc. calibration curve

| | | | |
|---|---|---|---|
| 1 | Be | 249.47 | nm |
| 2 | Ba | 493.42 | nm |
| 3 | B | 208.96 | nm |
| 4 | B | 249.77 | nm |

The Ba and Be analysis showed reasonable stability. However, the measured concentration of boron (both lines) is seen to decrease with time after a sharp increase. This underlines the serious memory effect experienced with boron. Since the washing time was short (30 sec) the blank intensity measured during the calibration procedure was higher due to boron still remaining in the system. During the first few analyses the apparent concentration increases slightly and with time and with further washing the relative intensity of 1 ppm solution decreases.

The experiment was carried out using standard solutions prepared in 0.05% TX-100 and the washing time was increased

to 60 seconds. The results are shown in figure 7.9. A small drift for all the lines is noticed and after 40 minutes of analysis the barium concentration had dropped by about 8%. This emphasises the necessity for frequent recalibration. Calibration change is often associated with background drift and this is shown in figure 7.10. The background intensity was monitored at about 0.1 nm from the centre of the 249.77 nm boron line.

The use of an "alternating blank routine" has been described by Larson et al [68]. The average concentrations for the blank analysed before and after each sample are subtracted from the measured concentration of the sample. The advantages of this procedure are:

1. Reduction of errors due to memory or carry over from previous samples.

2. Reduction of errors due to background drift.

3. Reduction of the importance of the calibration blank.

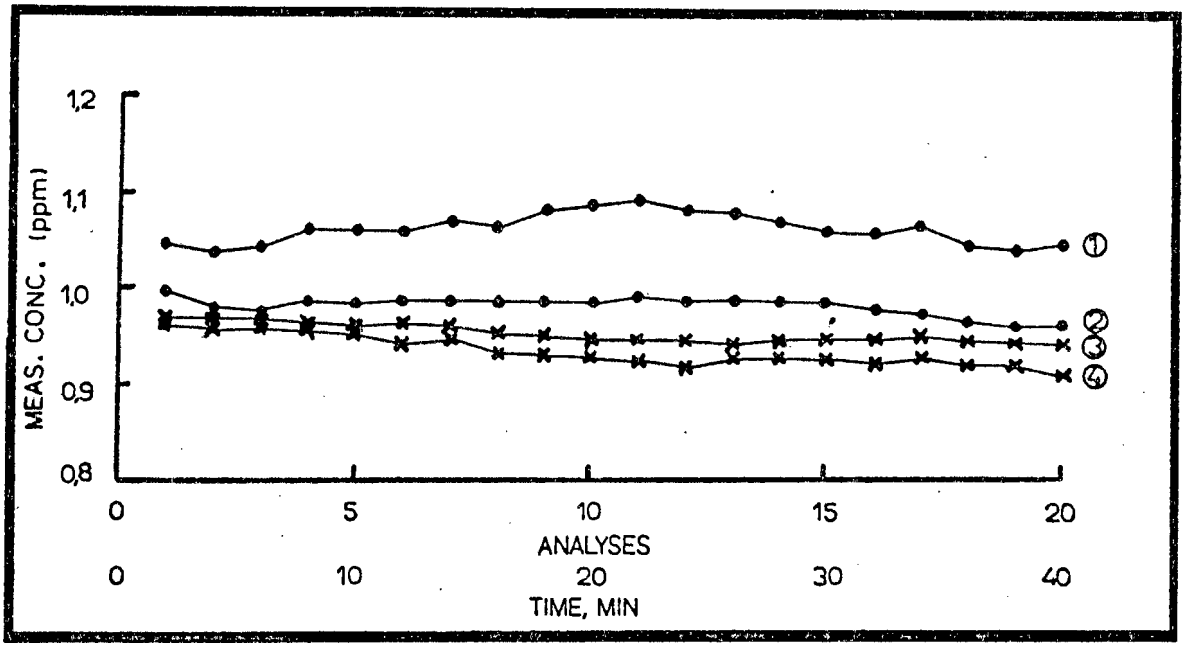


Figure 7.9 Stability of conc. calibration curve

| | | | |
|---|---|---|---|
| 1 | B | 208.96 | nm |
| 2 | B | 249.77 | nm |
| 3 | Be | 249.47 | nm |
| 4 | Ba | 493.41 | nm |

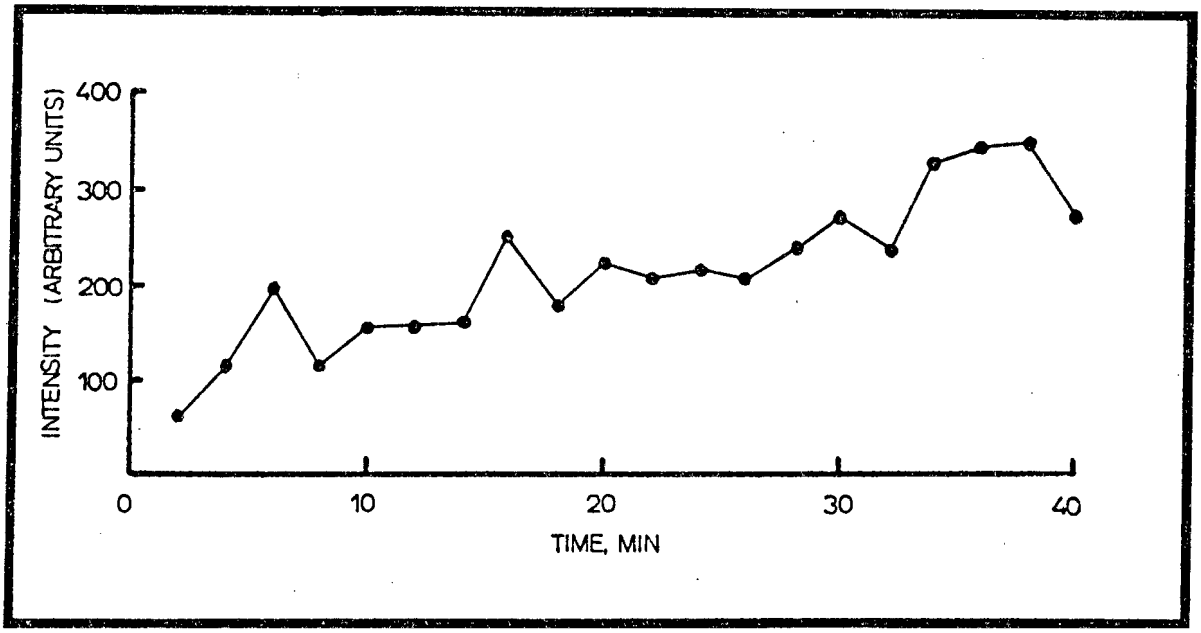


Figure 7.10 Background drift near B 249.77 nm line.

Analytical programmes have been developed for the analysis of trace amounts of boron in various samples (see below). A careful investigation of possible interferences from the matrices under study was done.

From table 7.1, the 249.77 nm line is shown to offer the best characteristics for trace analysis. However, serious spectral interference by iron is experienced at this wavelength [74]. Iron has a very complex and intense spectrum within this region. A wavelength scan near the B spectral line is shown in figure 7.11. Spectral overlap and background interference is noted. The magnitude and linearity of this interference by Fe was investigated by analysing a series of Fe standards containing 1000, 600, 400, 200 ppm in water. The interference effect was found to be linear over this range (see figure 7.12). A correction factor (CF) was calculated using:

$$CF = \frac{\text{Measured conc. (ppm) at B wavelength}}{\text{conc. of iron (ppm)}}$$

$$= 0.0012$$

When B is determined at this wavelength the Fe concentration in the sample $[Fe]_{sample}$ is measured using a programme line for Fe and the correction applied to the measured boron concentration:

ie, corrected [B] = measured [B] - CF x $[FE]_{sample}$.

The CF value was found to vary slightly ($0.0012 \pm 0.0002$) from day to day and with variation of other parameters, eg observation height, torch power and the use of the background

corrector. It is thus recommended that the correction factor be determined before analysis once the plasma is stabilized and other parameters chosen, in order that proper corrections are applied. The effect of 1000 ppm Fe on 1 ppm B at 208.96 nm could not be seen.

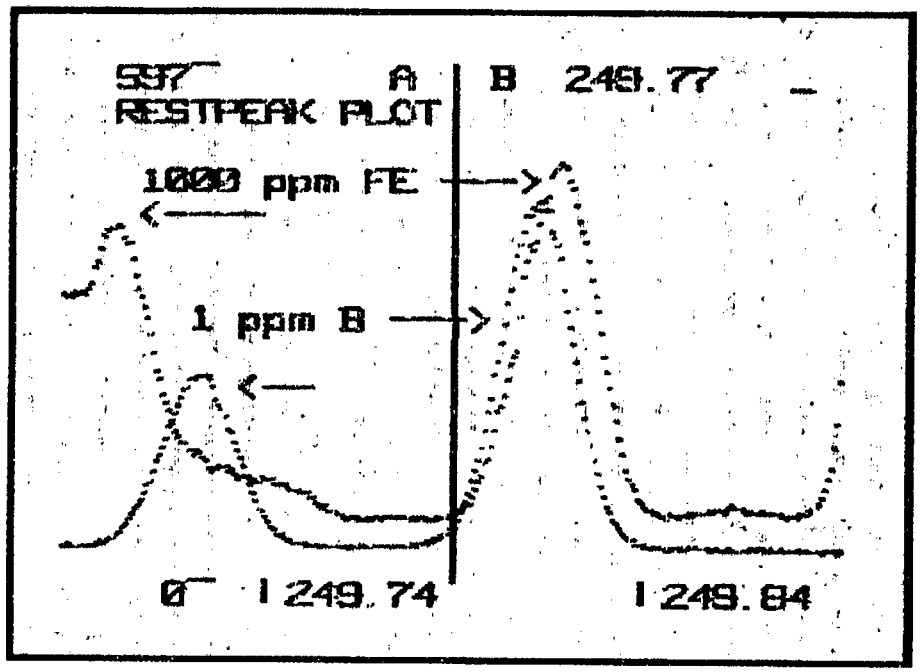


Figure 7.11 Interference by iron

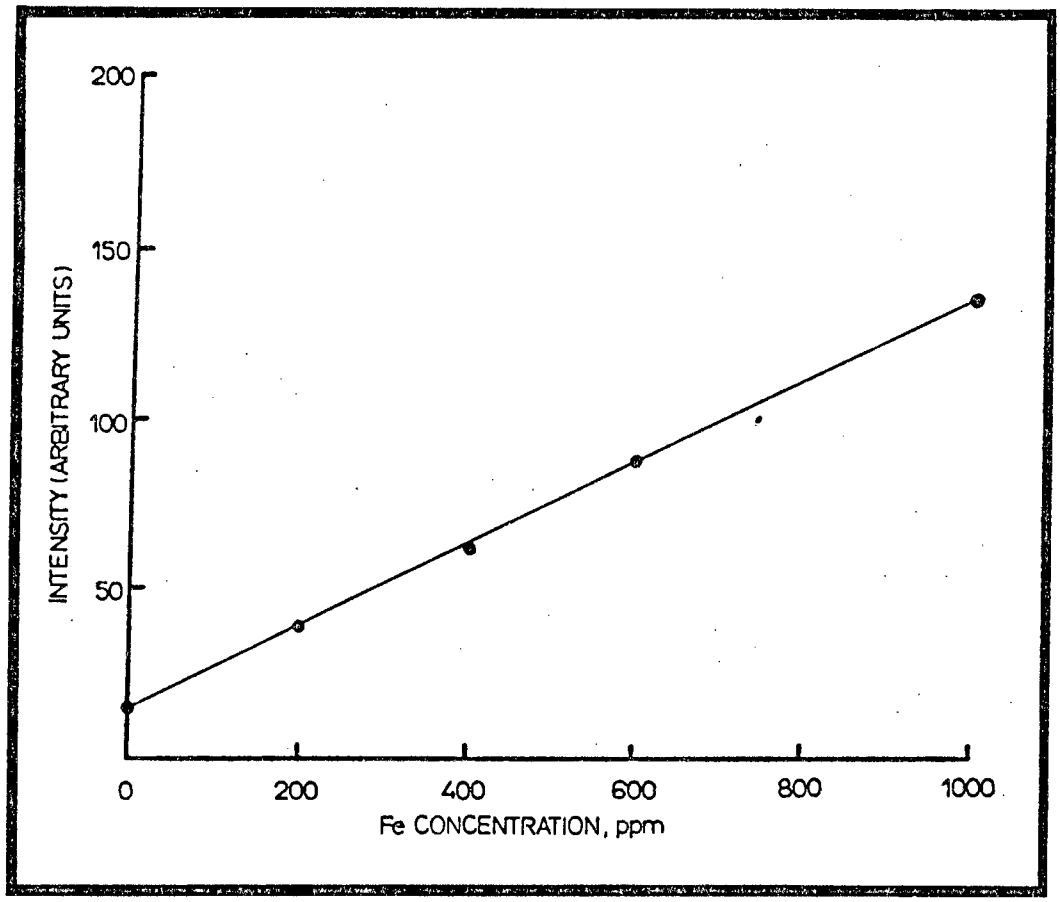


Figure 7.12 Calibration curve for Fe emission at 249.77 nm

The Fe spectral line at 233.28 nm is used for measuring the Fe concentration in the samples because of its reduced sensitivity compared with other lines and its linearity at levels up to 1000 ppm ($C_L$ = 0.02 ppm).

Serious spectral interference by Mo was noted on both B doublets (figures 7.13 and 7.14). The correction factor for Mo on B at 208.96 nm was calculated to be 0.0121. However, in coal and fly ash, Mo is present at trace levels (usually less than 20 ppm), thus it is not a serious interferent in these analyses.

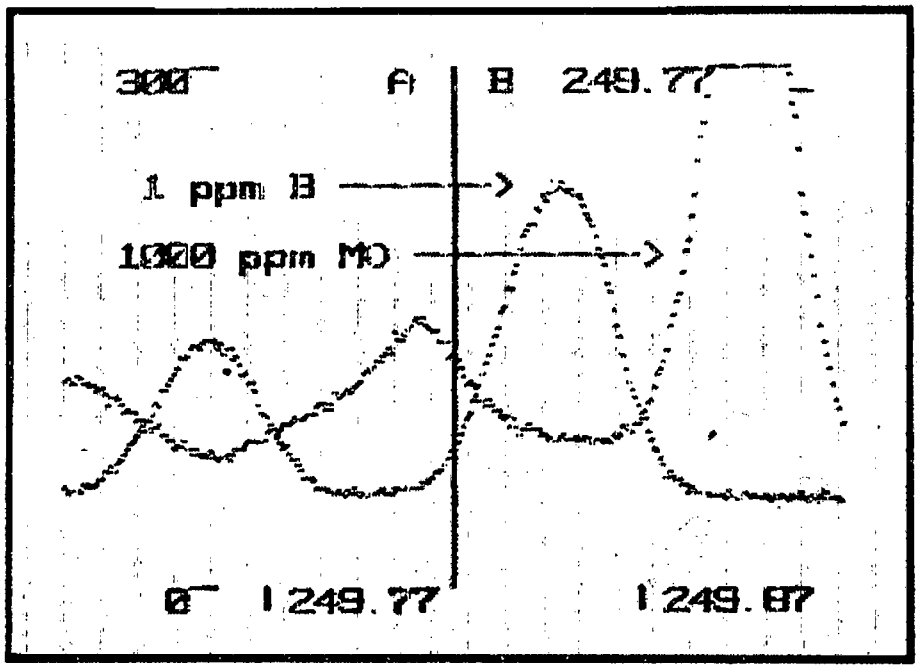


Figure 7.13 Interference by Mo at 249.77 nm.

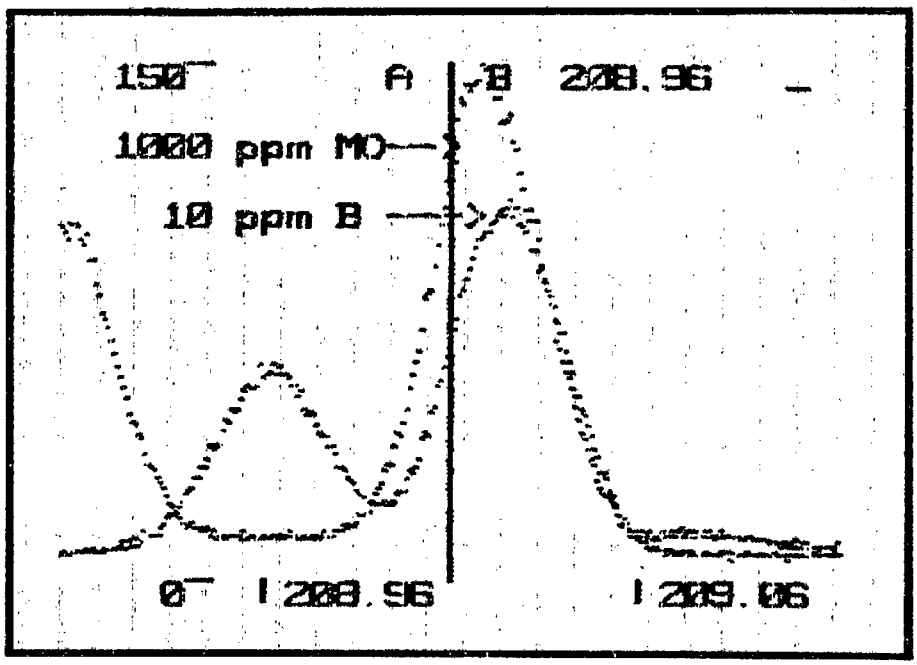


Figure 7.14 Interference by Mo at 208.96 nm.

Aluminium was found to cause background interference near 208.96 nm. This is shown in figure 7.15. In this case the background correction routine must be used by observing regions about 0.05 nm on one side or both sides of the peak depending on the sample background emission near the analyte

peak. In the case of high Fe concentration, the background was similarly corrected for at the 249.77 nm line.

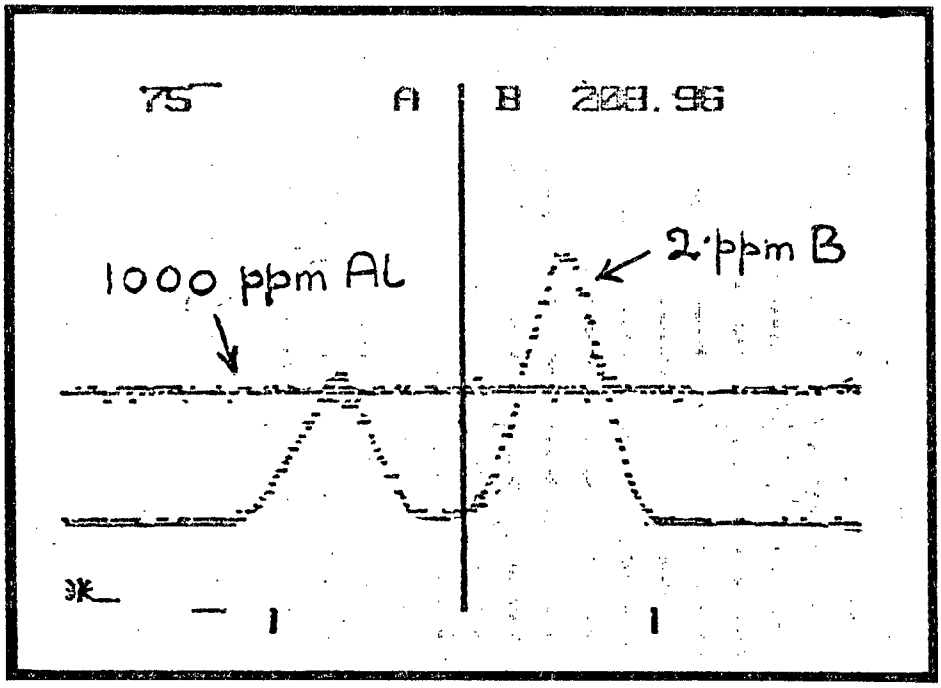


Figure 7.15 Background interference by Al.

High concentrations of other elements normally found in coal and fly ash were also investigated. No other interferences were noted.

## 7.1 Analysis of coal and fly ash

The aim of this study was to determine the boron concentration of coal and ash samples from different locations in South Africa. The samples were supplied by Dr Kruger of the Co-operative Scientific Programme Group, Council for Scientific and Industrial Research, South Africa, as finely ground powders.

Because boron is present at trace levels in these samples, a sample preparation method similar to the one used for major element analysis (method B) was used to obtain higher concentrations in the prepared samples than obtainable by the Parr

bomb method where the amount of sample used is limited to about 0.05 g.

Sample preparation

About 0.5 g dry sample aliquots were placed in polypropylene flasks and 5 ml concentrated $HNO_3$, 10 ml of water and 10 ml HF (48%) were added. The flasks were sealed and shaken gently in a water bath at 70°C for about 15 hours. After cooling 25 ml of water and 2 ml of 1% TX-100 were added and the flasks shaken for a few minutes. The samples were filtered before analysis through Whatman filter paper (No 541, ashless hardened). Blanks were prepared in the same way. The working standards were prepared by spiking the blank solutions with 1000 ppm B standard solutions. The calibration of the spectrometer was done using 5, 2, 0.5 ppm standards and a blank.

The 208.96 nm line was used and each analysis was a mean of two readings for 6 seconds. A two point background correction programme was used. The blank was analysed between each sample to monitor drift. Recalibration was done after 10 determinations. The NBS-SRM 1633a, 1632a and 1635 were analysed to test the accuracy of the method. Two wavelength scans of samples and a B standard are shown in figures 7.16 and 7.17. The background correction positions are also shown in figure 7.17.

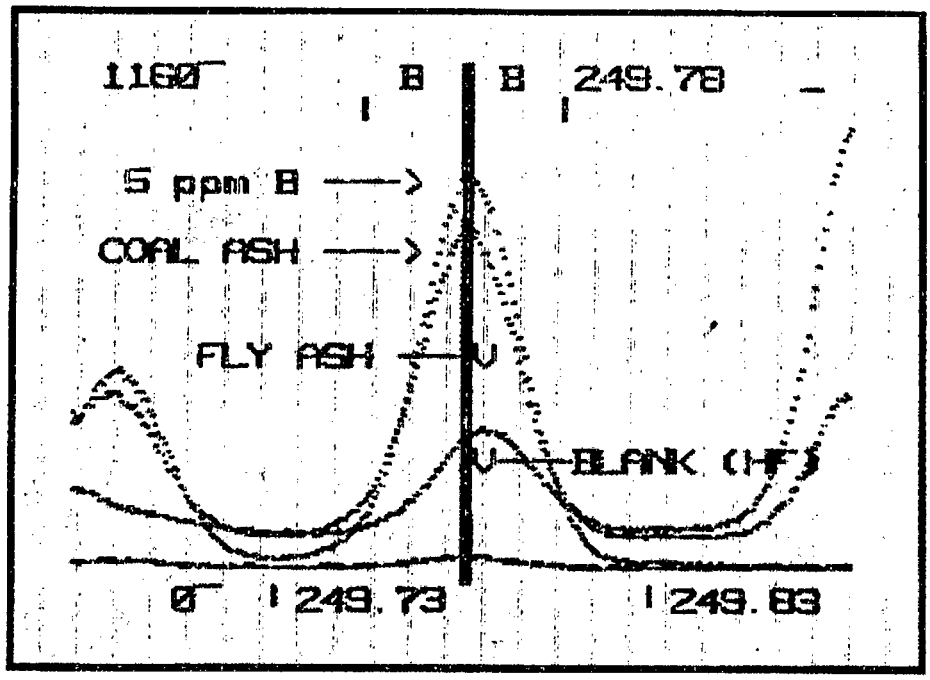


Figure 7.16 Wavelength scan for sample at 249.77 nm.

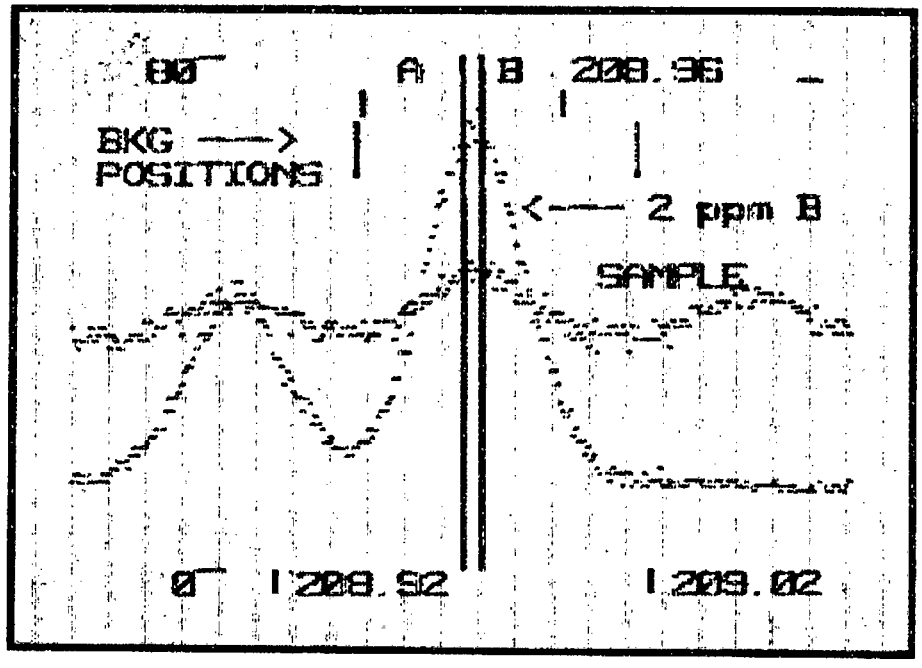


Figure 7.17 Wavelength scan for fly ash sample at 208.96 nm.

The boron concentrations of the reference materials from different sources are listed in table 7.2. No NBS certified values are available.

Table 7.2 Boron concentration in NBS-SRM materials.

| Sample | REPORTED VALUES (ppm) | | | |
|---|---|---|---|---|
| | [54] | [50] | [69] | [73] |
| 1633a | 39.2 | 39 ± 1 | 39.2 ± 0.7 | - |
| 1632a | 53 | - | 52.7 ± 1.8 | 53 ± 2 |
| 1635 | 105 | - | 104.5 ± 2.6 | 105 ± 3 |

[50] ICP-AES, fusion method.
[69], [73] Neutron-capture prompt x-ray activation analysis.

The results obtained for the NBS standards and for 30 South African samples are shown in table 7.3.

Table 7.3 Analytical results.

| Samples | Concentrations (ppm) |
|---|---|
| 1633a Fly ash | 40.0 ± 1.5 (3) |
| 1632a Bituminous coal | 53.3 ± 2 (3) |
| 1635 Sub-bituminous coal | 107.0 ± 5 (3) |
| 45 Fly ash | 123.0 |
| 46 Fly ash | 300.0 |
| 47 Fly ash | 407.0 ± 5 (2) |
| 48 Fly ash | 513.0 |
| 49 Fly ash | 209.0 |
| 50 Fly ash | 343.0 ± 4 (2) |
| 51 Fly ash | 396.0 |
| 52 Fly ash | 522.0 |
| 53 Fly ash | 218.0 ± 2.5 (2) |
| 54 Fly ash | 186.0 |
| 56 Fly ash | 406.0 |
| 57 Fly ash | 158.0 |
| 58 Fly ash | 248.0 ± 3 (2) |
| 59 Fly ash | 352.0 |
| 60 Fly ash | 410.0 |
| 61 Coal | 60.0 ± 1 (2) |
| 62 Bituminous ash | 118.0 |
| 63 Coal | 53.0 |
| 64 Bituminous ash | 108.0 |
| 65 Boiler ash | 97.0 ± 3 (2) |
| 66 Fly ash | 215.0 |
| 67 Fly ash | 347.0 |
| 68 Fly ash | 436.0 |
| 69 Fly ash | 473.0 |
| 70 Boiler ash | 97.0 ± 1.5 (3) |
| 71 Fly ash | 214.0 |
| 72 Fly ash | 422.0 |
| 73 Fly ash | 517.0 |
| 74 Fly ash | 488.0 ± 4 (2) |
| 101 Coal | 60.0 |

Values in parentheses are the number of separate determinations.

The B values obtained for the NBS standards are in close agreement with reported values. Because of the large numbers of samples to be analysed and the long sample preparation time, duplicate analysis for all the samples was not possible. Frequent instrument breakdowns during the course of this work also delayed the analyses. Several analyses of a few samples yielded better than 5% RSD (4.67% for NBS-SRM

1635). The concentration of B in fly ash ranged from 123 to 513 ppm (av 344 ppm) and 60 to 118 ppm in coal.

A much faster sample preparation method is highly desirable for routine analyses and, at present, a fusion technique using NaOH is being developed for the determination of boron, lithium, beryllium and possibly other elements in coal, coal ashes and mineral samples. Complete decomposition of fly ash samples has been achieved (except for unburnt carbon) in less than fifteen minutes.

## Leaching of boron from fly ash

An experiment was performed to investigate leaching of boron from fly ash by water.

About 1 g samples were shaken with 100 ml of water in 200 ml polypropylene flasks for 20 hours. The residues were filtered off and the filtrate analysed, using the 208.98 nm line. The % B leached was calculated (table 7.4).

Table 7.4 Leaching of boron from ash by water. (Duplicate analysis).

| Sample | Total B (ppm) | pH of filtrate | % B leached |
|---|---|---|---|
| NBS-SRM 1633a | 40 | 5 | 24.0 |
| 45 | 123 | 10 | 33.0 |
| 46 | 300 | 11 | 12.0 |
| 47 | 407 | 11 | 1.5 |
| 48 | 513 | 11 | 20.0 |
| 49 | 209 | 11 | 15.0 |
| 50 | 343 | 11 | 2.4 |
| 51 | 396 | 11 | 1.8 |
| 52 | 522 | 11 | 19.0 |
| 74 | 488 | 10 | 23.0 |

Pagenkopf and Connolly [82] mentioned that the release of boron from coal ash to leachate waters is dependent upon:

(i) contact time;

(ii) pH of the leachate water;

(iii) ash particle size;

(iv) ratio of ash to leachate water.

An increase of pH was noted (table 7.4) due to the presence of alkaline compounds, such as CaO. If the boron is present as borates (borax) and boric acid, these are readily soluble in water at room temperature over a wide range of pH. Less-soluble species like borosilicates may be formed at elevated temperatures. Cox et al [52] reported that approximately 50% boron present in a Southern Illinois (USA) fly ash was water leachable. They agitated 0.5 g of ash in 200 ml of water. James et al [53] analysed leachability of boron from 19 ash samples from different power plants (USA). The amount of boron leached varied from 17 to 64%. However, one ash from a magneto-hydrodynamic (MHD) high temperature (3000 K) pilot plant was found to contain only 7% leachable boron. This suggests the possibility of thermal fixation of the boron at high temperatures and a thus significant factor in reducing boron availability.

A proper investigation of boron leaching from South African ash heaps in power station areas is desirable and should involve a simulation of the effect of rain water on the ash heaps. The above points (i) to (iv) would have to be taken

into consideration. It has been shown here that ICP-AES is a useful tool for this kind of investigation.

## 7.2 Determination of boron in Kornerupine

### Reasons for study

This was to investigate the mineralogy and geochemistry study of a rare boron-bearing metamorphic mineral (Kornerupine) hitherto unknown from the Namaqualand Metamorphic Complex, Cape Province, South Africa.

### Experimental

The sample materials consisted of coarse crystals which were crushed in a steel Siebtechnik swing-mill grinder to ca.90 mesh after which inclusion impurities were removed using a magnetic separator. The samples were then crushed to -300 mesh particle size using an electric agate mortar and pestle.

Two methods for sample preparation were used:

**Method A :** Fusion decomposition.

The fusion method described by Owens et al [50] for boron determination in geological materials was used.

About 0.4 g aliquots of the samples were mixed thoroughly with 1 g of sodium carbonate. About 0.5 g $Na_2CO_3$ was placed into a Pt-Au crucible (cleaned by fusing $Na_2CO_3$ in it over a burner and rinsing in 10% HCl) followed by the sample

mixture and about 0.5 g $Na_2CO_3$ to cover the mixture (total $Na_2CO_3$ = 2 g). Samples were fused for 15 minutes at 850°C followed by 15 minutes at 950°C in an oven. After cooling the melts were dissolved in hot water. These solutions were filtered to remove insoluble residues, neutralized with perchloric acid and diluted to 100 ml with water. Solutions were left standing overnight to remove dissolved $CO_2$.

**Method B** : Acid dissolution

About 0.02 g aliquots of the samples were weighed in the teflon cups of the Parr bombs and 2 ml concentrated nitric acid and 3 ml 48% hydrofluoric acid were added. The bombs were sealed and held at 130°C for 5 hours. After cooling, samples were diluted to 50 ml with water. A white precipitate was obtained and this was filtered off.

For both methods, blanks were prepared following the procedure described while working standards were prepared by spiking blank solutions.

The 249.77 nm B line was used for B determination in the samples prepared by method A and the two lines 249.77 and 208.96 nm were used for method B samples. Iron was also determined in all the samples using the 238.20 nm line. The ICP parameters are listed in table 7.5. Background correction was done on each side of the boron peaks (about 0.05 nm off-line). The method of "alternating blank routine" was used. A 40 second washing time was allowed.

Table 7.5 ICP parameters.

| Element | Wavelength (nm) | Torch Power | Neb.Press (psi) | Obs.Ht (mm) | Sample flowrate (ml/min) |
|---|---|---|---|---|---|
| B | 249.77 | 3 | 32 | 10 | 1 |
| B | 208.96 | 3 | 32 | 10 | 1 |
| Fe | 238.20 | 3 | 32 | 12 | 1 |

## Results

The results obtained by the two methods are shown in tables 7.6 and 7.7. No iron could be detected in the samples prepared by method A. Consequent x-ray diffraction analysis (XRD) indicated the presence of Fe together with other elements in the residues. The amounts of Fe determined in samples from method B are shown in table 7.8. A comparison with data obtained by electron microprobe (EM), table 7.8, shows higher Fe concentrations in the samples (calculated as FeO). It is possible that Fe was present in the precipitates. The Fe data was used to correct for Fe interference at 249.77 nm. A comparison of the values obtained by using the two B lines (table 7.7) indicates the need for correction when Fe concentrations are large. The correction factor was calculated as 0.0014.

Satisfactory agreement between the two methods was obtained. The fusion technique is much faster and has the advantage of the removal of the interfering Fe from the samples. However, it is shown that the 208.96 nm line can be used instead when Fe concentrations are large, as in the case of

fly ash analysis. XRD analysis of the residues from method A showed no presence of Kornerupine indicating complete breakdown of the mineral.

Table 7.6 Method A, Analytical results.

| Sample | % B | Mean % B | % $B_2O_3$ |
|---|---|---|---|
| 1 (a) | 0.287 | 0.279 | 0.90 |
| (b) | 0.271 | | |
| 2 (a) | 0.553 | 0.541 | 1.74 |
| (b) | 0.528 | | |
| 3 (a) | 0.971 | 1.026 | 3.30 |
| (b) | 1.081 | | |

Table 7.7 Method B, Analytical results.

| Sample | Wavelength (nm) | % B | % B Corr. at 249.77 nm | Mean % $B_2O_3$ |
|---|---|---|---|---|
| 1 | 249.77 | 0.299 | 0.297 | 0.96 |
| | 208.96 | 0.298 | 0.298 | |
| 2 | 249.77 | 0.561 | 0.554 | 1.78 |
| | 208.96 | 0.552 | 0.552 | |
| 3 | 249.77 | 1.027 | 1.020 | 3.29 |
| | 208.96 | 1.021 | 1.021 | |

Table 7.8 Method A, Fe determination.

| Sample | Fe measured (ppm) | % FeO | % FeO (EM) |
|---|---|---|---|
| 1 | 7.35 | 2.26 | 3.3 |
| 2 | 15.90 | 4.82 | 6.2 |
| 3 | 32.16 | 8.01 | 11.0 |

## 7.3 Determination of boron in water samples

An analysis of water is described in chapter 8. Here boron was determined in sea water and in some lake water samples.

The analysis of trace elements in sea water is often difficult because of the high dissolved solid concentrations. However, with the high temperatures of the ICP source where interelement interferences are claimed to be very small, analysis of sea water directly without preconcentration and/or salt removal has been attempted.

High concentrations of sodium are shown to cause enhancement of the boron lines in figures 7.18 and 7.19. For both lines, the enhancement is found at low viewing heights. At observation heights larger than 22 mm, the effect is seen to be negligible. However, the sensitivity decreases rapidly with increase of viewing heights in the plasma. The background is also found to be higher at lower observation heights.

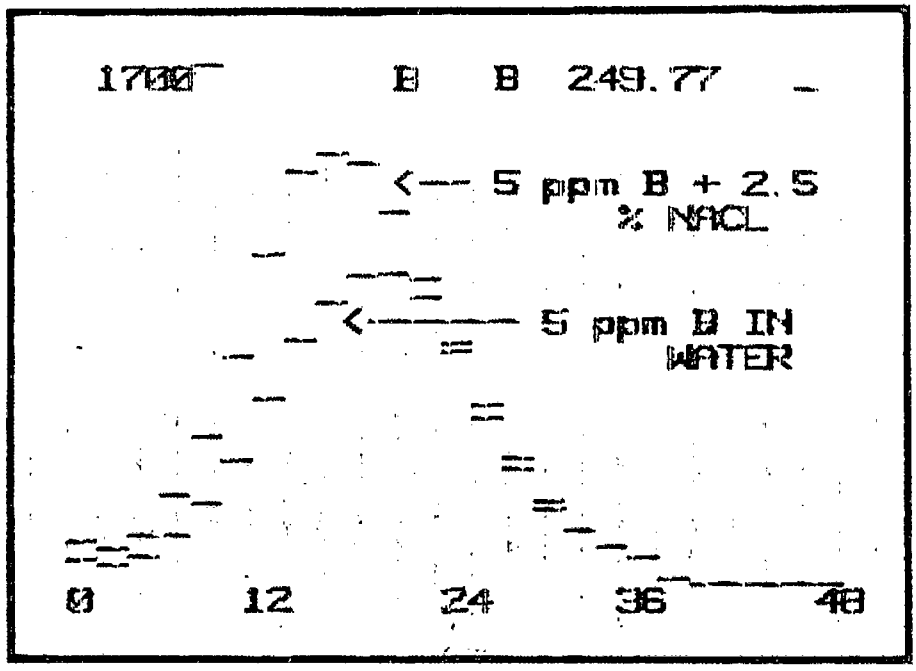


Figure 7.18 Effects of Nacl on boron emission at 249.77 nm.

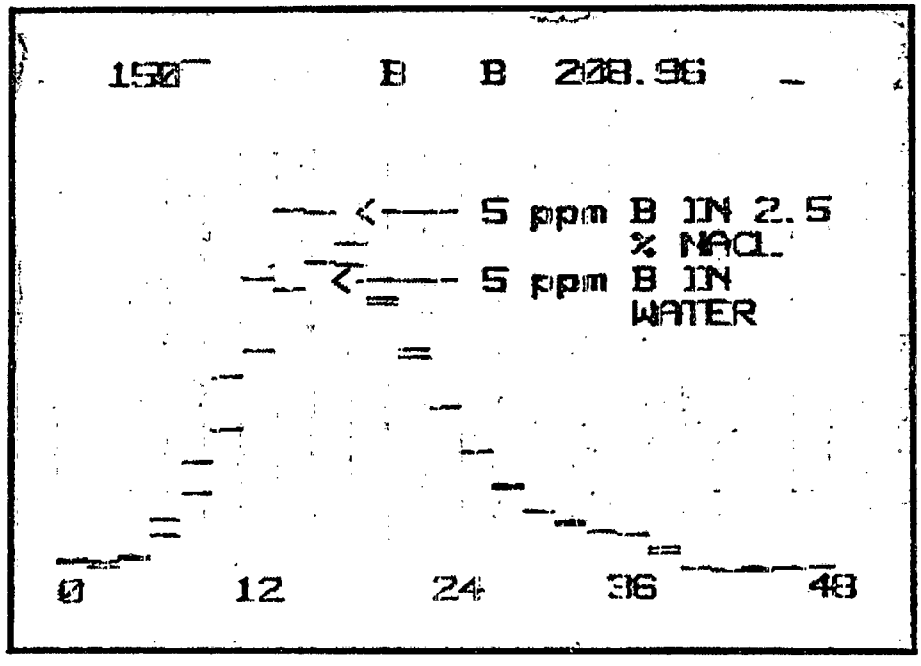


Figure 7.19 Effects of Nacl on boron emission at 208.96 nm.

Sea water was analysed directly using aqueous standards for calibration (10, 2, 0.5 ppm). The following parameters were

used: Power 4, 1 ml/min, 36 psi, 18 mm, 10 RDG of 6 sec. The background correction programme was used on the high wavelength side of the peaks.

The two lines were used and a mean value of 4.51 ppm (0.78% RSD) was obtained which is in good agreement with reported values of boron in sea water, eg 4450 µg/l [83].

Boron was also determined in 12 lake water samples (4 samples from 3 different lakes collected at different periods). Only three readings for eight seconds were taken. A scan of the sample emission at 249.77 can be seen in figure 7.20. The results obtained are shown in table 7.9. RSD varied from 0.5 to 4%.

Table 7.9 Boron in lake water.

| Sample | ppm B measured (mean) |
|---|---|
| L 1A | 0.19 |
| B | 0.17 |
| C | 0.16 |
| D | 0.09 |
| L 2A | 0.11 |
| B | 0.05 |
| C | 0.05 |
| D | 0.08 |
| L 3A | 0.08 |
| B | 0.08 |
| C | 0.17 |
| D | 0.07 |

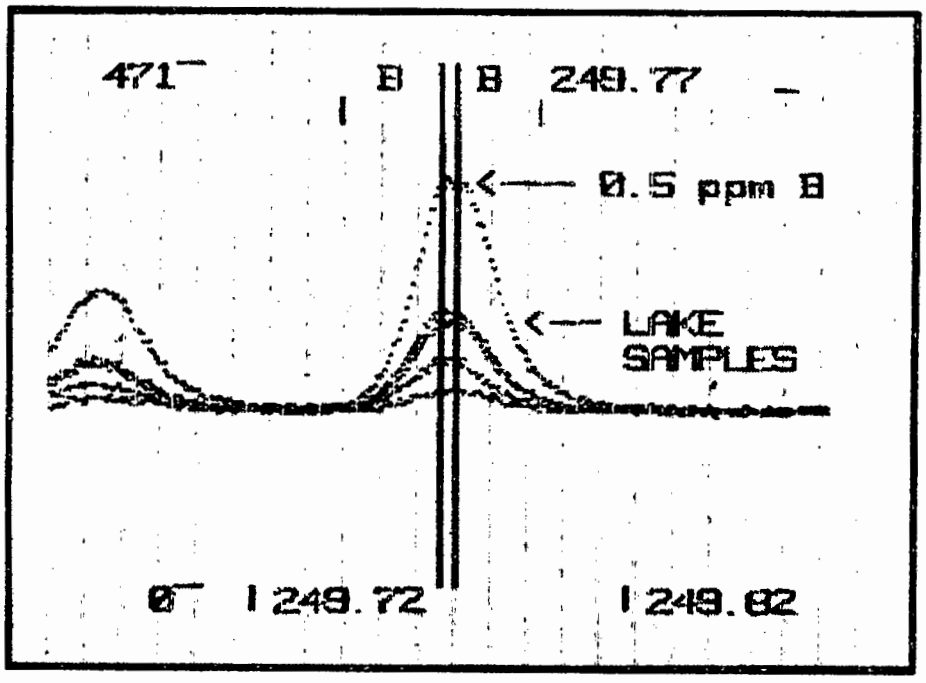


Figure 7.20 Lake water emission at 249.77 nm.

It must be noted that the measurements made above ranged from 10 to 40 times the detection limits for boron determination.

A tap water sample was aspirated but no boron could be detected, ie Cape Town tap water contains less than 0.005 ppm B. The Fe concentrations in the lake water samples were less than 0.2 ppm. Since small variation of the background intensity would yield large errors when working at these levels, great care must be taken to monitor variation of the background during analysis and a stable plasma is imperative.

The use of two spectral lines for the analysis of difficult samples, eg fly ash, has been shown to be useful for detecting interferences. However, it is not practical for routine analysis unless two monochromators are used for single element determinations.

# CHAPTER 8. ANALYSIS OF WATER SAMPLES FROM A POWER PLANT BY ICP-AES AND FAAS

Since the introduction of the FAAS technique, it has been widely used for trace element analysis of water. There has been remarkable progress in the application of ICP-AES to the analysis of environmental samples. In the case of a sample containing high concentrations of salt, for example sea water, spectral interference arising from stray light and other interferences have been observed, so that pretreatment or background correction is necessary. Samples of river water and industrial waste water can often be quickly analyzed without any pretreatment and with little or no interference corrections being required.

10 water samples from different locations of the SASOL I plant (South Africa) were received in 2 litre plastic containers. The pH values were determined using Universalindikator (Merck). The samples were then filtered through Whatman No 1 filter paper and stored in plastic bottles. Some samples contained large amounts of solids and some of them were yellow or brown in colour. The samples are listed together with their properties in table 8.1.

Table 8.1 Water samples from the SASOL I plant.

| Origin of sample | Sample Code | pH | Colour |
|---|---|---|---|
| Sewage storm water | 10 | 6 , | colourless |
| Underflow from thickener (AB) | 11 | 9 | colourless |
| Overflow from thickener (AB) | 12 | 5 | |
| Gas liquor | 13 | 6 | dark brown |
| Underflow from thickener (c) | 14 | 12 | colourless |
| Overflow from thickener (c) | 15 | 11 | light brown |
| From classifier | 16 | 12 | colourless |
| Underflow from precipitator ($CO_2$) | 17 | 6 | light brown |
| From a water treatment section | 18 | 5 | light yellow |
| Overflow from precipitator ($CO_2$) | 19 | 7 | light brown |

## 8.1 ICP-AES analysis

Calcium, magnesium, silicon and boron were determined quantitatively and the levels of Al, Fe, Ti and P were estimated.

### Method

Wavelength scans were performed with standards, samples and water blanks (MQW) to investigate possible interferences. Scans for Ca and Mg are shown in figures 8.1 and 8.2. No interferences were detected and the samples did not contain large elemental concentrations. Similar scans were done for Al, Fe, Ti and P and their concentrations were found to be very small. Using the RESTPEAK-PLOT routines after optimization, the concentrations were estimated on the VDU by

comparison of peak heights with standard solutions.

Experience has shown that very good estimates are obtainable by using the VDU as such.

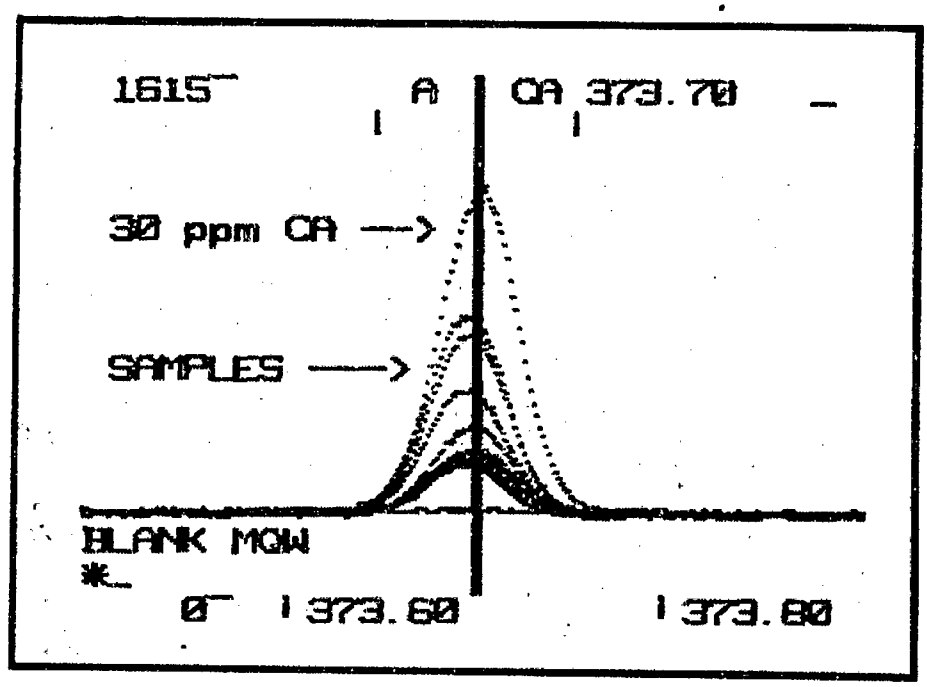


Figure 8.1 Wavelength scan for Ca.

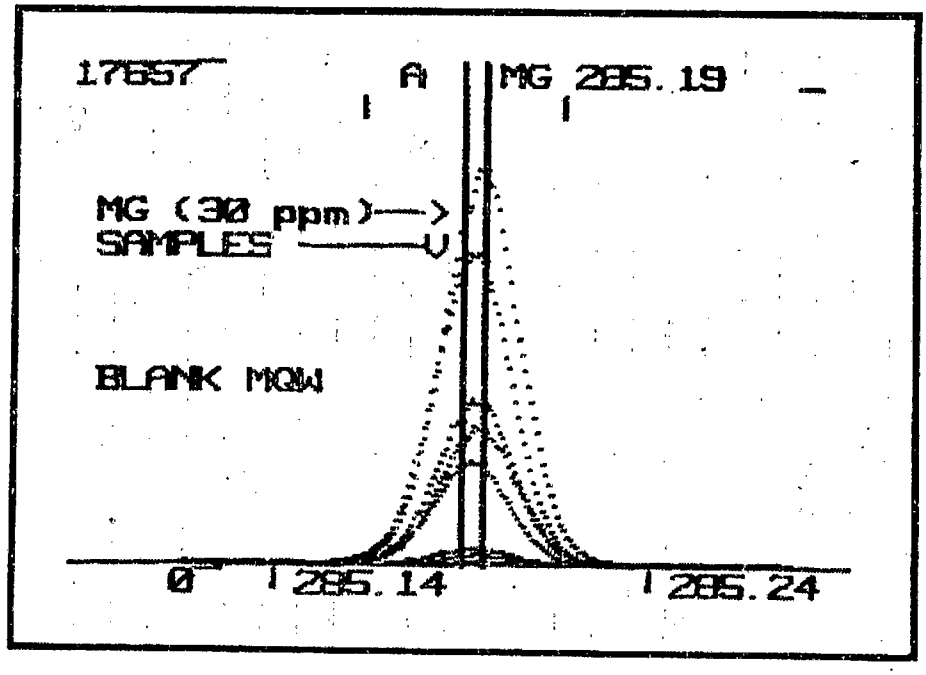


Figure 8.2 Wavelength scan for Mg.

Two analyses of three readings each for 3 seconds were done for each water sample. The torch power was kept at 3. the nebulizer driving pressure was 30 psi in all cases and the pump delay was 40 seconds. Other parameters are shown in table 8.2.

Table 8.2 Instrumental parameters.

| Element | Spectral line (nm) | Obs Height (mm) | Sample flow rate (ml/min) |
|---|---|---|---|
| Ca | 373.60 | 12 | 2.0 |
| Mg | 285.21 | 14 | 1.5 |
| Si | 288.16 | 12 | 2.0 |
| Al | 308.22 | 12 | 2.0 |
| Fe | 259.94 | 14 | 2.0 |
| Ti | 337.28 | 14 | 2.0 |
| P | 213.61 | 12 | 2.0 |

Determination of boron

The analytical parameter for boron determination is shown in figure 8.3.

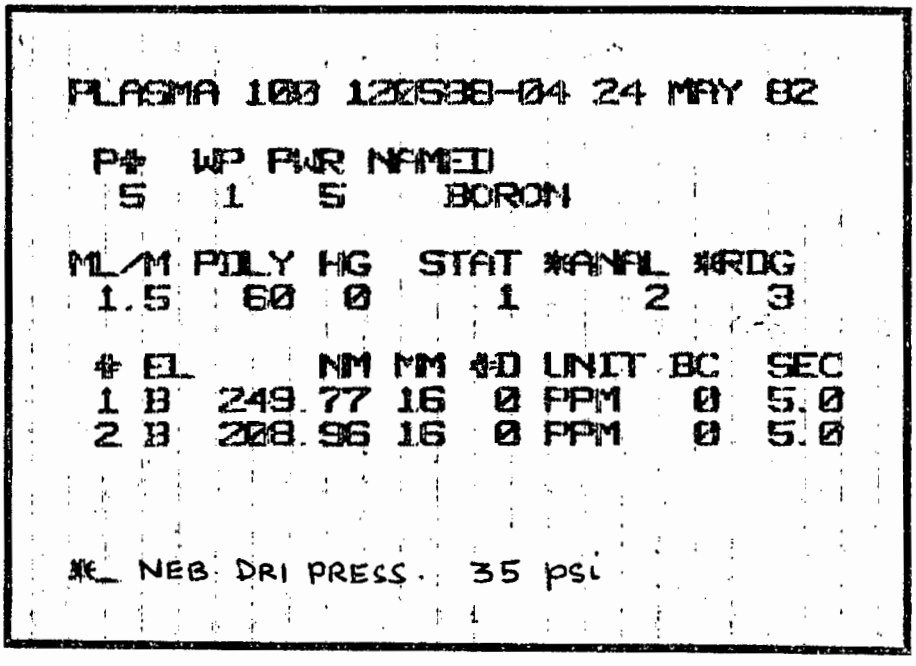


Figure 8.3 Boron analytical programme.

A rough estimate of the boron concentration in the water samples was obtained by calibrating the instrument with a 100 ppm boron standard in water and a water blank. The 208.96 nm line was used and 1 reading of 2 seconds for each water sample was recorded. The results obtained are listed in table 8.3 for comparison with the more accurate results using the parameters in figure 8.3 where the instrument was calibrated with 10, 5 ppm B standards and a water blank. For boron determination TX-100 (0.05%) was added to the water samples and standards. Recalibration was done after the analysis of three samples.

Table 8.3 Analytical results for boron determination (ppm).

| Sample | Spectral lines (nm) | | |
|---|---|---|---|
| | 208.96* | 208.96 | 249.77 |
| 10 | 2.44 | 2.53 | 2.55 |
| 11 | 7.73 | 7.62 | 7.64 |
| 12 | 3.08 | 3.19 | 3.20 |
| 14 | 0.21 | 0.57 | 0.60 |
| 15 | 7.36 | 6.96 | 7.05 |
| 16 | 2.86 | 3.00 | 3.03 |
| 17 | 16.99 | 15.99 | 16.08 |
| 18 | 4.60 | 4.53 | 4.60 |
| 19 | 7.38 | 7.12 | 7.16 |

* Line used for "rough" analysis.

The two sets of data obtained by using the two spectral lines are in very good agreement. However, systematically higher results were obtained by using the 249.77 nm line. This difference can probably be attributed to a small background shift at one of the lines. Surprisingly, the results obtained by the rough analysis (*) using a large calibration range and very short reading time agree reasonably well with

the more careful analysis, except for sample 14. It took only about 12 minutes to obtain the results and for most purposes, they should be adequate.

## 8.2 FAAS analysis

Vanadium, nickel, cobalt and molybdenum were determined by FAAS because of their very low concentration.

### Method

Preliminary AAS measurements were made to establish the drying, ashing and atomization temperatures and times. The instrumental parameters are listed in tables 8.4 and 8.5. Peak heights were recorded and the background corrector was used for all determinations. Maximum power mode of atomization was used for V, Ni and Mo.

Table 8.4 Spectrophotometer parameters.

| Element | Line (nm) | Slit width (nm) | Lamp current (mA) |
|---|---|---|---|
| V | 318.4 | 0.7 | 18 |
| Ni | 232.0 | 0.2 | 22 |
| Co | 240.7 | 0.2 | 29 |
| Mo | 313.3 | 0.7 | 27 |

Table 8.5 HGA-500 parameters.

| Step | Element | Temp (°C) | Ramp time (sec) | Hold time (sec) | Int flow (ml $min^{-1}$) |
|---|---|---|---|---|---|
| DRY | Vi, Ni, Co, Mo | 110 | 12 | 30 | 300 |
| CHAR | V | 1000 | 5 | 12 | 11 |
| | Ni | 800 | 5 | 12 | 11 |
| | Co | 1000 | 5 | 12 | 11 |
| | Mo | 1600 | 5 | 12 | 11 |
| ATOMIZE | V | 2700 | 0* | 5 | 10 |
| | Ni | 2300 | 0* | 6 | 10 |
| | Co | 2400 | 2 | 5 | 10 |
| | Mo | 2700 | 0* | 5 | 10 |

* Maximum Power mode.

A 20 µl micropipette was used for dispensing the standards and samples inside the HGA tubes (all pyrolytically coated) except for Co determination, when a 50 µl pipette was used.

Difficulties with dispensing some of the samples was encountered, especially those having dark colours, due to wetting of the pipette tips. New tips were used as required. The tips were also washed with water between injections.

The calibration curves (Peak height, absorbance versus elemental concentration) prepared for the four elements are shown in figures 8.4 to 8.7. Results were calculated from a linear regression curve fit using calibration data within the linear part of the calibration curves. Each analysis was a mean of at least three readings. Some samples were also analysed by the standard addition method and good agreement

was obtained with the above method. This shows that the use of aqueous standards for the analysis of water samples containing low concentrations of V, Co, Ni, Mo is satisfactory.

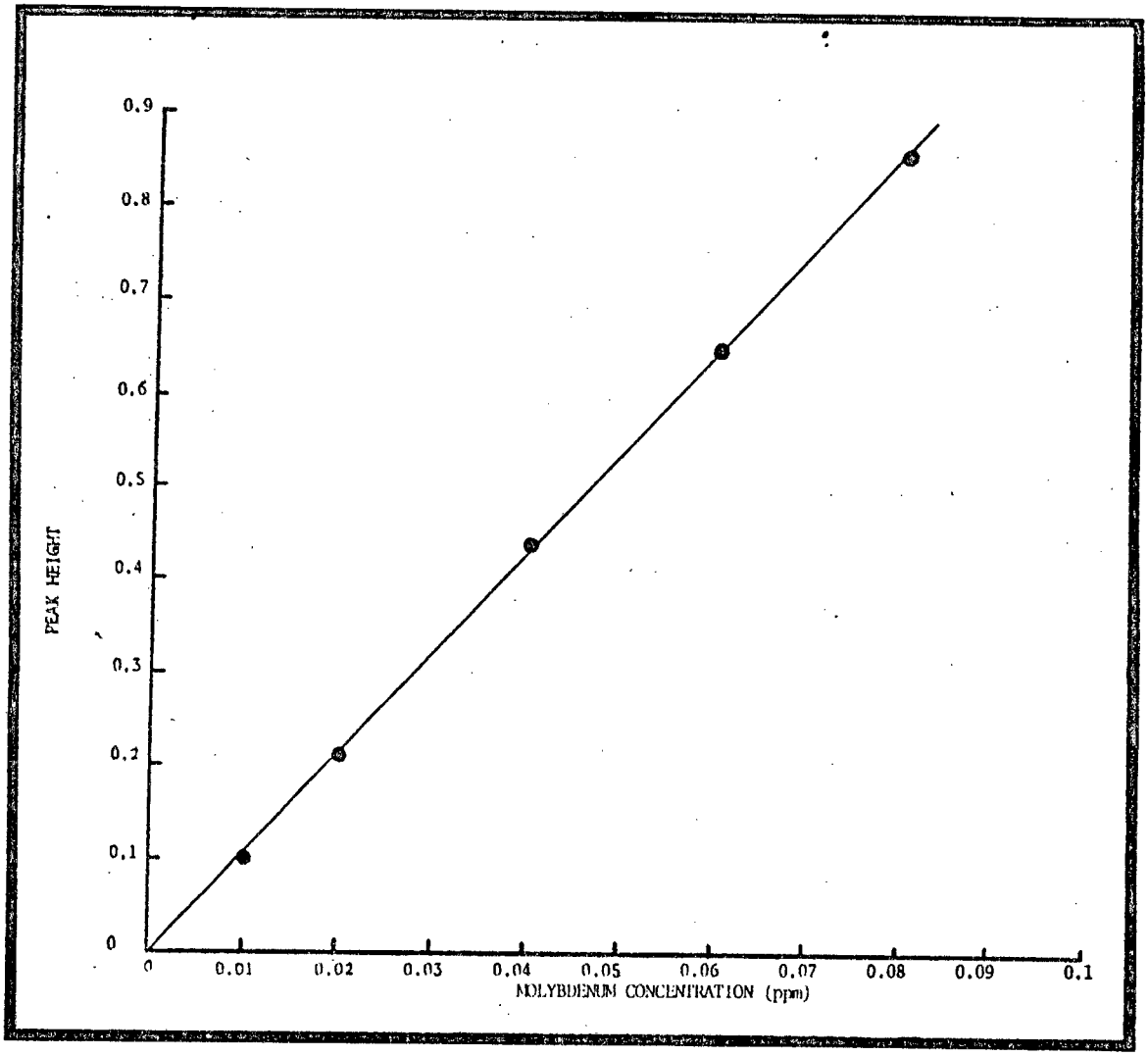


Figure 8.4 Molybdenum calibration curve.

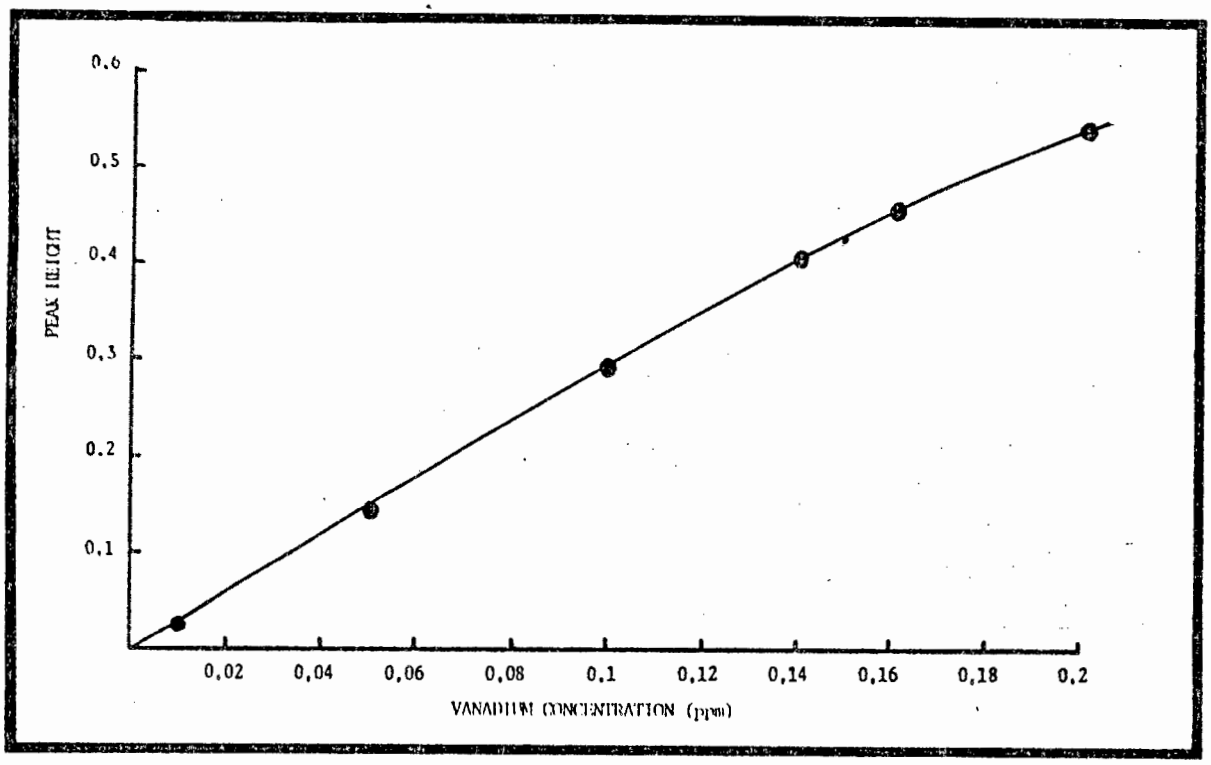


Figure 8.5 Vanadium calibration curve.

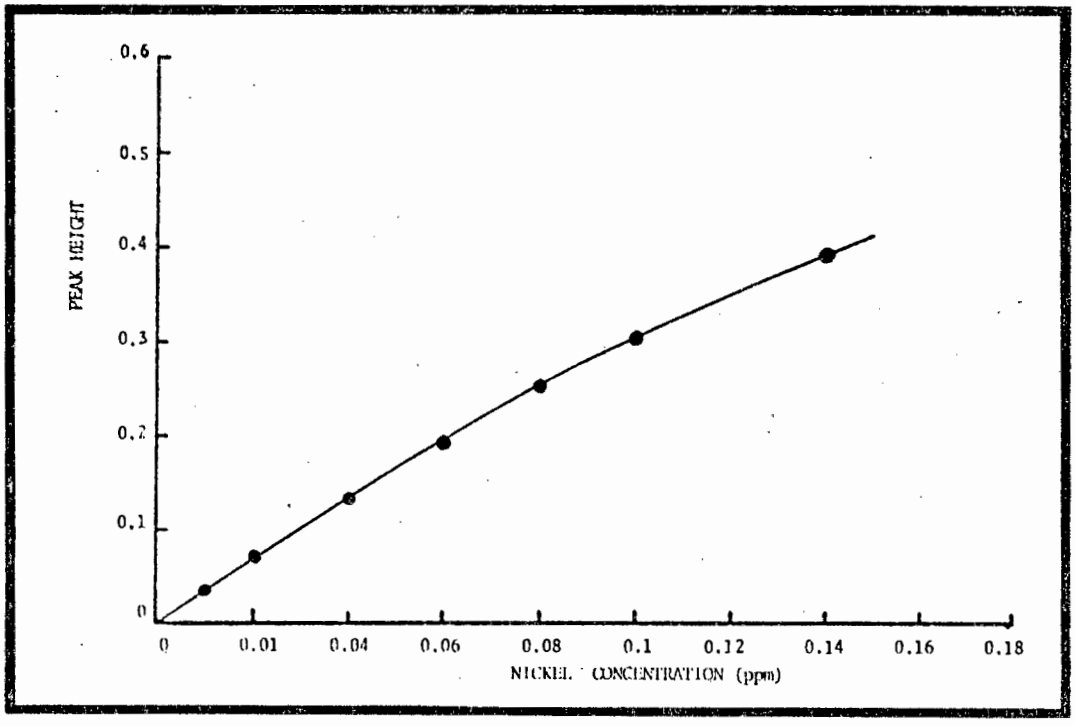


Figure 8.6 Nickel calibration curve.

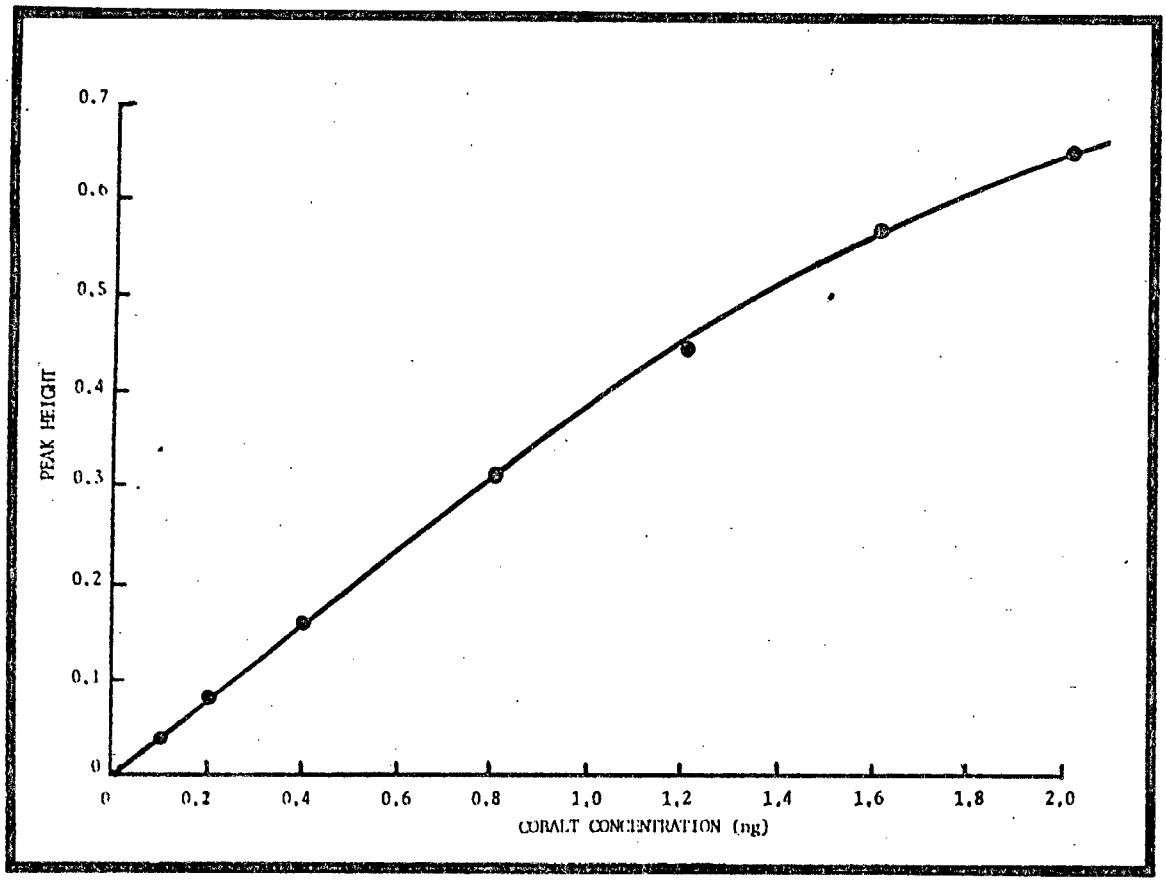


Figure 8.7 Cobalt calibration curve.

## 8.3 Results and discussion

Analytical results for Ca, Mg, Si and B are listed in table 8.6. Less than 0.5 ppm Al was found in most water samples; however, samples 13 and 15 were found to contain about 2 ppm Al. The concentration of Fe and Ti was less than 0.3 ppm in all samples. Less than 0.5 ppm P was found, except for sample 18 which contained about 2 ppm P. The analytical results for V, Ni, Co and Mo are shown in table 8.7.

The average %RSD for ICP-AES analyses was 0.6 and for FAAS analyses it varied from 0.5 to 7% at very low levels.

Table 8.6 Analysis by ICP-AES.

| Sample | Concentration (ppm) | | | |
|---|---|---|---|---|
| | Ca | Mg | Si | B* |
| 10 | 112.2 | 20.6 | 18.5 | 2.54 |
| 11 | 115.6 | 0.7 | 9.7 | 7.63 |
| 12 | 111.8 | 12.6 | 11.1 | 3.20 |
| 13 | 5.2 | 2.7 | 7.4 | - |
| 14 | 813.0 | <0.5 | 1.2 | 0.59 |
| 15 | 359.4 | <0.5 | 5.9 | 7.01 |
| 16 | 556.5 | <0.5 | 0.7 | 3.02 |
| 17 | 89.2 | 42.3 | 2.6 | 16.04 |
| 18 | 96.0 | 7.0 | 5.6 | 4.57 |
| 19 | 84.2 | <0.5 | 4.9 | 7.14 |

* Mean of results from table 8.3.

Table 8.7 Analysis by FAAS.

| Sample | Concentration ( µg/l) | | | |
|---|---|---|---|---|
| | V | Ni | Co | Mo |
| 10 | 110 | 35 | 3.10 | 14 |
| 11 | 164 | 39 | 1.40 | 32 |
| 12 | 152 | 39 | 2.80 | 19 |
| 13 | 9 | 10 | 1.20 | 4 |
| 14 | 24 | 103 | 0.60 | 94 |
| 15 | 136 | 70 | 1.60 | 38 |
| 16 | 25 | 96 | 0.90 | 69 |
| 17 | 78 | 31 | 1.99 | 55 |
| 18 | 343 | 57 | 1.90 | 15 |
| 19 | 114 | 17 | 1.60 | 36 |

The effect of pH on elemental concentration was studied by plotting elemental concentrations against pH of the water samples. These are shown in appendix 4. The calcium, molybdenum and nickel concentrations are larger at high pH values (pH 12) while magnesium and cobalt show the reverse trend. No clear trends for silicon, vanadium and boron were seen. More samples and a better sampling technique would be required to fully understand the variation of concentrations of these elements within the plant. Variation of the concentration at one location of the plant is expected to vary with time.

The boron concentrations in some samples, eg 17, 11, 15, 19 seem very high. The water samples were analysed several months after they were collected (the other elements were determined within a month from collection). In most cases the samples were in contact with solids, mostly ash, and these high concentrations seem to indicate that boron was leached out of the ash (chapter 7.4) in the sample bottles or within the power plant.

# CHAPTER 9. DETERMINATION OF BERYLLIUM BY ICP-AES

In recent years, the acute toxicity of beryllium compounds to humans has been fully recognised. A relatively small intake of beryllium can lead to acute or chronic disease. Determination of trace quantities of this toxic element in geological and environmental samples is gaining increased importance. A number of techniques for beryllium measurements have been reported [55] : fluorimetry, gas chromatography, mass spectrometry, spectrophotometry [56], polarography, gravimetric methods, flame atomic absorption [57, 58, 59] and emission spectroscopy, as well as electro- thermal atomic absorption [60, 61, 100, 101]. Because of the very low concentrations of beryllium in environmental samples, and the usually complex matrices (eg coal), direct determination of trace beryllium is difficult. Pretreatment must be used both to pre-concentrate the beryllium and to separate it from other interfering elements. Methods used include extraction by acetyl acetone into chloroform or carbon tetrachloride, and ion exchange separations [56, 58, 59, 60].

Graphite furnace atomic absorption spectroscopy has considerable advantages in sensitivity over many of the above techniques. Direct determination of beryllium in coal by a solid sampling technique has been reported by Gladney [55], and Geladi and Adams [51] determined Be in a fly ash standard (NBS-SRM 1633)..

After investigating methods of beryllium determination in coal and fly ash by FAAS using: (i) samples prepared in the digestion bombs, and (ii) the slurry technique described in chapter 3, a study of the possibilities of using ICP-AES for

trace beryllium determination, was done.

Standard solutions were used to optimize the conditions for Be determination. The analytical programme shown in figure 9.1 was used to obtain spectral characteristics of four Be emission lines. The results are shown in table 9.1.

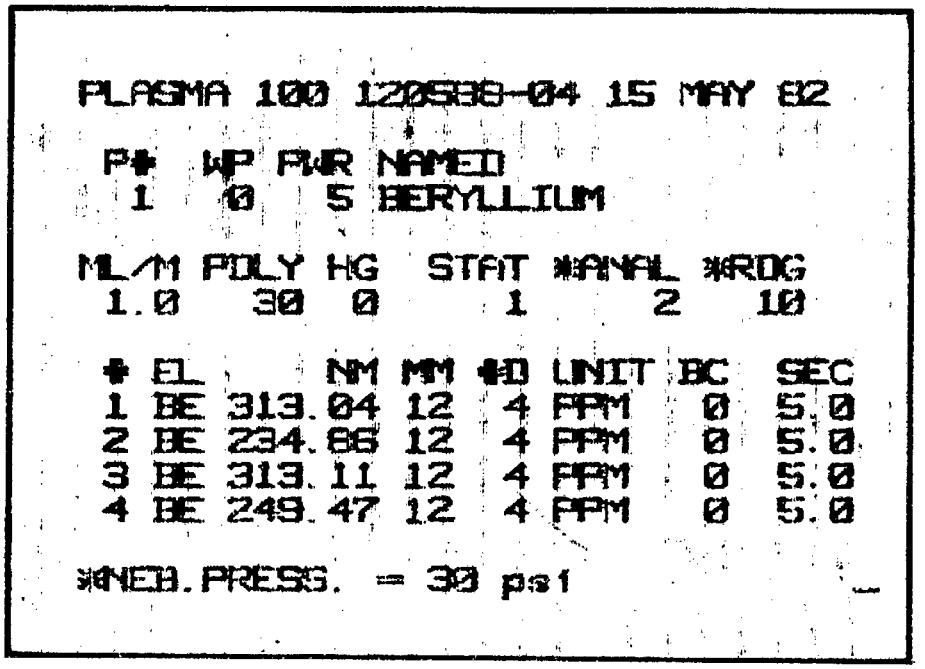


Figure 9.1 Be analytical programme.

Table 9.1 Be lines characteristics.

| Spectral line (nm) | $I_N/I_B$ (1 ppm Be) | $C_L$ (ppm) |
|---|---|---|
| 313.04 II | 46.0 | 0.00014 |
| 313.11 II | 25.0 | 0.00040 |
| 234.86 I | 45.0 | 0.00022 |
| 249.47 I | 1.9 | 0.0048 |

The first two lines are close to each other but are sufficiently well resolved by the IL-100 optical system. From table 9.1 the Be 313.04 and 234.86 nm the lines are the two lines

of choice because of their higher $I_N/I_B$ and better $C_L$ values. The 249.47 nm line is not sensitive enough for low level determinations.

An interference study was carried out for the first three lines in table 9.1. Serious interference by an iron line near the 234.89 nm Be line makes this line difficult to use since the ratios of iron to beryllium in fly ash samples are very large. This interference is shown in figure 9.2. A high blank is noted on the short wavelength side of the Be line which coincides with the iron line. It is not clear whether the high blank is due to spectral overlap from argon or other molecular band.

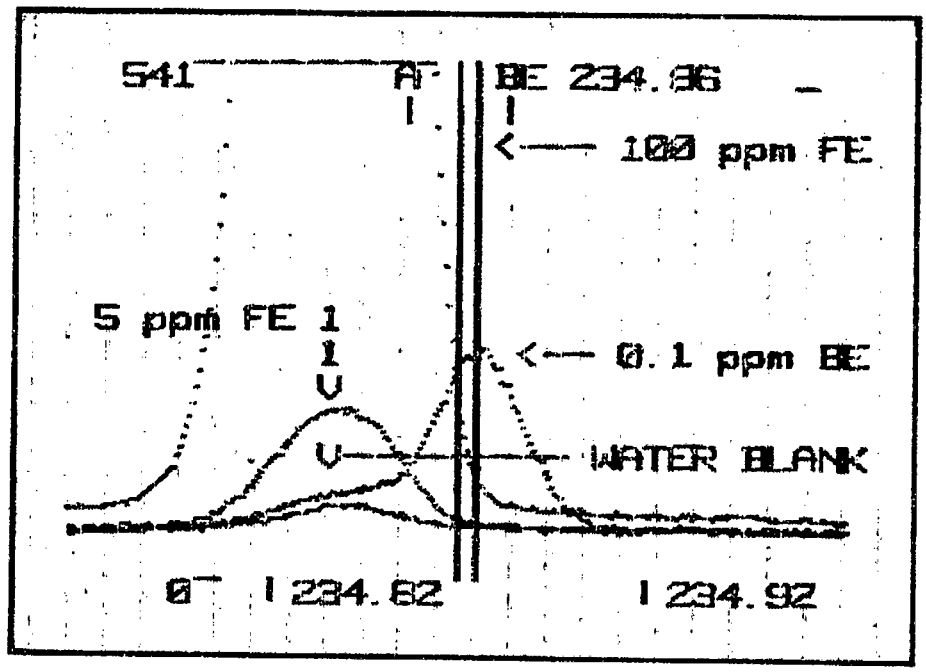


Figure 9.2 Interference by Fe at Be 234.86 nm.

Vanadium interference on the Be 313.04 nm and a titanium peak between the two Be lines are shown in figure 9.3.

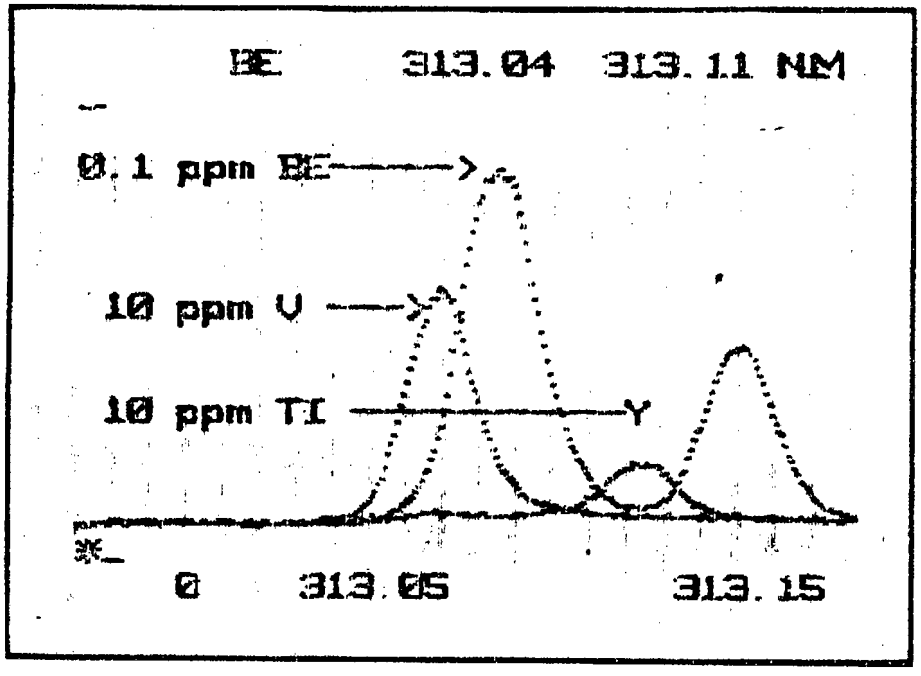


Figure 9.3 Interferences at Be 313.04 and 313.11 nm lines.

Figure 9.4 shows scans of a fly ash sample, a Be standard, a blank solution and a titanium standard (all containing the same concentrations of acids as the sample). The high blank at 313.04 nm is caused by OH emission bands situated in this region [45]. These appear to be two poorly resolved peaks that cannot be seen at high Be concentrations but causes a broadening of the Be peak. The titanium peak from the sample interferes severely with both Be lines.

TPROFILE scans of the above solutions, figure 9.5, show that emission from the blank and titanium is stronger at high observation heights. Therefore, to decrease the interference by titanium, lower observation heights can be used, eg 10 mm. An attempt to use the background correction "marker" positioned near point A (figure 9.4) gave "over correction" probably because it does not lie on a "flat" part

of the spectrum. The small window was used for beryllium determination and correction factors were obtained for the interferences. Under those conditions Ti interference at the 313.04 nm line was found to be negligible and at 313.11 nm the correction factor was 0.00015. A correction factor of 0.0043 was obtained for V interference at the Be 313.04 nm line.

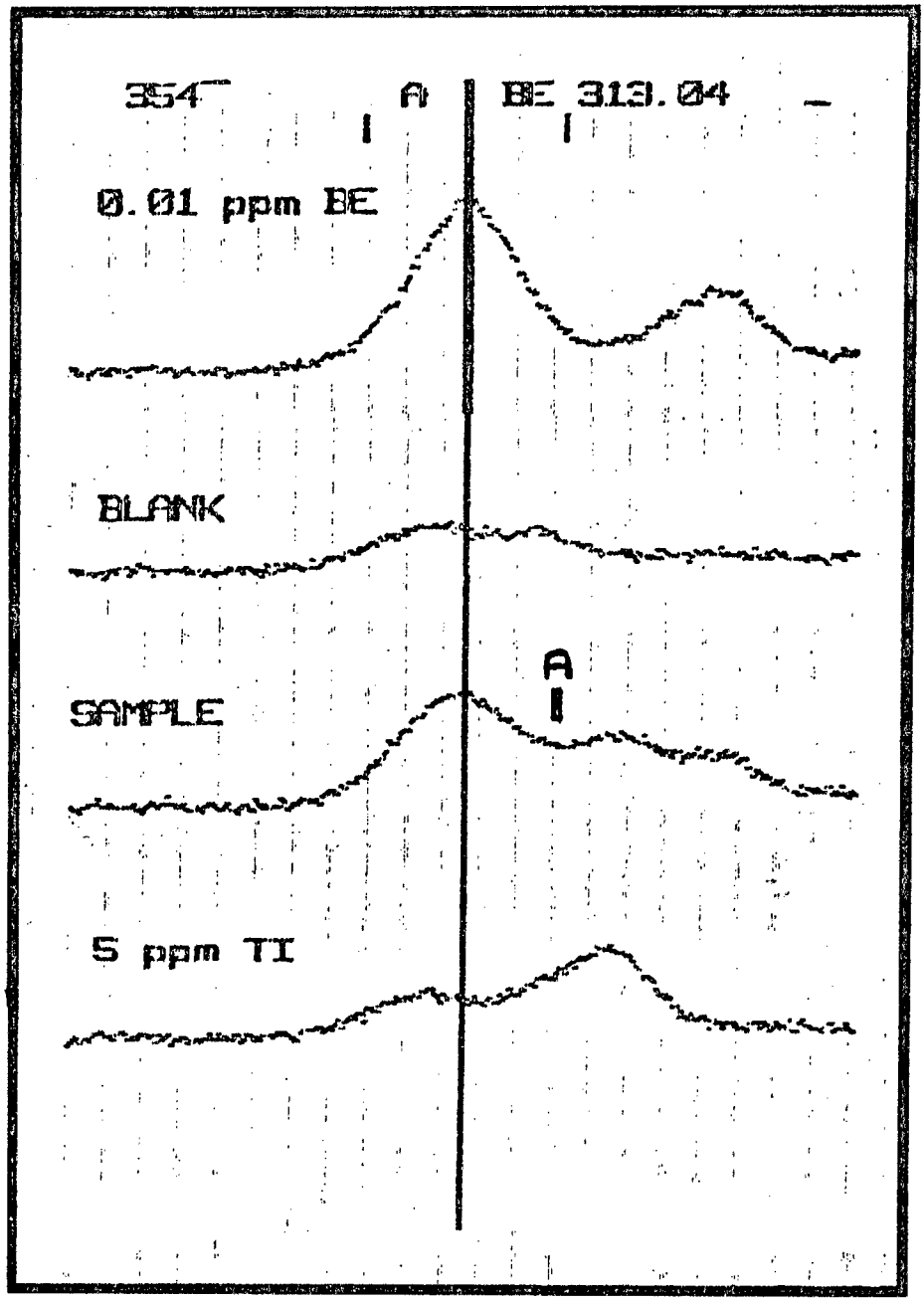


Figure 9.4 Wavelength scans near the 313.04 nm line.

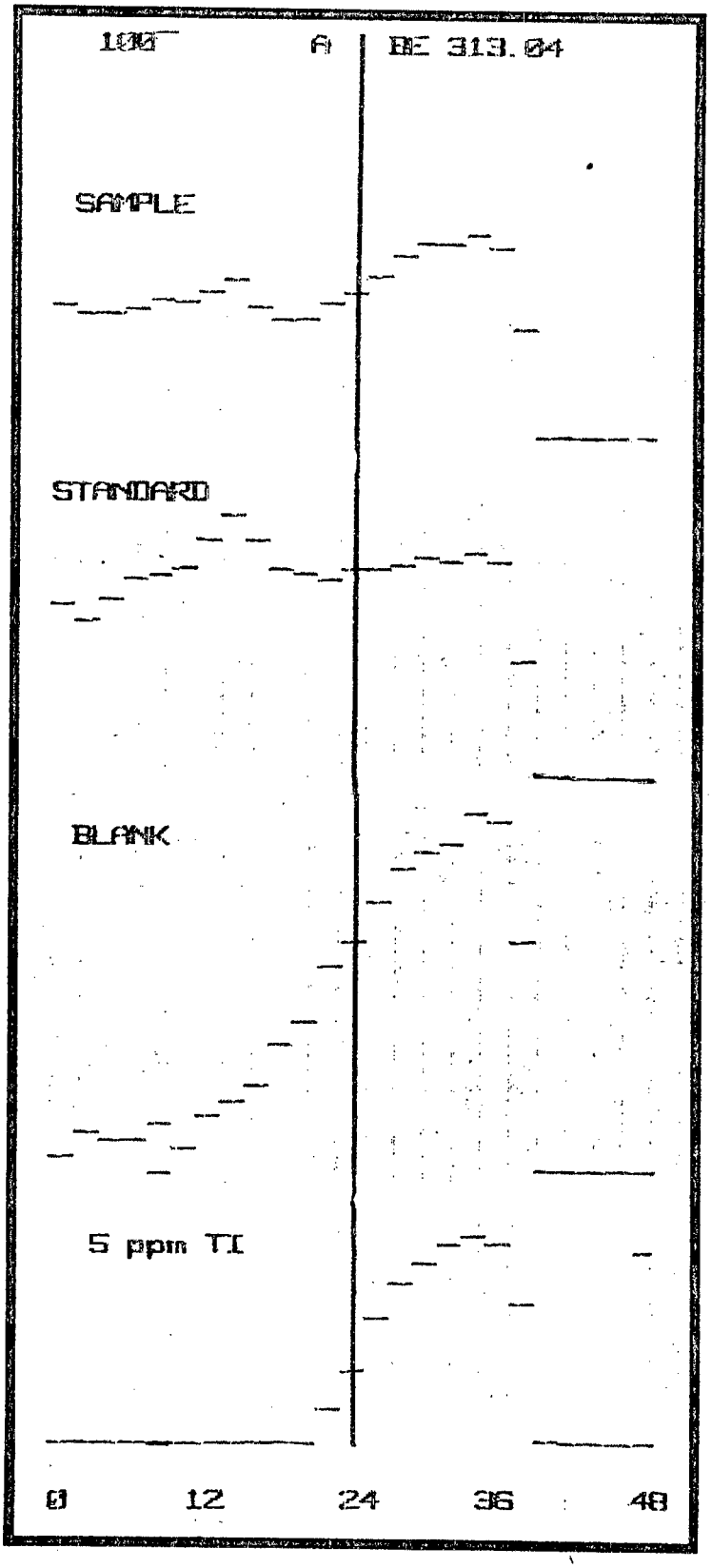


Figure 9.5 TPLOT scans near the 313.04 nm line.

Analysis of the NBS fly ash sample 1633a

Samples were prepared in the following way:

About 0.05 g aliquots were dissolved in the digestion bombs with 2 ml of aqua regia (1 conc $HNO_3$ : 3 conc HCl) and 3 ml of 48% HF at 115°C for four hours. The dissolved samples were transferred to 50 ml polypropylene volumetric flasks and diluted to the mark with water. The blanks were prepared in the same way and standards were prepared by spiking the blank solutions. All the solutions contained about 0.05% TX-100 for ICP-AES analysis.

Samples prepared in the same way (but without TX-100) were used for Be determination by FAAS using the standard addition method. Pyrolytically coated graphite tubes and small homemade "L'vov platforms" [104] were used. The platforms were made by cutting small pieces from a graphite tube. Good sensitivities were obtained with FAAS. However, the use of these platforms (to reduce matrix interference) was not very practical since for each platform the furnace had to be realigned and the temperature programme altered. The instrumental parameters for Be determination by FAAS are shown in table 9.2. The Ar flow rate during atomization was 100 ml $min^{-1}$.

Table 9.2 FAAS parameters.

| Step | Temp (°C) | Ramp time (sec) | Hold time (sec) |
|---|---|---|---|
| Dry | 180 | 1 | 40 |
| Ash | 1500 | 1 | 20 |
| Atomize | 2600 | 0* | 5 |
| Clean | 2700 | 1 | 3 |

* Maximum Power mode

Four samples were analysed by FAAS and ICP-AES. The 234.9 nm was used for FAAS and the 313.04 nm line for ICP-AES. The ICP was calibrated with four standards and a blank (0.001, 0.01, 0.1, 0.5 ppm).

The results obtained were as follows:

FAAS : 12.68 $\pm$ 0.68 ppm (5.34 %RSD)
ICP-AES : 13.53 $\pm$ 0.75 ppm (5.54 %RSD)

During the ICP-AES analysis, drift was noticed and the method of alternating blank routine was used.

One of the samples was also analysed using the standard addition method with ICP-AES. Net intensity values were plotted against Be concentrations spiked into the sample. The correlation coefficient was 0.9987 and the concentration of Be in the sample was calculated to be 13.49 ppm, which agrees with the values obtained above.

The samples were analysed again by ICP-AES using the 313.04 nm line and applying the correction for V interference. The V 310.23 nm line was used with background correction on one side of the peak since aluminium causes large background shifts. The V 309.31 nm line suffers from

spectral interference by high Al concentrations (Al 309.28 nm) and the V 292.40 nm line is interfered with by an iron line. Since the Be 313.11 nm line has less sensitivity two samples prepared for boron analysis (chapter 7.1) were analysed at this wavelength using the Ti 334.94 nm line (low observation height of 8 mm to reduce its sensitivity) for correction.

The results were 12.16 and 12.36 ppm Be respectively. the relative standard deviation in the analysis if interferences are not corrected was about 10%.

The uncertified value quoted by NBS [25] for this reference material is 12 ppm.

The beryllium concentration in 30 South African fly ash samples were found to vary from 5.5 to 14.3 ppm. The samples were prepared in the digestion bombs by the method described above.

It was concluded that both Be lines are suitable for trace analysis of fly ash samples. The choice of one line depends on the Be, V and Ti concentrations present in the samples.

# CHAPTER 10. DETERMINATION OF POTASSIUM AND LITHIUM BY ICP-AES

## 10.1 Potassium determination

During major element analyses of coal and fly ash (chapter 5), potassium could not be determined because of the low sensitivity found at the 766.49 nm line. The other lines at 404.72 and 404.71 nm were also found to lack sensitivity. The photomultiplier tube in one of the monochromators (R106, Hamamatshu TV Co, Ltd, supplied by the manufacturers) of 160 ~ 650 nm was replaced by a R955 tube sensitive over a wider range of 160 ~ 930 nm. The spectral responses of the two tubes are shown in figure 10.1.

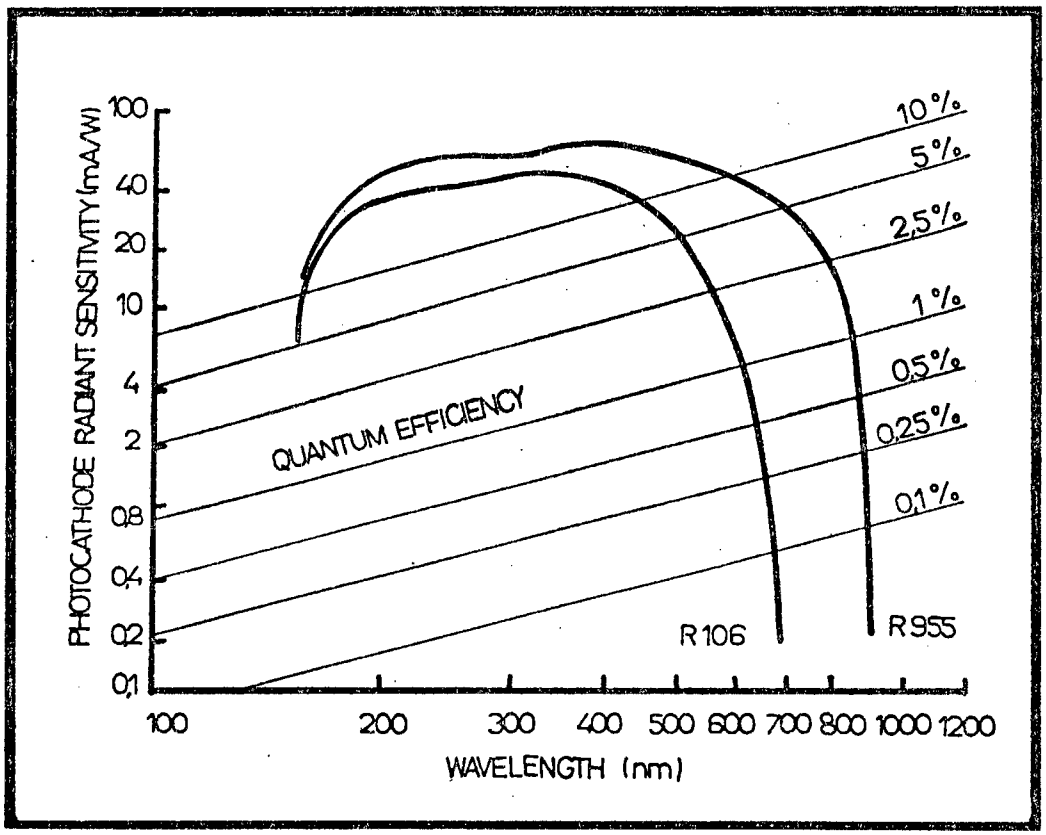


Figure 10.1 Photomultiplier responses.

A 100 ppm potassium standard was used to optimize the ICP parameter. Like the other alkali metals, maximum emission was found to occur at low observation heights. The best intensities were obtained at low powers (1), high nebulizer driving pressures (40 psi) and high sample flow rates (1.8 ml $min^{-1}$) which suggests that the mechanism of atomic emission by this element of low excitation energy is more efficient under "cooler" conditions. Cross flow nebulizers perform better at high driving pressures, the signal intensity is more stable and better precision is obtained. Under those conditions, the presence of sodium was found to enhance K emission, especially at low observation heights (0 to 10 nm). This is illustrated in figure 10.2.

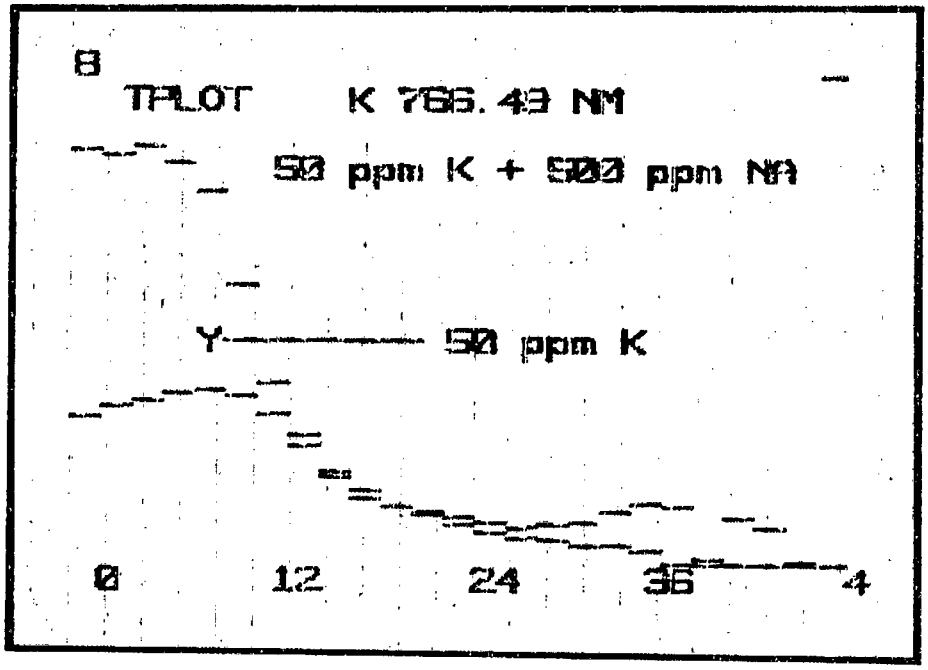


Figure 10.2 Enhancement of K emission by Na.

The effect is minimal between 12 and 24 mm. Since in coal and ashes the ratio of sodium to potassium is much smaller than 10, interference by Na on potassium determination is not a problem and 14 mm observation height can be used.

Serious spectral interference by magnesium on the potassium line is illustrated in figure 10.3. However, a TPLOT in figure 10.4 of the two elements shows that under the conditions used, magnesium emits more strongly higher in the plasma. Thus, when the emission is measured lower in the plasma, interference is diminished. The effect is shown in figure 10.5.

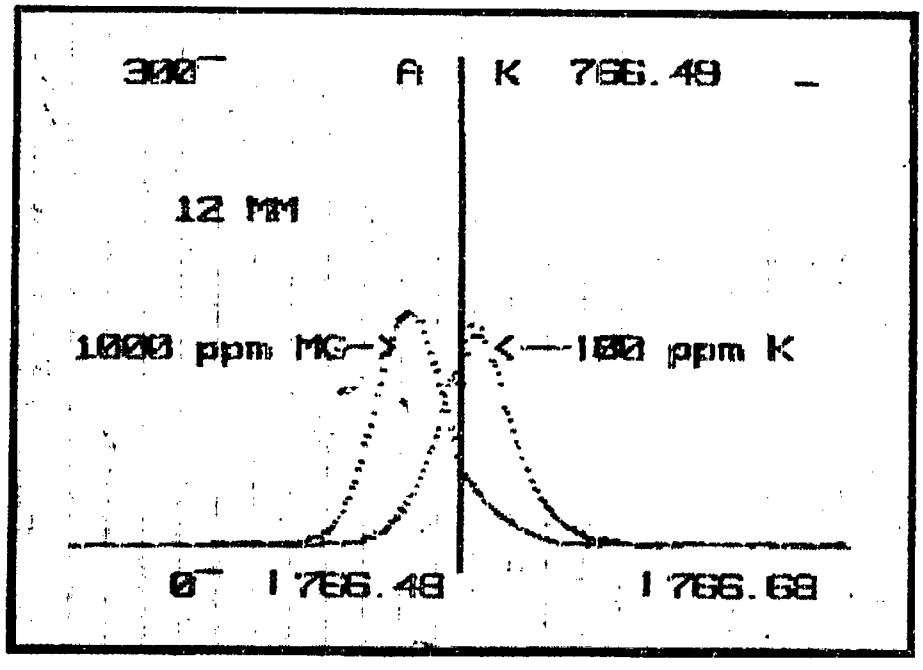


Figure 10.3 Interference of Mg on K.
at 12 mm observation height.

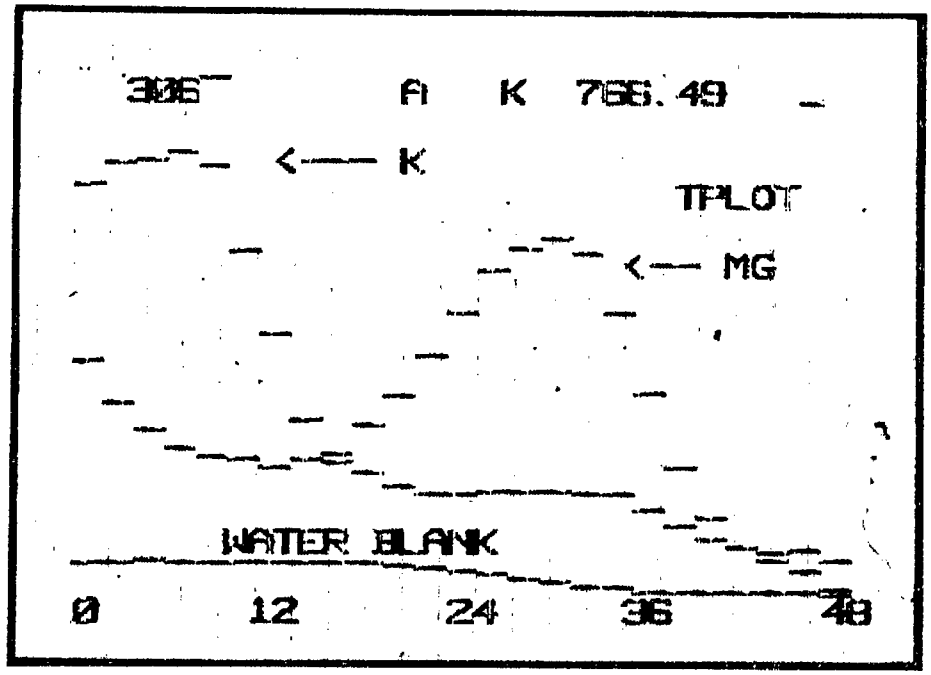


Figure 10.4 TPLOTS for K and Mg.

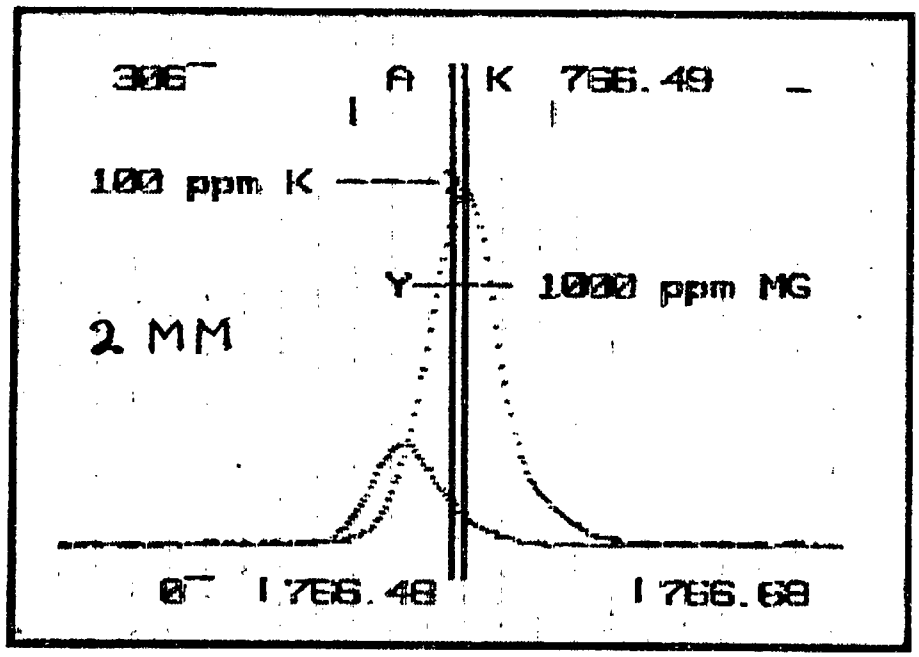


Figure 10.5 Interference of Mg on K at 2 mm observation height.

The IEC values calculated for a 1000 ppm Mg solution at 2 and 12 mm above the coil were 33.0 and 114.2 respectively.

The spectral characteristics in table 10.1 at 2 and 12 mm were calculated using the following parameters: Power 1, Nebuliser driving pressure 40 psi, sample flow rate 1.8 ml/min.

**Table 10.1** K spectral characteristics.

| Obs Ht (mm) | $C_A$ (ppm) | $I_N/I_B$ | $C_L$ (ppm) |
|---|---|---|---|
| 2 | 100 | 9.3 | 0.094 |
| 12 | 100 | 9.4 | 0.077 |

The $I_N/I_B$ and $C_L$ values are similar at the two observation heights since although the $I_A$ values at 2 mm are larger, the blank intensity is also larger and slightly better precision is obtained at 12 mm.

## 10.2 Lithium determination

Lithium is present in coal and ashes at trace levels. The possibilities of determining this element at low levels were investigated. Several lines are available for analysis and these are listed in table 10.2. spectral characteristics obtained from different sources are also listed.

Table 10.2 Li emission lines.

| Spectral line (nm) | $C_L$ (ppm) | $I_N/I_B$ [45] (for 100 ppm Li) |
|---|---|---|
| 670.78 I | 0.013 [79] | - |
| 610.36 I | 0.043 [79] | - |
| 460.29 I | 1.35 [79] | 3.5 |
| 323.26 I | 1.1 [45] | 2.8 |
| 274.12 I | 1.6 [45] | 1.9 |

For this work only the most sensitive line at 670.78 nm was investigated. Standard solutions were used to optimize the ICP parameters. A remarkable dependence of the stability of the signal (precision) with (i) the nebulizer driving pressure, and (ii) the viewing height above the torch was experienced. Figure 10.6 shows TPLOTS for a 10 ppm Li standard solution at three different nebulizer pressures. At 35 psi, emission is seen to nearly double at low observation heights. The variation of signal stability with change of viewing height in the plasma is shown in figure 10.7.

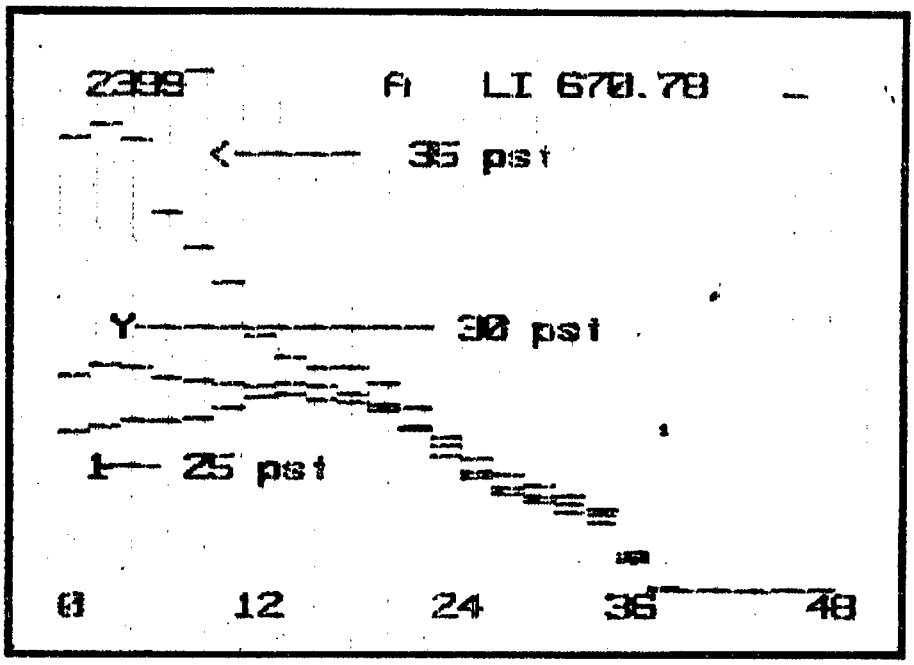


Figure 10.6 Effect of nebulizer pressure on Li emission.

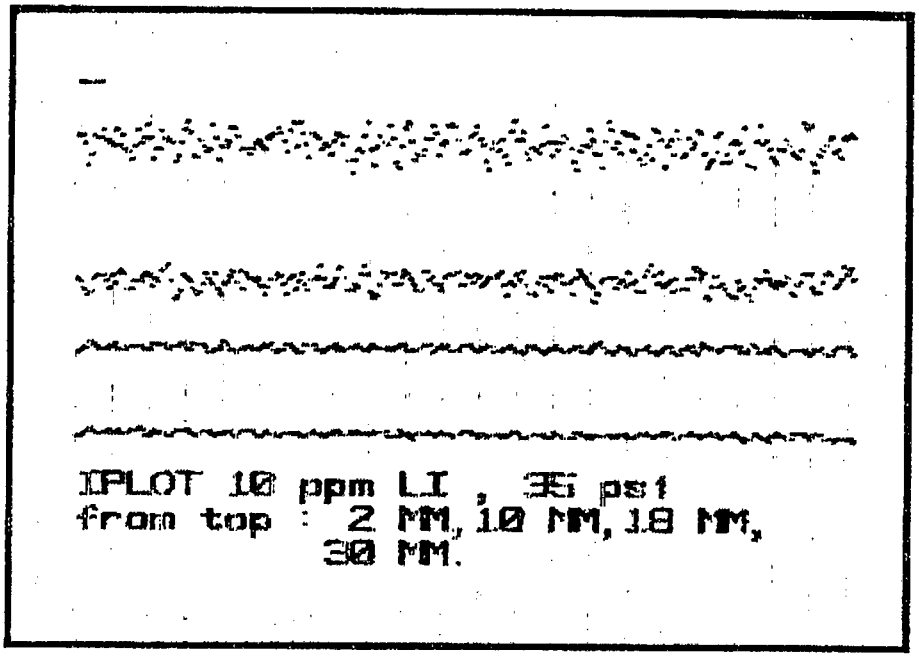


Figure 10.7 Signal stability at different viewing heights.

A 10 ppm Li standard was used to investigate the precision of analysis at different nebulizer driving pressures (25, 30, 35 psi) and viewing heights (2 to 30 mm). The results are shown in figure 10.8. Each % RSD value was calculated using 10 readings of three seconds each.

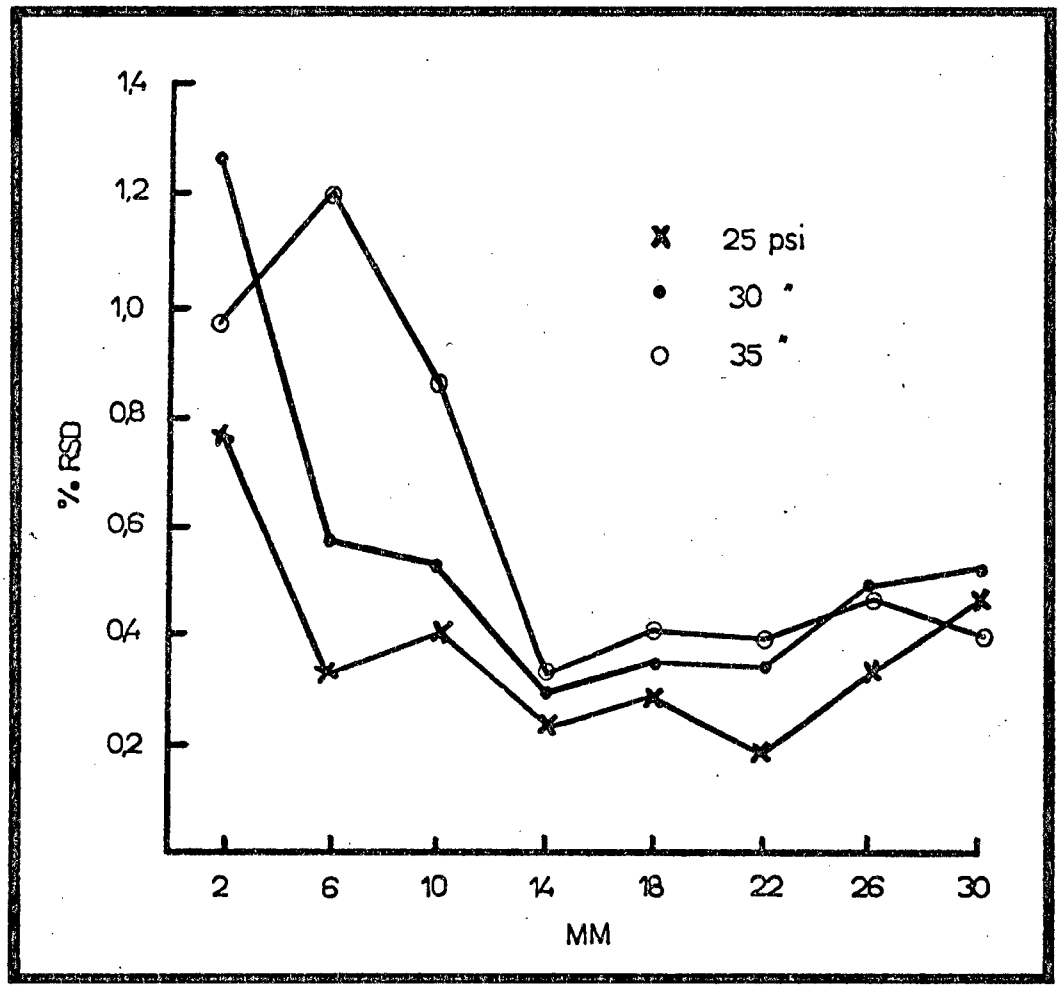


**Figure 10.8** Effects of Neb dri pressures and viewing heights on precision of analysis.

The best precision is obtained at low pressures and a viewing height of about 14 mm. The detection limit was found to be 0.008 ppm and the $I_N/I_B$ value for a 10 ppm Li solution (0.28 %RSD) was 4.2 using the following parameters:

| | |
|---|---|
| Power | 3 |
| Nebuliser Driving Pressure | 27 psi |
| Observation height | 14 mm |
| Sample flow rate | 1 ml/m |

The close dependence between the signal characteristics and ICP parameters for this element indicates that the mechanism by which emission occurs is complicated and very sensitive to slight plasma changes.

As in the case of potassium, an emission enhancement by high concentrations of sodium (500 ppm Na to 10 ppm Li) was noted at low observation heights. However, the enhancement was very small compared with K and at heights of about 14 mm was not noticeable. No other interference by other major elements was experienced.

Lithium was determined in a sea water sample directly using the parameters listed above. A plot of an aqueous Li standard and the sea water sample is shown in figure 10.9. A background shift is noted and in order to obtain an accurate analysis, background correction was used on the low wavelength side of the peak (position shown in figure 10.9).

The instrument was calibrated with a water blank and two standards (2 and 0.5 ppm Li in water).

The value obtained for two analyses of 5 readings for 5 seconds each was 0.177 $\pm$ 0.008 ppm (4.6 %RSD) which is in close agreement with reported values, eg 173 µg/l [80].

Lithium was determined in 32 South African fly ash samples using the Parr bomb dissolution method for sample preparation. The concentrations were found to vary from 65 to 402 ppm.

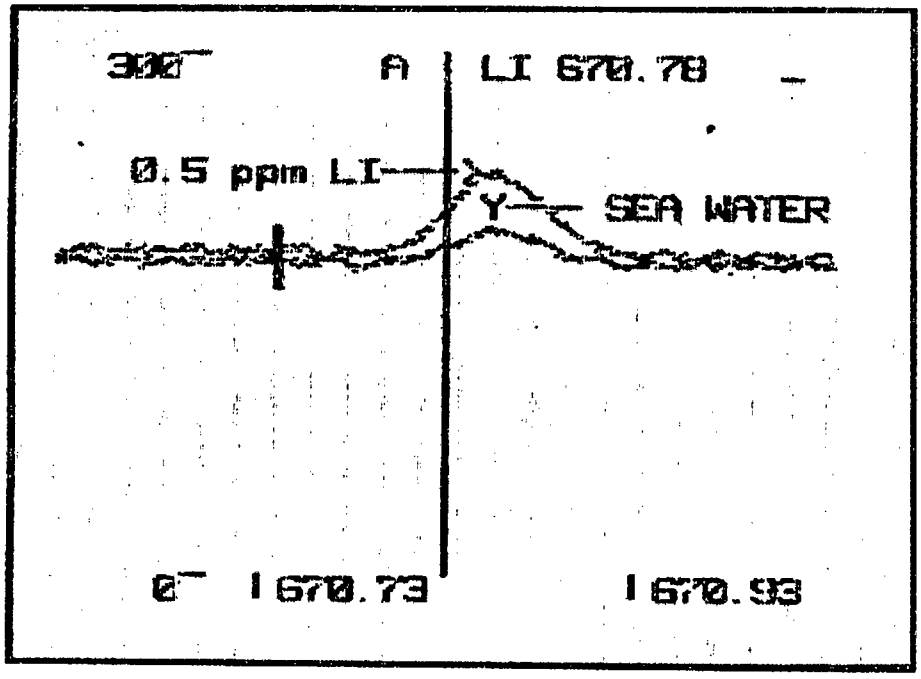


Figure 10.9 Comparison of intensity peaks for a Li standard and the sea water sample.

This investigation showed that determination of trace elements of Li in complex matrices by ICP-AES is possible. In the case of sea water no matrix matching is required if the instrumental conditions are chosen carefully and aqueous standards can be used for accurate measurements. Once again, the choice of instrumental parameters is shown to be critical for certain elements.

# CHAPTER 11. MATRIX INTERFERENCES IN ICP-AES

One of the major factors leading to the popular acceptance of ICP-AES is the claimed freedom from chemical interference in a properly optimized system. However, numerous reports have indicated that large matrix dependent changes in emission intensities do occur under certain plasma conditions. During the past decade interelement effects have been investigated [84 - 92, 95] and the general conclusion is that these effects do occur to a much lesser extent in the plasma, compared with flames used for atomic absorption and emission spectroscopy, the reason being that the higher temperature of plasma sources. Conflicting statements about observed interferences and their magnitude in different situations are common in this field of research and this is supported by the following quotations:

"These conflicting statements, often by the same authors, demonstrate that it is probably erroneous to compare the data from differently operated ICP's. Indeed, several studies show that the observed interferences depend critically on such plasma parameters as observation height, RF power and carrier gas flow rate. However, even for apparently similar conditions the observed interferences can be significantly different, even for the same laboratory and the same species studied" [93].

Koirtyohann et al [89, 94] attributed the difficulties encountered when comparing ICP's amongst authors and laboratories to the lack of a nomenclature system for various

zones of the plasma which have different properties. They suggested the following nomenclature illustrated in figure 11.1.

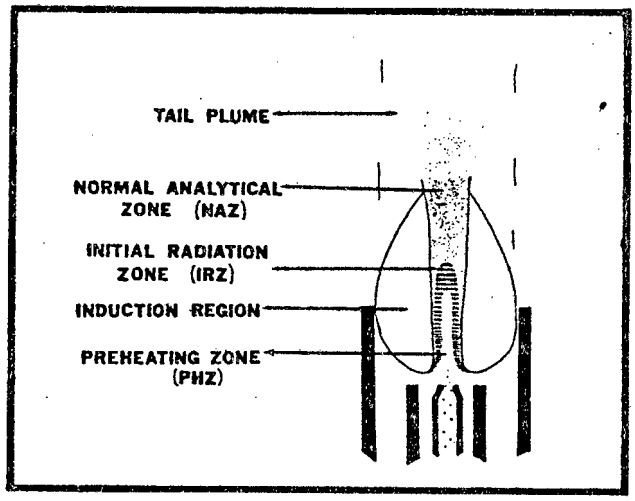


**Figure 11.1** Schematic view of a toroidal low power argon ICP and suggested nomenclature for the various zones [89, 94].

Blades and Horlick [90] surveyed reported interferences from easily ionizable element (EIE) matrices in ICP-AES and they quoted the following:

"A literature survey of the effects of an excess of an easily ionizable element (EIE) such as Na, K or Cs as a concomitant on analyte emission intensity in ICPs is a study in confusion Virtually every ICP spectroscopist has studied the effect of this type of matrix, and the literature abounds with tables and graphs on the magnitude and characteristic of the effect. The driving force for these studies is the fact that EIEs, especially Na and K, turn up in a variety of natural matrices for which emission spectroscopy is used as an analytical probe. These include animal and plant materials, blood, seawater and geological samples.

The sources of much of this confusion are two fold. First, much of the data which have appeared has not been consistent, some investigators observing analyte emission 'enhancement', some observing 'depressions', and some 'no effect'. Secondly, there is still no satisfactory explanation for the observed effects at a fundamental level".

To clarify some of these observations and offer rational arguments on the nature of the effect, a spacial study of the effect was undertaken by the authors. They discussed possible mechanisms of EIE interferences, eg shifts in ionization equilibrium, enhanced collisional excitation, volatilization effects, ambipolar diffusion, and nebulizer effects. The dependence of the effect, eg depression or enhancement of signal, on ICP parameters and spatial position observed was illustrated. For example, enhancement of the emission intensities was found to occur at lower regions of the plasma and depression of the intensities at higher regions.

The enhancement of boron and potassium emission intensities by large concentrations of sodium at lower observation heights has been illustrated in chapters 7.4 and 10.1 respectively. An experiment was done to investigate the effects of high sodium (EIE) concentrations on several elemental emission lines. Both atomic and ionic lines of Ca, Cr, Zn and Ni, two atomic B lines and one atomic V line were used for the investigation.

Solution preparations:

1. Solution A : 40 g NaOH (Analar, BDH) + 50 ml conc $HNO_3$ in 200 ml water.

2. 1% TX-100.

3. 100 ml of the following solutions contained 5 ml 1% TX-100:

| Solution # | Vol of A per 100 ml (ml) | |
|---|---|---|
| 1 | 0.5 | + 0.5 ml 1000 ppm elements |
| 2 | 1.0 | |
| 3 | 5.0 | |
| 4 | 10.0 | |
| 5 | 15.0 | |
| 6 | 20.0 | |
| 7 | 30.0 | |
| 8 | 0.5 | Na blanks |
| 9 | 1.0 | |
| 10 | 5.0 | |
| 11 | 10.0 | |
| 12 | 15.0 | |
| 13 | 20.0 | |
| 14 | 30.0 | |
| 15 | - | + 0.5 ml 1000 ppm elements |
| 16 | - | water blank |

These solutions (3) were analysed using the analytical programme in figure 11.2 in the following order:

16, 15, 8, 1, 9, 2, 10, 3, 11, 4, 12, 5, 13, 6, 14, 7.

Between each analysis, adequate washing with #16 was done. (The deep orange glow due to Na in the plasma can be observed visually should large memory effects occur).

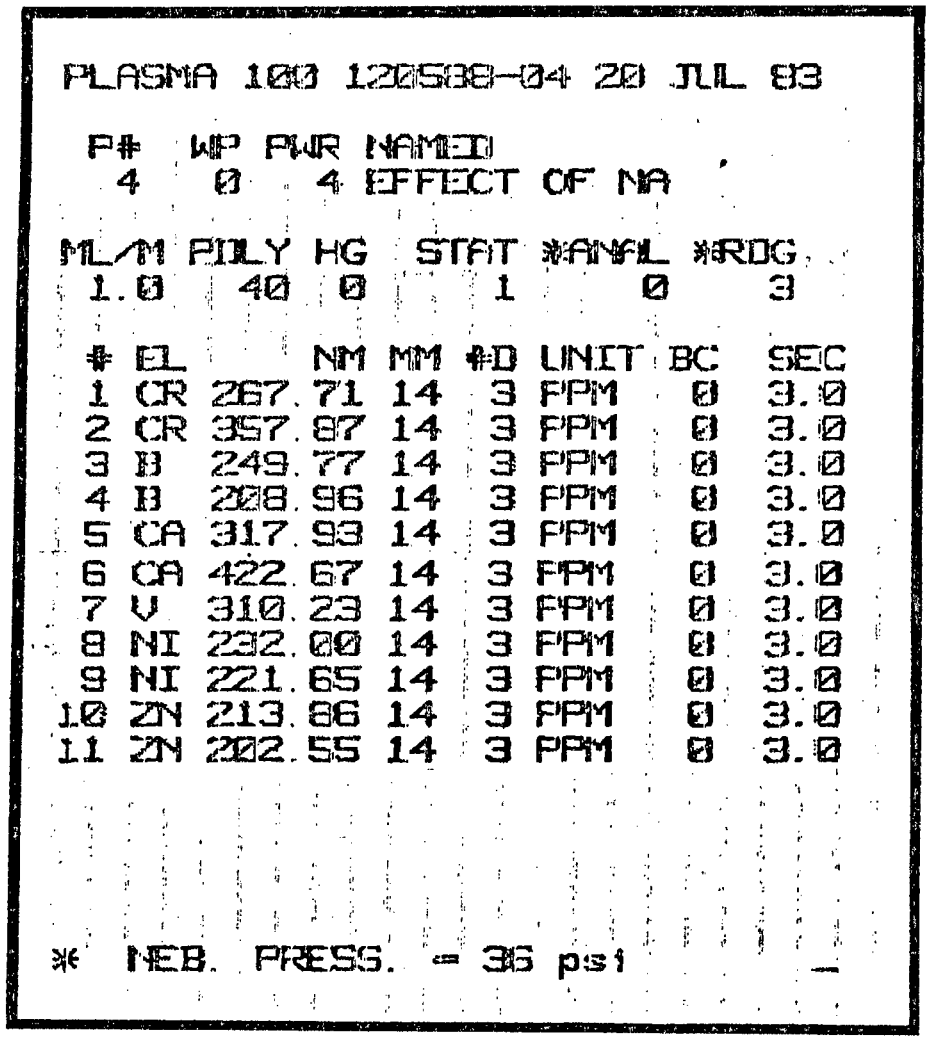

PLASMA 100 120588-04 20 JUL 88

| P# | WP | PWR | NAME |
|---|---|---|---|
| 4 | 0 | 4 | EFFECT OF NA |

| ML/M | PRLY | HG | STAT | *AVG | *RDG |
|---|---|---|---|---|---|
| 1.0 | 40 | 0 | 1 | 0 | 3 |

| # | EL | NM | MM | #D | UNIT | BC | SEC |
|---|---|---|---|---|---|---|---|
| 1 | CR | 267.71 | 14 | 3 | PPM | 0 | 3.0 |
| 2 | CR | 357.87 | 14 | 3 | PPM | 0 | 3.0 |
| 3 | B | 249.77 | 14 | 3 | PPM | 0 | 3.0 |
| 4 | B | 208.96 | 14 | 3 | PPM | 0 | 3.0 |
| 5 | CA | 317.93 | 14 | 3 | PPM | 0 | 3.0 |
| 6 | CA | 422.67 | 14 | 3 | PPM | 0 | 3.0 |
| 7 | V | 310.23 | 14 | 3 | PPM | 0 | 3.0 |
| 8 | NI | 232.00 | 14 | 3 | PPM | 0 | 3.0 |
| 9 | NI | 221.65 | 14 | 3 | PPM | 0 | 3.0 |
| 10 | ZN | 213.86 | 14 | 3 | PPM | 0 | 3.0 |
| 11 | ZN | 202.55 | 14 | 3 | PPM | 0 | 3.0 |

* NEB. PRESS. = 35 psi

Figure 11.2 Analytical programme.

The results obtained are shown in figures 11.3 to 11.8. Plots of relative intensities for analytes and blanks are shown:

(A) $(I_N)_{Na} / (I_N)_{aq}$ v/s [Na]

(B) $(I_B)_{Na} / (I_B)_{aq}$ v/s [Na]

$(I_N)_{Na}$ = net intensities for analyte signal in the presence of Na.

$(I_N)_{aq}$ = net intensities for analyte signal in the absence of Na.

$(I_B)_{Na}$ = sodium blanks.

$(I_B)_{aq}$ = water blank, ie #16.

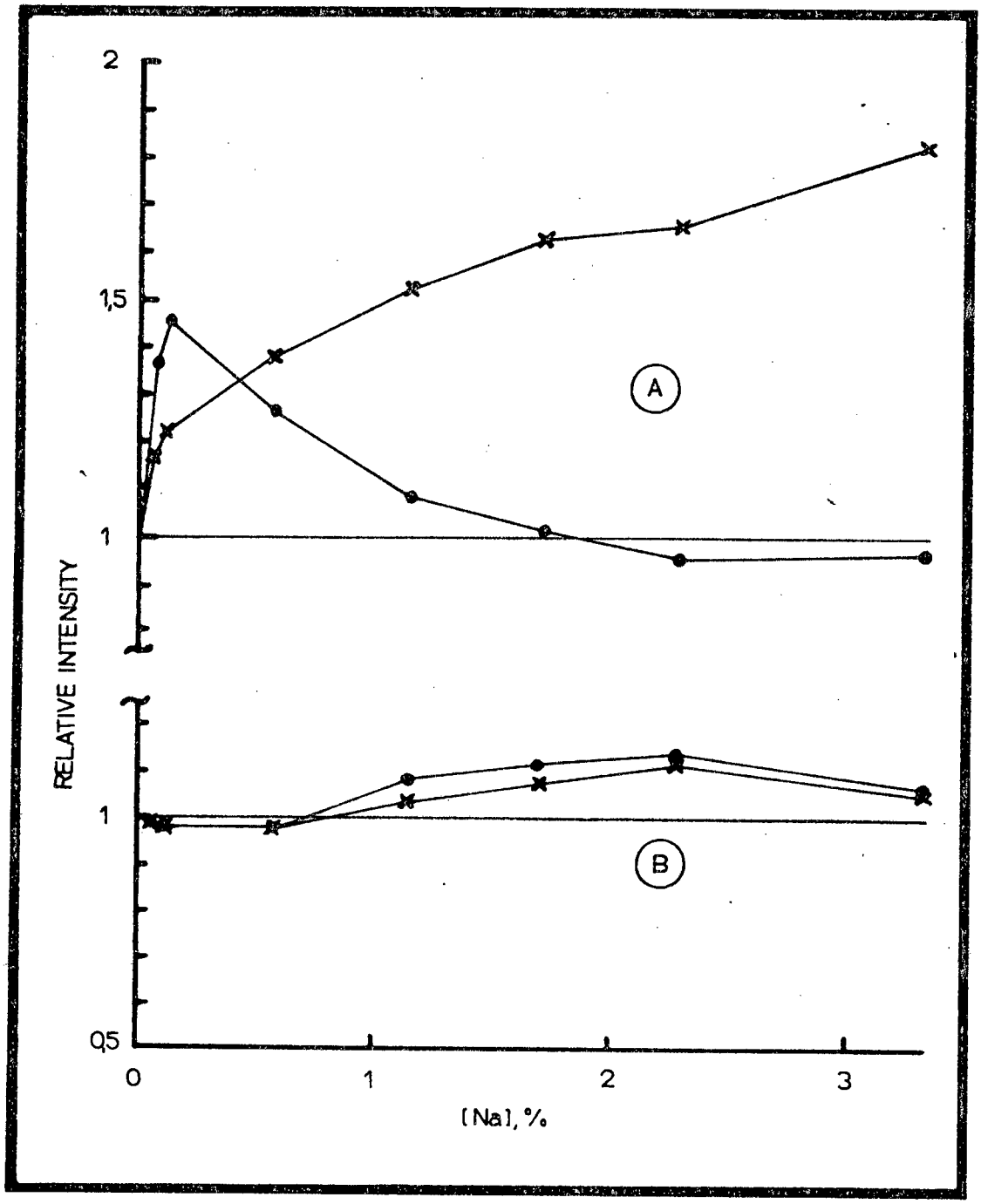


Figure 11.3 Effect of Na on (A) Ca, (B) blank emission.
. Ca I 422.67 nm
x Ca II 317.93 nm

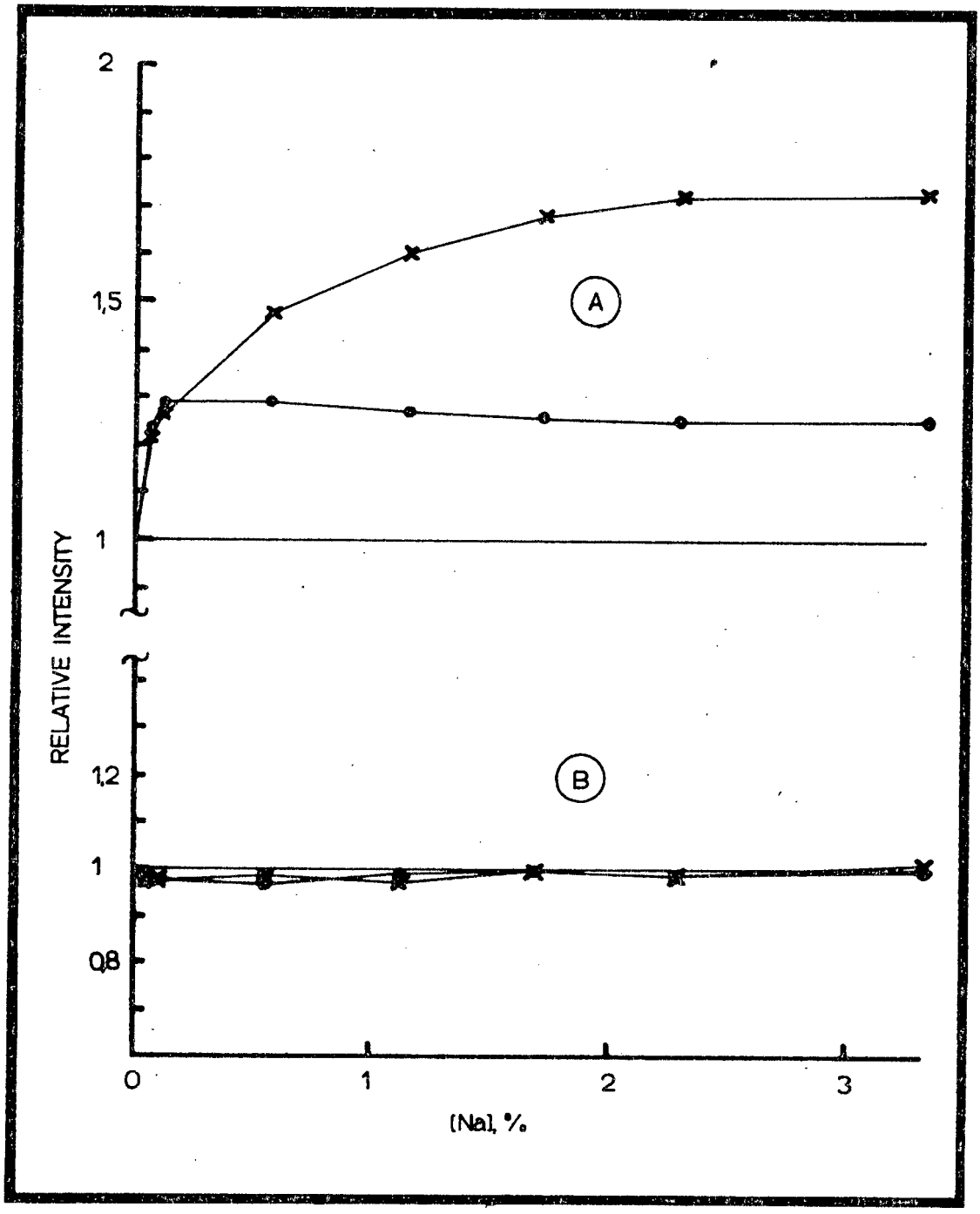


Figure 11.4 Effect of Na on (A) Cr, (B) blank emission.
. Cr I 357.87 nm
x Cr II 267.71 nm

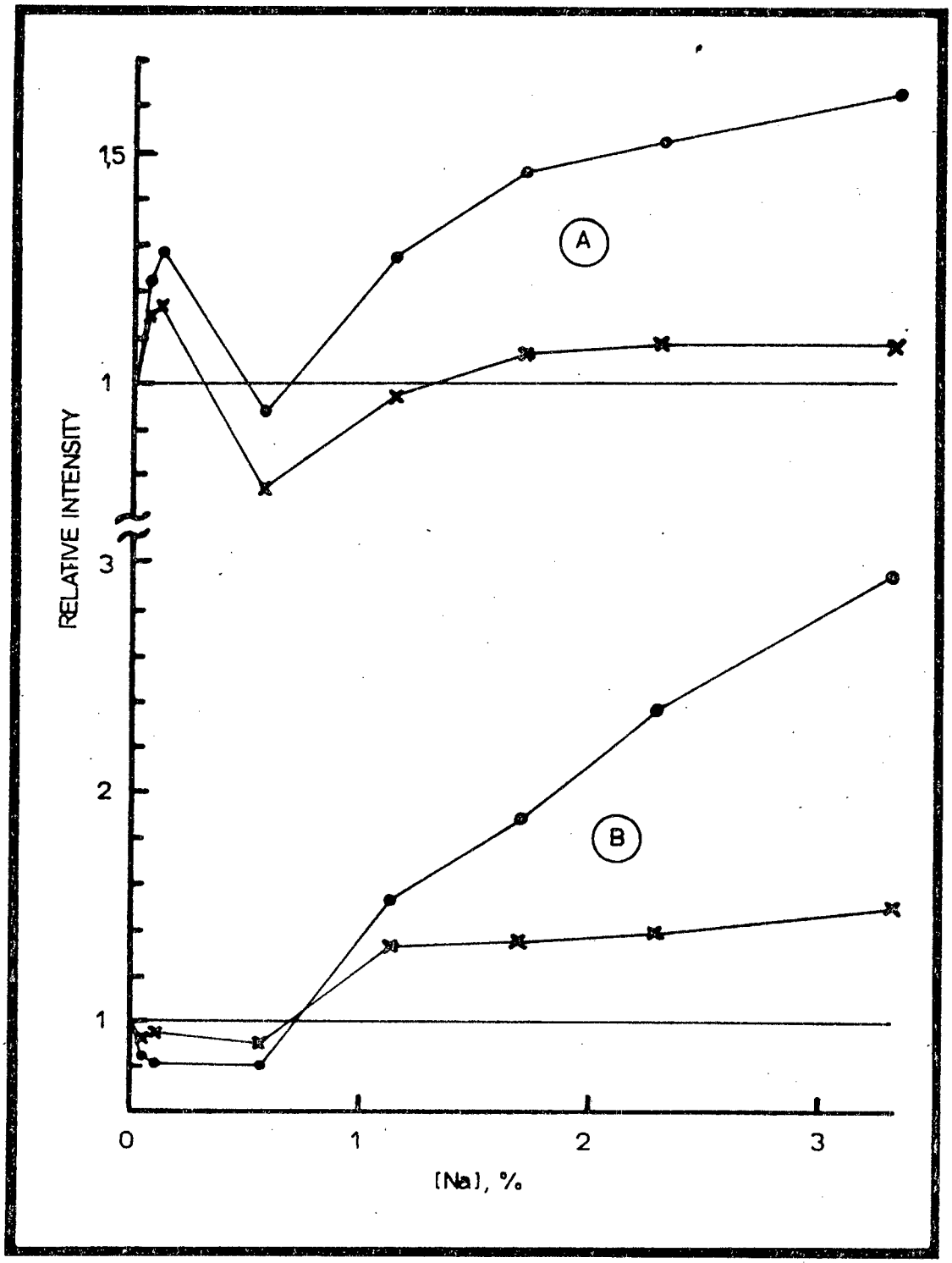


Figure 11.5 Effect of Na on (A) Zn, (B) blank emission.
. Zn I 213.86 nm
x Zn II 202.55 nm

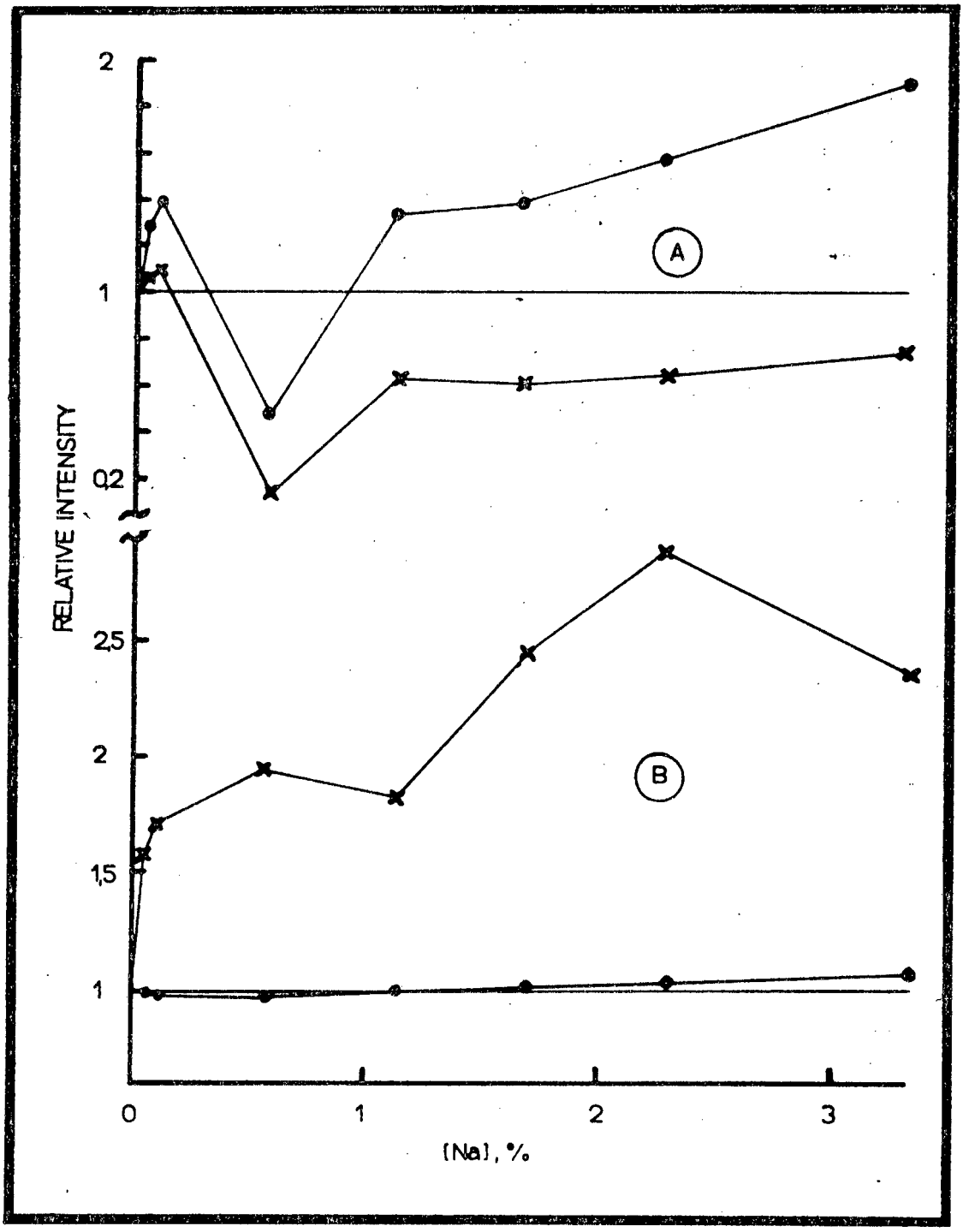


Figure 11.6 Effect of Na on (A) Ni, (B) blank emission.
. Ni I 232.00 nm
x Ni II 221.65 nm

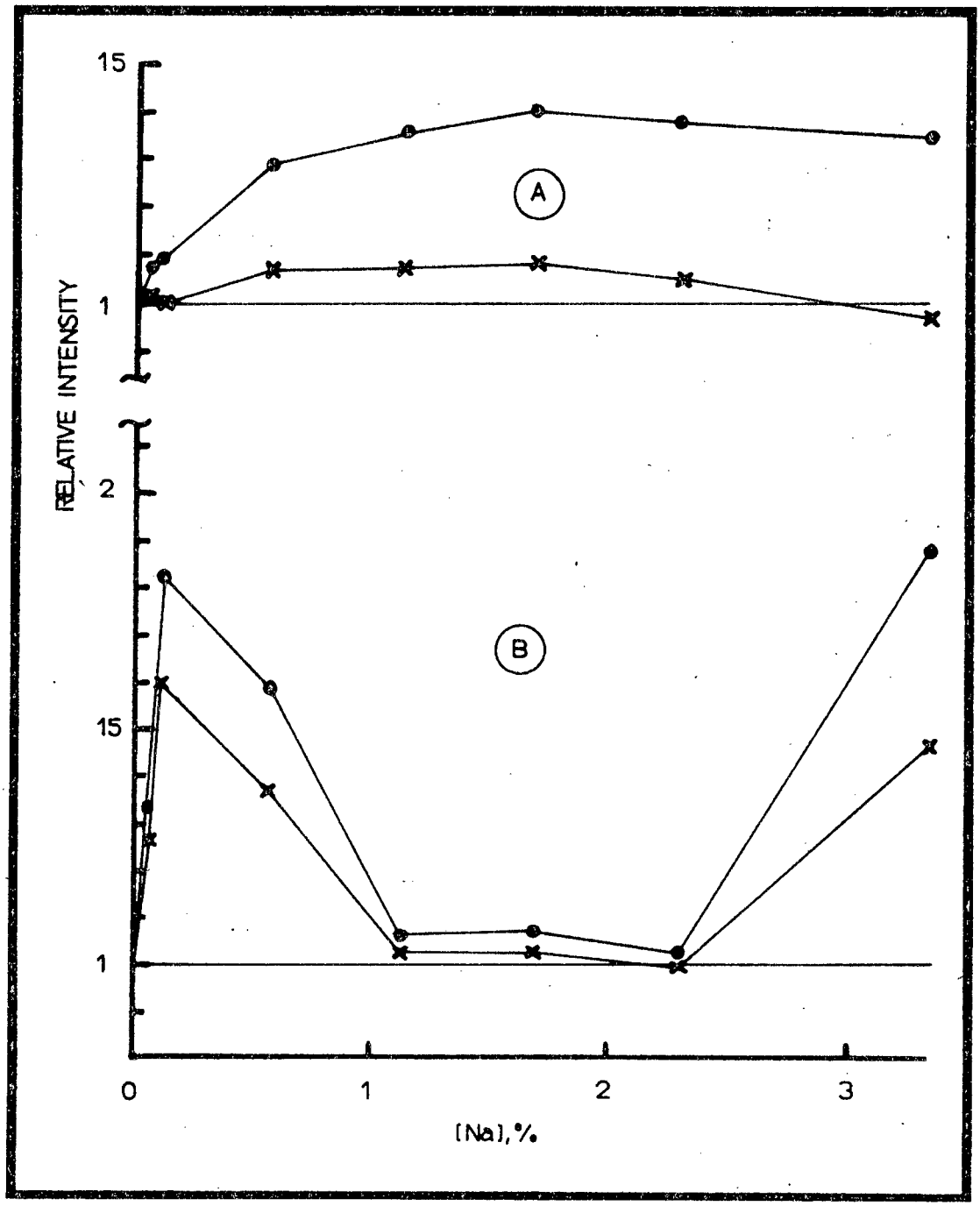


Figure 11.7 Effect of Na on (A) B, (B) blank emission.
. B I 249.77 nm
x B I 208.96 nm

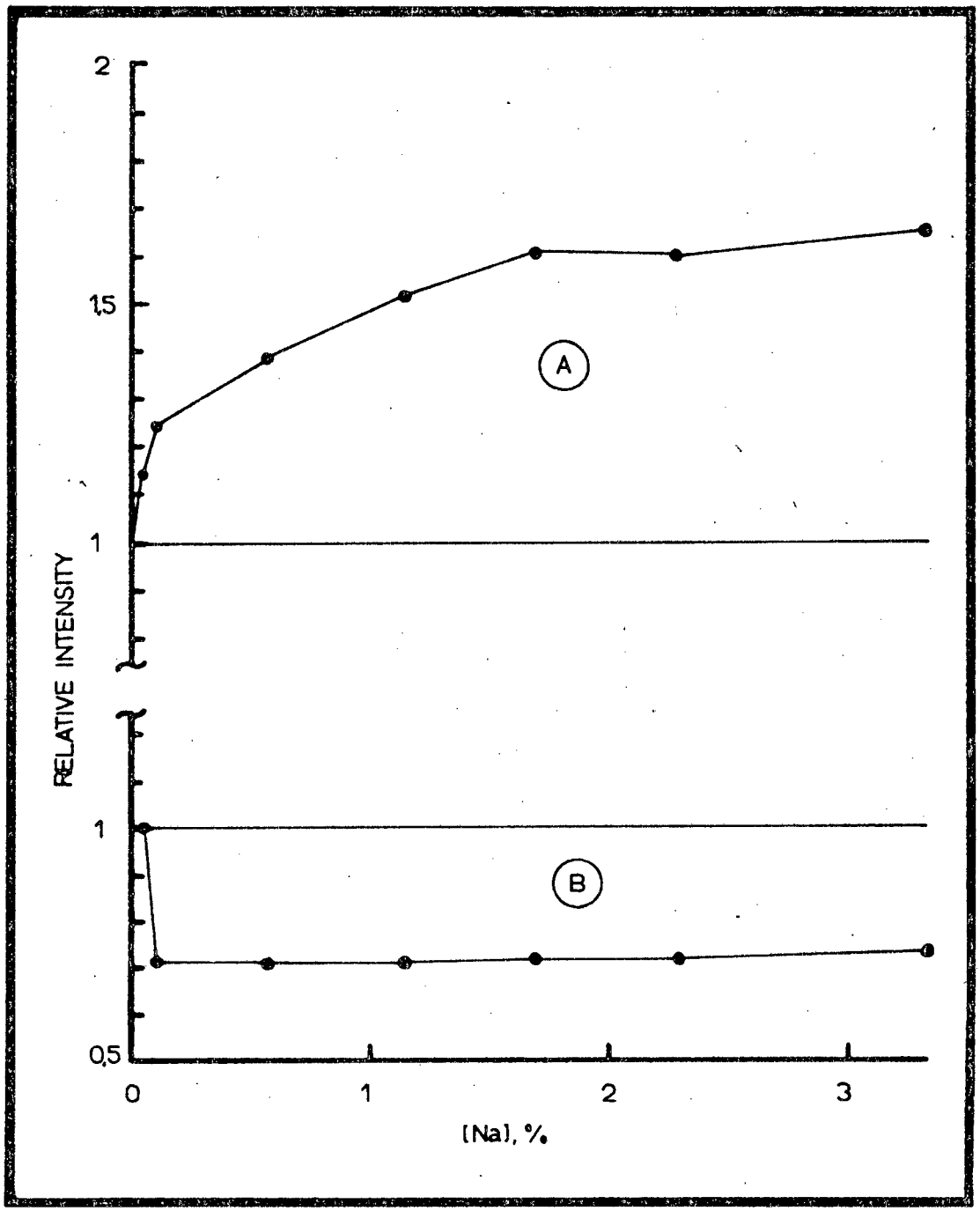


Figure 11.8 Effect of Na on (A) V, (B) blank emission.
. V II 309.31 nm

In general, all the lines showed enhancement of the emission intensities. The Ca I line showed a sharp enhancement at low %Na and the intensities decreased with higher %Na and a small depression was obtained at concentrations larger than 1.5% Na. The atomic and ionic lines of Zn and Ni are shown to be enhanced at low %Na, followed by a depression at concentrations of about 0.5% Na and increase in intensities at higher %Na. The nickel II line displayed a depression of its intensity at levels larger than about 0.15% Na. The ionic linies of Ca and Cr showed larger enhancement than the atomic lines. The opposite was found with Zn and Ni lines. A comparison of both boron atomic lines shows a larger enhancement of intensities for the 249.77 nm line.

The blank intensities for the Cr lines and the atomic Ni line showed very small changes and the Ca lines showed a small depression followed by small enhancement at higher % Na. The other blank intensities generally showed enhancements except for the V line.

From these observations, no general trend seems to be present except that the magnitude of the effect seems to differ for atomic and ionic lines. However, the two boron atomic lines are affected to different extents which is probably related to their different excitation potentials.

The explanation of these results is obviously not simple. The observations are thought to be the result of a complex interaction of several mechanisms rather than a single dominant one. Separation of these would be practically impossible. For example, if a shift in ionization

equilibrium is considered, an increase in electron density of the plasma would cause systematic enhancement of atomic emission and depression in ionic emission which is not always observed. Enhancement due to increased collision rate by an increase in electron density seems to be significant since both atomic and ionic lines are enhanced. The problem is further complicated by the fact that each region in the plasma has different properties which are related to the instrumental parameters. This means that the effect and magnitude of an interference in a plasma system will vary with the chosen instrumental parameters. For example, the use of a different torch with a different argon flow rate will definitely require re-investigation of an observed effect. Probably the best solution in difficult situations would be to "matrix-match" the samples, working standards and the blank. Although extensive research is required to improve instrumental designs towards better understanding of certain effects in plasma systems, the analyst using commercial instruments should be more concerned with the proper recognition and investigation of such interferences in order to obtain precise and accurate results.

The influence of varying acid concentration on line intensity has been reported by many authors [96, 97, 47]. It is thought that the cause of a depression of intensity is due to lower nebulization efficiency in the presence of acids and related to the transport of the aerosol into the plasma. The effect of nitric acid on two zinc and two calcium atomic and ionic lines and sulfuric acid on the two zinc lines are shown in figures 11.9 and 11.10. The difference in magnitude of the effect between the atomic and ionic calcium line seems to

indicate that the effect might be related to atomization or ionization since the intensities of the two lines were measured at the same time. Up to 30% HCl and 10% HF had very small effect (<5%) on the net intensities of the zinc lines. These illustrate the importance of acid matching the standards and blanks with the samples.

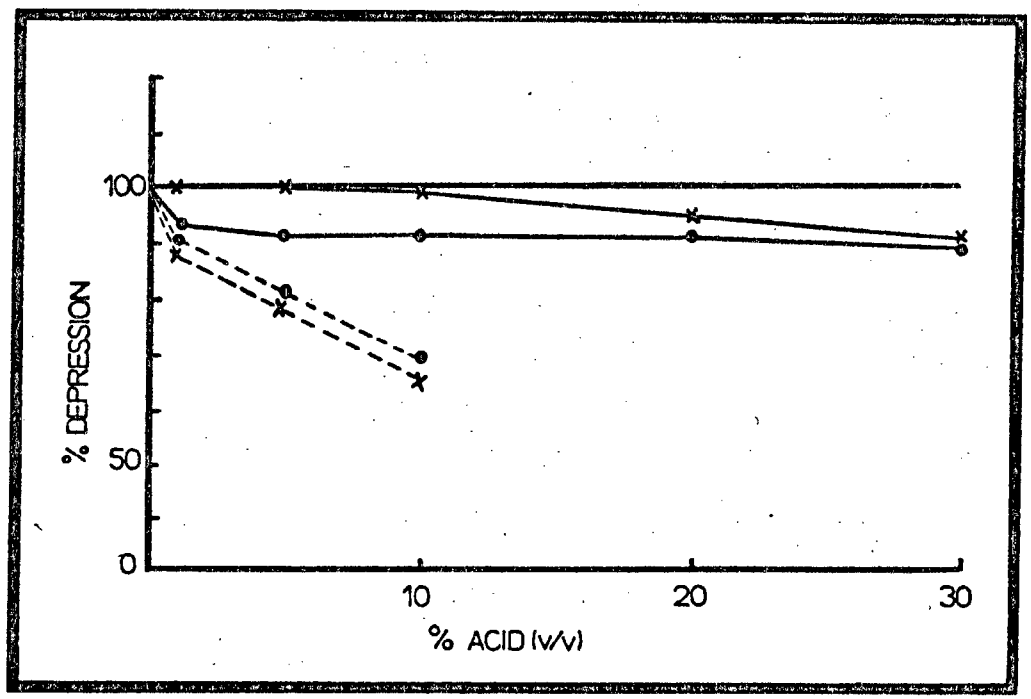


Figure 11.9 Plot of percent depression of Zinc II 202.55 nm (·) and Zinc I 213.86 nm (x) with acid concentration
_____ $HNO_3$
----- $H_2SO_4$

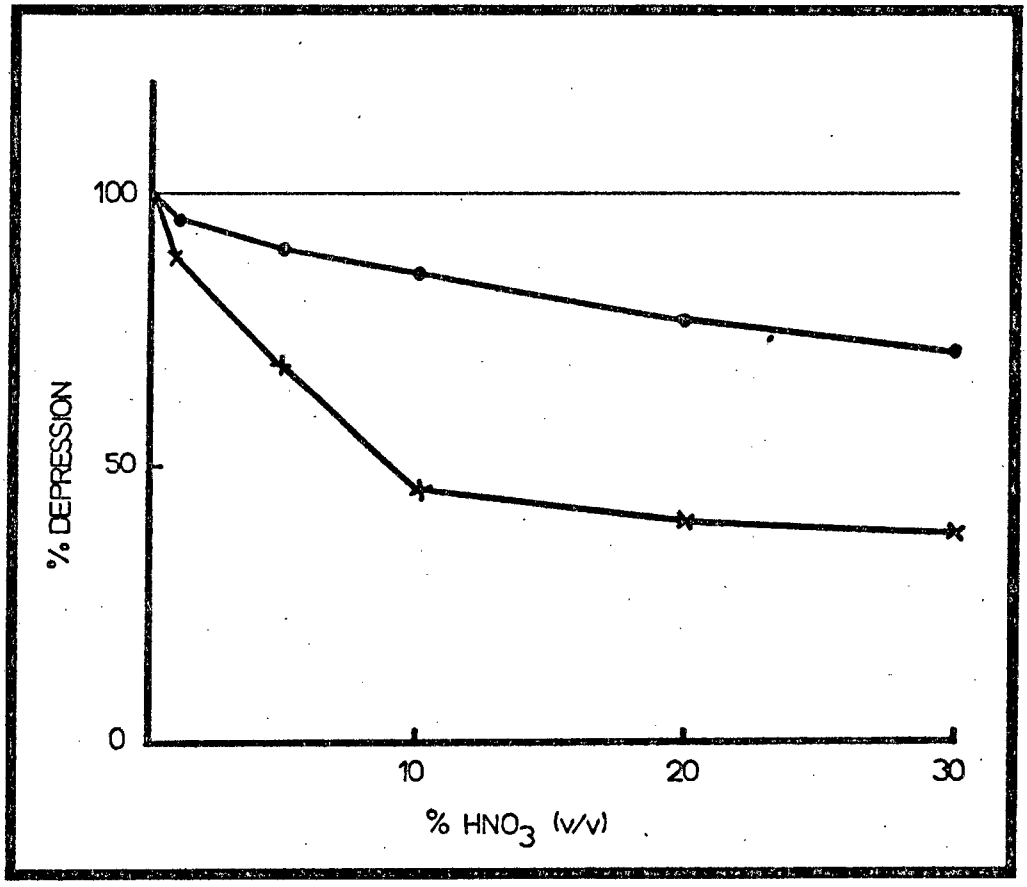


Figure 11.10 Plot of percent depression of Calcium I 422.67 nm(·) and II 317.93 nm (x) with acid concentration.

# CHAPTER 12. CONCLUSIONS

This work has demonstrated the wide applicability of ICP-AES for the determination of a large number of elements in many sample matrices. Although less attention was paid to FAAS during this work, its advantages for trace element analysis must be emphasized. Some trace elements such as Hg, Pt, Mo, As, Se, Sn, and Pb are present at such low levels in coal that the final concentrations in samples prepared, as at present, would be near detection limits for ICP-AES and the numerous spectral interferences by major elements at the most sensitive emission lines would make their determination difficult or almost impossible unless some preconcentration and separation steps are involved. FAAS offers detection limits which range from 60 to 3500 times smaller than those attainable with ICP-AES for the above elements. Dilute solutions can be used directly, using normal, dissolution methods, for example acid dissolution in the digestion bombs. The development of the slurry injection technique has proved useful and is already being applied to the determination of other elements in different matrices, eg Be in fly ash and coal ash.

The choice between AAS or ICP-AES for coal and ash analysis depends on many factors, eg the number of elements to be determined, the number of samples, the accuracy of the analysis required. ICP-AES has definite advantages over AAS when large numbers of elements are to be determined routinely. Moderately accurate results can be obtained with

only a few seconds reading time for each element. Many problems with complicated matrices such as coal and fly ash occur in flame AAS analysis and release agents must be added for certain elements. Many matrix interferences have been found in FAAS and these must be checked carefully when developing analytical methods. The numerous interferences in ICP-AES have been demonstrated. Although background shifts that are frequently encountered can be easily corrected for by most modern instruments, spectral interferences remain the most critical problem in emission spectroscopy, especially when trace level determinations are required. The steps required for proper investigation of interferences from a complicated sample pose a difficult task for the analyst and a fair amount of experience is essential. As was shown, the graphic facilities in modern instruments makes this investigation simpler and should help to identify many spectral overlaps that have not yet been reported. Because of the need to investigate interference, method development for ICP-AES is time consuming.

The sensitivity for Be by ICP-AES was exceptionally good and trace determination of this element in many environmental samples is possible. Boron determination at low levels is another advantage of ICP-AES and since very little information on boron concentrations in South African coal and ash samples is available, this technique will be put to good use. Lithium is another element of interest and no difficulties in determining this element in fly ash were encountered.

The aim now is to use a multielement programme for major and trace elements determination. One of the problems

associated with multielement programmes is in the preparation of multielement standards since high purity solutions are required and some elements are not mutually compatible. Calibration of each programme line (ie, each element) individually is possible but this is a lengthy procedure. The use of a well characterized sample as a standard is probably the best solution. In that respect, the availability of standard reference materials with certified values for the elements of interest, is highly desirable. For example, no data for beryllium concentrations in the NBS-SRM coal samples were available and lithium concentrations are largely unknown. The lack of information on certain elemental concentrations makes it difficult for the analyst to test the accuracy of a new method.

Some recommendations concerning ICP-AES analysis can be summarised here:

1. Calibration drift is frequent and must be monitored especially when low concentration levels are measured.

2. For some elements the instrumental parameters are critical for good precision and accuracy and the instrumental parameters must be carefully optimized.

3. Memory effects in the torch-nebulizer system occur unexpectedly and must be investigated. Some examples are B and Si, while high salt concentrations (eg NaCl) tend to remain in the system for long periods.

   The use of different aqueous solutions has been shown to diminish or prevent memory effects. Long washing times and the use of "alternate blank routine" is useful.

4. Nebulization efficiency can be improved by the use of a surfactant and the adjustment of the cross flow nebulizer is critical for obtaining good precision.

5. High acid concentrations (eg, 10% HF, $HNO_3$) can be aspirated, preferably using a surfactant, but depression of signals (eg, by 10% $HNO_3$ on Ca, Mg and P emission) and other physical interferences must be investigated. Acid matching of standards, blanks and samples is the easiest solution.

6. It is suggested that correction factors be recalculated before analysis since they will change from day to day, and especially after realigning the torch and nebulizer system or any other alteration or adjustment to the instrument.

7. Calibration can be done with two points, ie a blank and a standard but the linearity up to the high standard must be ascertained. Experience has shown that it is wisest to calibrate the instrument with several standards (eg, 5) checking the linearity of the calibration curve and then recalibrating with only the blank and the highest standard which can be freshly prepared for subsequent analysis.

8. Stabilization time of the plasma must be allowed (10 to 15 minutes after igniting the torch) and when varying certain parameters such as the torch power and nebulizer driving pressure, at least one minute stabilization is usually necessary before investigating the effects of such a change or taking any reading.

9. High powers and high nebulizer pressures are recommended for samples containing high dissolved solids and proper washing is needed at frequent intervals to avoid clogging of the system. The sample flow rate can also be decreased.

10. When using low powers (eg, power 1), liquid must always be aspirated to avoid air entering the system and possibly extinguishing the plasma.

    Finally, the torch-nebulizer system should be cleaned (eg, by soaking in an ultrasonic bath containing a detergent) periodically for optimum performance and especially after running samples containing organics.

Although little work was done with organics, the plasma was found to be stable when aspirating xylene solutions, water saturated with methylisobutylketone (MIBK) and hexane. Power 3 and 1.5 ml/min sample flow rates could be used. The determination of Sn and Ru in those solutions was shown to be possible.

The use of internal standards to improve precision and accuracy in ICP-AES has been discussed by many authors, eg [81], and its usefulness seems to be critically dependent on the choice of analyte/internal standard emission line pairs. This was not investigated here and it might help improve trace element analysis in complex samples.

The acid dissolution procedures for sample preparation have been shown to be satisfactory. However, they are time consuming and are not suitable for routine analysis of very large numbers of samples unless the laboratory has a large

number of bombs available. A fusion method using NaOH is being investigated and preliminary work has shown some promise. It is fast and four samples can be prepared in less than half an hour.

Future work should include determination of Li, Be and B in South African coal and ash samples, boron leaching from coal ash which is an interesting environmental study fundamental interference problems in ICP-AES and, possibly, the coupling of a graphite furnace to the ICP for investigating the volatility of trace elements from coal under different temperature cycles.

# CHAPTER 13. REFERENCES


[1] S TORREY, Trace contaminants from coal, Pollution Technology Review No 50, Noyes Data Corporation, USA, 1978.

[2] J C MILLS and C B BELCHER, Prog analyt atom spectrosc, 1981, 4, 49-80.

[3] J P MATOUSEK, Prog analyt atom spectrosc, 1981, 4, 247-310.

[4] F J LANGMYHR and U AADALEN, Anal Chim Acta, 1980, 115, 365-368.

[5] F J LANGMYHR, J R STUBERGH, Y THOMASSEN, J E HANSSEN and J DOLEZAL, Anal Chim Acta, 1974, 71, 35-42.

[6] F J LANGMYHR, R SOLBERG and L T WOLD, Anal Chim Acta, 1974, 69, 267-273.

[7] E L HENN, Anal Chim Acta, 1974, 73, 273-281.

[8] J A NICHOLS, R D JONES and R WOODRIFF, Anal Chem, 1976, 50, (14), 2071-2076.

[9] D A LORD, J W McLAREN and R C WHEELER, Anal Chem, 1977, 49, (2), 257-261.

[10] C L CHAKRABARTI, C C WAN and W C LI, Spectrochimica Acta, 1980, 35B, 93-105.

[11] G BURNET, M J MURTHA and J W DUNKER, "Recovery of Metals from Coal Ash", An Annotated Bibliography, Ames Laboratory, Iowa State University, January 1983.

[12] F J LANGMYHR and J AAMODT, Anal Chim Acta, 1976, 87, 483-486.

[13] J P WILLIS and J CRANK, Geochemistry Department, University of Cape Town, 1980.

[14] G HORLICK, Analytical Chemistry, Fundamental Review, April 1982, 54, (5), 281 R - 285 R.

[15] P T GILBERT, Anal Chem, 1962, 34, 1025-1026.

[16] M KASHIKI and S OSHIMA, Anal Chim Acta, 1970, 51, 387-392.

[17] J B WILLIS, Anal Chem, 1975, 47, (11), 1752-1758.

[18] J E O'REILLY and D G HICKS, Anal Chem, 1979, 51, (12), 1905-1915.

[19] Analytical Chemistry, Fundamental Review, April 1982.

[20] C W FULLER, R C HUTTON and B PRESTON, Analyst, 1981, 106, (1266), 913-920.

[21] C W FULLER, Analyst, 1976, 101, 961-965.

[22] C W FULLER and I THOMPSON, Analyst, 1977, 102, 141-143.

[23] J E O'REILLY and D G HICKS, Abstr 51, ACS/CST, Chem Congr Honolulu, April 1979.

[24] L EBDON and W C PEARCE, Analyst, 1982, 107, 942-950.

[25] National Bureau of Standards Certificate of Analysis, Washington D C 20274, 1979.

[26] Vogel's Textbook of Quantitative Inorganic Analysis, 4th Ed, Longman, 1978.

[27] R BOCK, A handbook of decomposition methods in analytical chemistry, International Textbook Company, 1979.

[28] B BERNAS, Anal Chem, 1968, 40, (11), 1682-1686.

[29] A M HARSTEIN, R W FREEDMAN and D W PLATTER, Anal chem, 1973, 45, (3), 611-.614.

[30] D SILBERMAN and G L FISHER, Anal Chim Acta, 1979, 106, 299-307.

[31] C BLOCK, Anal Chim Acta, 1975, 80, 369-373.

[32] J N WALSH, Spectrochimica Acta, 1980, 35B, 107-111.

[33] E L OBERMILLER and R W FREEDMAN, Fuel, 1965, 44, 199-203.

[34] D E BUCKLEY and R E CRANSTON, Chem Geol, 1971, 7, 273-284.

[35] V A FASSEL, ICP Inf Newsl, 1982, 8, (2), 69-75.

[36] J R WILKINSON, L EBDON and K W JACKSON, Anal Proc, 1982, 305-307.

[37] R M DAGNALL, D J SMITH, T S WEST and S GREENFIELD, Anal Chim Acta, 1971, 54, 397-406.

[38] H G C HUMAN, R H SCOTT, A R OAKES and C D WEST, Analyst, 1976, 101, 265-271.

[39] R S BABINGTON, Popular Science, 1973, 43.

[40] R F SUDDENDORF and K W BOYER, Reference [42], pp 278-286.

[41] J M MERMET and C TRASSY, Ref [42], pp 245-250.

[42] R M BARNES (ed). Proceedings of International Winter Conference, San Juan, Puerto Rico, Heyden, Jan 1980.

[43] P W J M BOUMANS, Line coincidence tables for inductively coupled plasma emission spectrometry, Vol 1 and 2, Pergamon Press, 1980.

[44] I U P A C, Analytical Chemistry Division, II, Data interpretation, Spectrochimica Acta, 1978, 33B, 242.

[45] R K WINGE, V J PETERSON and V A FASSEL, Appl Spectros, 1979, 33, (3), 206-219.

[46] R N MERRYFIELD and J H RUNNELS, Ref [42], pp 396-403.

[47] S E CHURCH, Ref [42], pp 410-434.

[48] R I BOTTO, ICP Inf Newsl, 1981, 4, 49-80.

[49] S K KARACKI and F L CORCORAN, Jr, Appl Spectrosc, 1973, 27, (1), 41-42.

[50] J W OWENS, E S GLADNEY and D KNAB, Anal Chim Acta, 1982, 135, 169-172.

[51] P GELADI and F ADAMS, Anal Chim Acta, 1979, 105, 219-231.

[52] J A COX, G L LUNDQUIST, A PRZYJAZNY and C D SCHMULBACH, Environ Sci Technol, 1978, 12, 722.

[53] W D JAMES, C C GRAHAM, M D GLASCOCK and A G HANNA, Environ Sci Technol, 1982,16, (4), 195-197.

[54] E S GLADNEY, Anal Chim Acta, 1980, 118, 385-396.

[55] E S GLADNEY, At Absorption Newsl, 1977, 16, (2), 42-43.

[56] J A ADAM, E BOOTH and J D H STRICKLAND, Anal Chim Acta, 1952, 6, 462-471.

[57] B FLEET, K V LIBERTY and T S WEST, Talanta, 1970, 17, 203-210.

[58] J KORKISCH and A SORIO, Anal Chim Acta, 1976, 82, 311-320.

[59] J KORKISCH, A SORIO and I STEFFAN, Talanta, 1976, 23, 289-294.

[60] E Y CAMPBELL and F O SIMON, Talanta, 1978, 25, 251-255.

[61] D G HANNING and W SLAVIN, Appl Spectrosc, 1983, 37, (1), 1-11.

[62] A W BOORN and R F BROWNER, Anal Chem, 1982, 54, 1402-1410.

[63] D D NYGAARD, D S CHASE and D A LEIGHTY, Applications note #78, Instrumentation Laboratory, Analytical Instrument Division, Wilmington.

[64] F T BINGHAM, J Am Chem Soc, 1973, 95, 130-138.

[65] E S GLADNEY, E T JUNNEY and D B CURTIS, Anal Chem, 1976, 48, (14), 2139-2142.

[66] J L MANZOORI, Talanta, 1980, 27, 682-684.

[67] P D GOULDEN, D H J ANTHONY and K D AUSTEN, Anal Chem, 1981, 53, 2027-2029.

[68] G F LARSON, R T GOODPASTURE and R W MORROW, Ref [42], pp 611-626.

[69] M P FAILEY, D L ANDERSON, W H ZOLLER, G E GORDON and R M LINDSTROM, Anal Chem, 1979, 51, (13), 2209-2221.

[70] F J LANGMYHR and S SVEEN, Anal Chim Acta, 1965, 32, 1-7.

[71] F J LANGMYHR and P E PAUS, Anal Chim Acta, 1968, 43, 397-408.

[72] F J LANGMYHR and K KRINGSTAD, Anal Chim Acta, 1966, 35, 131-135.

[73] M S GERMANI, I GOKMEN, A C SIGLEO, G S KOWALCZYK, I OLMEZ, A M SMALL, D L ANDERSON, M P FAILEY, M C GULOVALI, C E CHOQUETTE, E A LEPEL, G E GORDON and W H ZOLLER, Anal Chem, 1980, 52, (2), 240-245.

[74] G F WALLACE, Atomic Spectroscopy, 1981, 2, (2), 61-64.

[75] I B BRENNER, I GAL, H ELDAD, L HALICZ and D HOFFER, ICP Inf Newsl, 1983, 8, (10), 568-572.

[76] S B SMITH, Jr, R G SCHLEICHER, A G DENNISON and G A McLEAN, Spectrochimica Acta, 1983, 38B (1/2), 157-163.

[77] P W J M BOUMANS and M BOSVELD, Spectrochimica Acta, 1979, 34B, 59-72.

[78] M BETTINELLI, Atomic Spectrosc, 1983, 4, (1), 5-9.

[79] Instrumentation Laboratory Memorandum, 9 Sept 1981.

[80] T J CHOW and E D GOLDBERG, J Mar Res, 1962, 20, 163-167.

[81] G J SCHMIDT and W SLAVIN, Anal Chem, 1982, 54, 2491-2495.

[82] G K PAGENKOPF and J M CONOLLY, Environ Sci Technol, 1982, 16, (9), 609-613.

[83] F CULKIN, The major constituents of sea water, In : Chemical Oceanography, Riley, Vol 1, London, 1965.

[84] P W J M BOUMANS and F J de BOER, Spectrochimica Acta, 1975, 30B, 309-334.

[85] G F LARSON, V A FASSEL, R H SCOTT and R N KNISELEY, Anal Chem, 1975, 47, (2), 238-243.

[86] M H ABDALLAH, J H MERMET and C TRASSY, Anal Chim Acta, 1976, 87, 329-339.

[87] G F LARSON and V A FASSEL, Anal Chem, 1976, 48, (8), 1161-1166.

[88] D J KALNICKY, V A FASSEL and R N KNISELEY, Appl Spectrosc, 1977, 31, (2), 137-150.

[89] S R KOIRTYOHANN, J S JONES, C P JESTER and D A YATES, Spectrochimica Acta, 1981, 36B, 49-59.

[90] M W BLADES and G HORLICK, Spectrochimica Acta, 1981, 36B, (9), 881-900.

[91] J P RYBARCZYK, C P JESTER, D A YATES and S R KOIRTYOHANN, Anal Chem, 1982, 54, 2162-2170.

[92] F J M J MAESSEN, H BALKE and J L M de BOER, ICP Inform Newsl, 1982, 8, (1), 21-22.

[93] G R KORNBLUM and L de GALAN, Spectrochimica Acta, 1977, 32B, 455-478.

[94] S R KOIRTYOHANN, J S JONES and D A YATES, Anal chem, 1980, 52, 1965-1966.

[95] P SCHRAMEL and XU-LI-GIANG, ICP Inform Newsl, 1982, 7, (9), 429-440.

[96] R L DAHLQUIST and J W KNOLL, Appl Spectrosc, 1978, 32, 1-29.

[97] P J Mc KINNON and K G GIESS, Ref [42], pp 287-301.

[98] S STIEG and A DENNIS, Anal Chem, 1982, 54, 605-607.

[99] D D NYGAARD and J H LOWRY, Anal Chem, 1982, 54, 803-807.

[100] J H RUNNELS, R MERRYFIELD and H B FISHER, Anal Chem, 1975, 47, (8), 1258-1263.

[101] W K ROBBINS, J H RUNNELS and R MERRYFIELD, Anal Chem, 1975, 47, (13), 2095-2101.

[102] Z GROBENSKI, R LEHMANN, R TAMM and B WELZ, Mikrochimica Acta, 1982, 1, 115-125.

[103] H UCHIDA, T UCHIDA and C IIDA, Anal Chim Acta, 1979, 108, 87-92.

[104] B V L'VOV, Spectrochimica Acta, 1978, 33B, 153.

[105] R L DAVISON, D F S NATUSCH, J R WALLACE and C A EVANS, Jr, Environ Sci Technol, 1974, 8, 1107.

# APPENDIX 1. REAGENTS AND STANDARD SOLUTIONS

## (a) Water (MQW)

High quality water from a Milli-Q-System (Millipore Corporation) fed with deionized water was used for washing and preparation of all samples and standard solutions.

## (b) Triton X-100 (TX-100)

BDH Chemicals Ltd, United Kingdom.

## (c) Acids

- Fuming Nitric acid; 100%, Merck
- Concentrated nitric (70%), hydrochloric (36%), sulphuric (98%), perchloric (72%) acids; "Analar" and "Aristar", BDH.

- Hydrofluoric acid; 40 and 48%, "Analar" and "Aristar", BDH.
- Boric acid ($H_3BO_3$), "Aristar", BDH.

## (d) Standard solutions (1000 ppm)

- V, Ni, Co, Mo, Mn, Cr, Zn, Cu, Pb, Fe, Mg, Ca, K, Na, Hg, Pt, Se; Standards for atomic absorption spectroscopy, "Spectrosol", BDH.

- Al, Si, Ba, Ti, Li, "Titrisol", (Merck), ampoule containing 1 g analyte dissolved in 1 litre of water.

- P; 4.26 g $(NH_4)_2\ HPO_4$, ("Analar", BDH) dissolved in 1 litre of water.

- B; 5.7195 g $H_3BO_3$, ("Aristar", BDH) per litre.
- Be; 22.7614 g Be $(NO_3)_2 \cdot 4H_2O$, (high purity, Merck) per litre.
- W; 0.3589 g $Na_2WO_4 \cdot 2H_2O$, (Analar, BDH) was dissolved in 200 ml of water containing 0.1% (m/v) NaOH to keep the tungsten in solution.

(e) Miscellaneous

All the reagents used, eg NaOH, $Na_2CO_3$ were of analytical reagent grade.

Glassware and other equipment were washed in a detergent solution, soaked in 10% $HNO_3$ and finally rinsed with MQW.

APPENDIX 2. IL PLASMA-100 GRAPHICS

(Method development, Chapter 4.2).

Figures 1 and 2 show an analytical programme and one of the programme's line respectively:

```
PLASMA 100 120588-04 15 MAY 82

 P#  WP PWR NAMED
  2   0   3 ANAL DE CHARBON

ML/M PDLY HG  STAT *ANAL *RDG
 1.0   30  1     1     2    3

 #  EL      NM  MM #D UNIT BC  SEC
 1  SI 251.61  14  2 PPM   0  5.0
 2  AL 308.22  16  2 PPM   0  5.0
 3  FE 239.56  14  2 PPM   0  5.0
 4  BA 455.40  16  3 PPM   1  6.0

*_
```

Figure 1. Analytical programme.

```
 #  EL      NM  MM #D UNIT BC  SEC
 1  SI 251.61  14  2 PPM   0  5.0

 #  B#      CONC      #  B#      CONC
 0  99       0.00     1   1      50.00
 2   2      20.00     3   3      10.00
 4                    5

 SENSITIVITY    BLNK-SENSIT    CH
           1              0     A

 I/S   1I/E   1S/F   2I/E   2S/F

*_
```

Figure 2. Programme line.

The meaning of the different symbols used above are as follows:

| | |
|---|---|
| P# | Programme number. |
| WP | WRITE PROTECT, locks the instrumental parameters for each programme, preventing an accidental change. |
| PWR | Power level. |
| NAMED | Programme name. |
| ML/M | Aspiration rate in ml $min^{-1}$. |
| PDLY | Pump delay in minutes. The pump operates at maximum flow rate for adequate washout of the nebulizer-torch system before a reading is taken. |
| HG | Mercury lamp used for spectrometer calibration can be switched ON (1) or OFF (0) during analysis. |
| *ANAL | Number of analyses. |
| *RDG | Number of readings for each analysis. |
| MM | Observation height in mm. |
| #D | Decimal placement. |
| UNIT | Units of measurement (ppm, %, wt % or ppb). |
| BC | Background correction, correction on one or two sides of peak. |
| SEC | Integration time per reading, in seconds. |
| CH | Selected channel (monochromator A or B). |

The other symbols in figure 2 are calibration and interference correction parameters.

Computer routines for graphic display:

The TRIM routine

To optimize the wavelength location, test solutions are aspirated and the TRIM routine is used to obtain a display of intensity versus wavelength as shown in figure 3. The standard peak search routine utilizes a scan of the 0.1 nm window to find the exact location of the analyte emission line. The signal intensity is the number at the top left corner. The channel used (A or B) appears near the element symbol and the spectral line used. The vertical cursor can be moved left or right to choose the position of the peak relative to the window whose size and location is indicated by the two small vertical lines. Three window sizes are available: 0.033 nm, 0.067 nm and 0.1 nm. Only one window size may be selected for each programme.

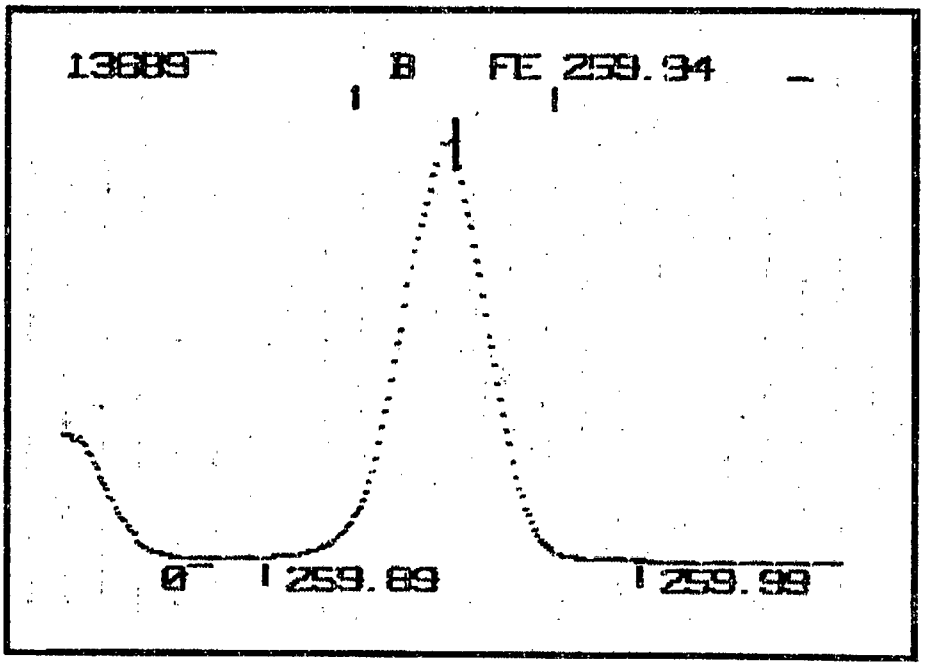


Figure 3. Wavelength scan, TRIM routine.

The TPROFILE routine:

To determine the optimal observation height, the test solution is aspirated and the TPROFILE routine used to obtain a display of intensity versus observation height as in figure 4. After scanning, the height at which maximum intensity is obtained is displayed, in this case 16 mm (top righthand side).

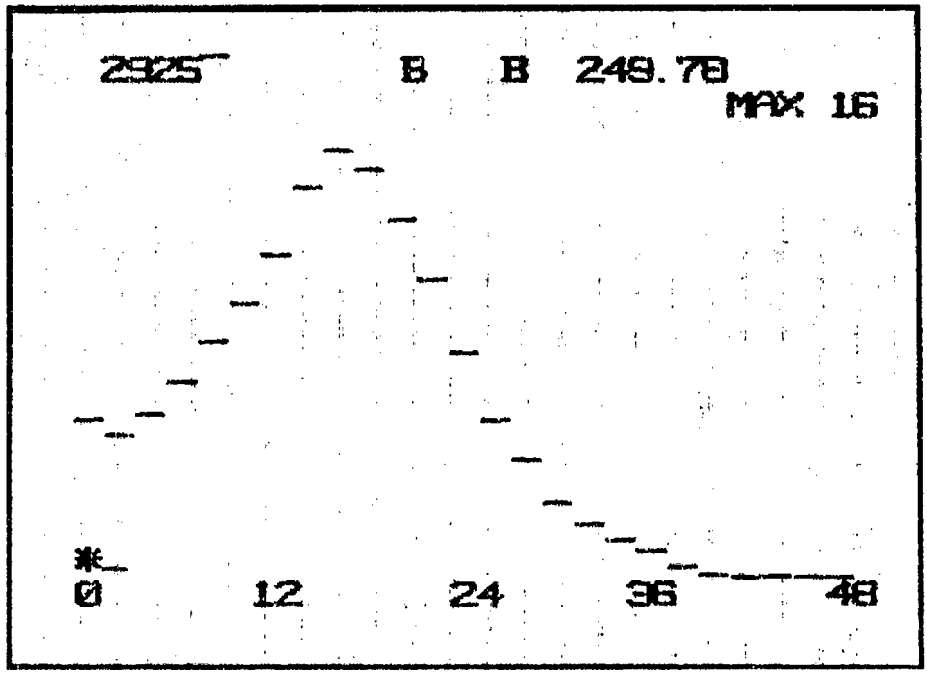


Figure 4. TPROFILE routine for an aqueous solution containing boron.

The RESTPEAK and PLOT routines:

After using the TRIM routine, the RESTPEAK routine is used to check for interferences. In this routine, the microcomputer scans a region around the corrected wavelength and draws a line where it computes the peak maximum to be.

To qualitatively study interferences between standards, blanks and samples, a subroutine of RESTPEAK or TPROFILE called PLOT is used. In this routine the stepper-controlled refractor

plate of the monochromator is used to scan the desired wavelength region. More than one emission plot can be superimposed on the CRT over the original plot by aspirating standards, blanks, samples or concomitants containing elements that may produce interference.

Figure 5 illustrates background interference at the 204.60 nm MO line caused by high concentrations of Al (1000 ppm).

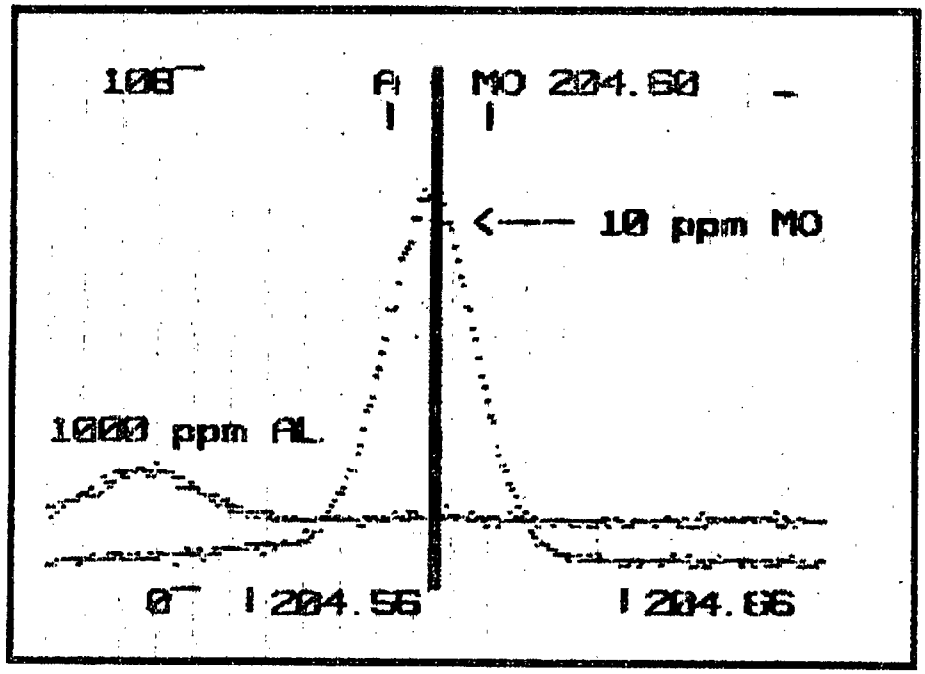


Figure 5. Background interference.

In figures 6 and 7 spectral overlap is illustrated. An argon line is shown to interfere with sodium determination (figure 6). In this case a small window and the background corrector are used.

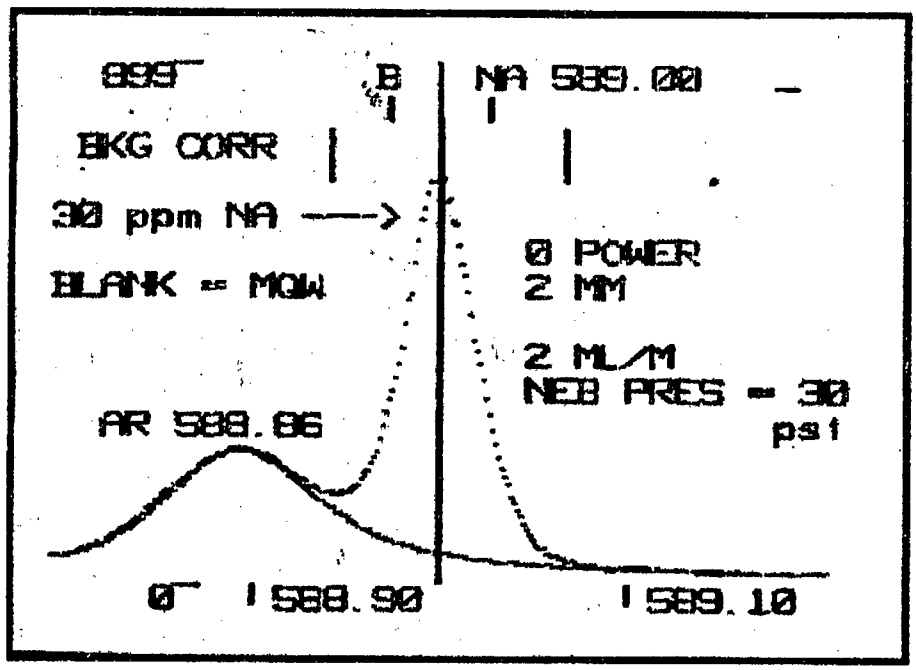


Figure 6. Spectral interference of Ar on Na.

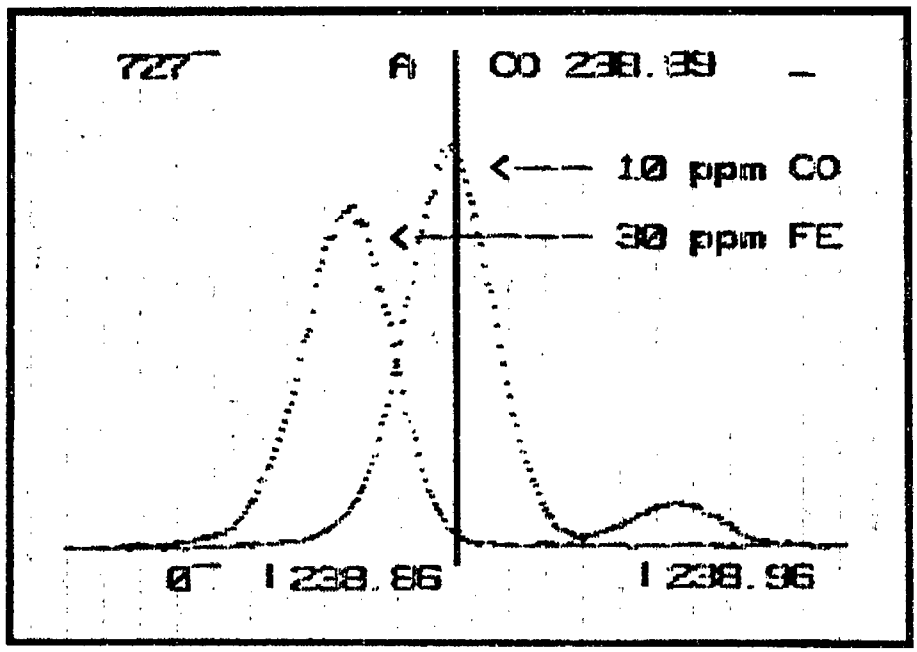


Figure 7. Spectral inteference of Fe on Co.

Other sub-routines are TPLOT, IPLOT and GPLOT. TPLOT is used to study intensity versus observation heights for different solutions. This is illustrated in figure 8. In this case maximum intensities for the three test solutions were obtained at the same height.

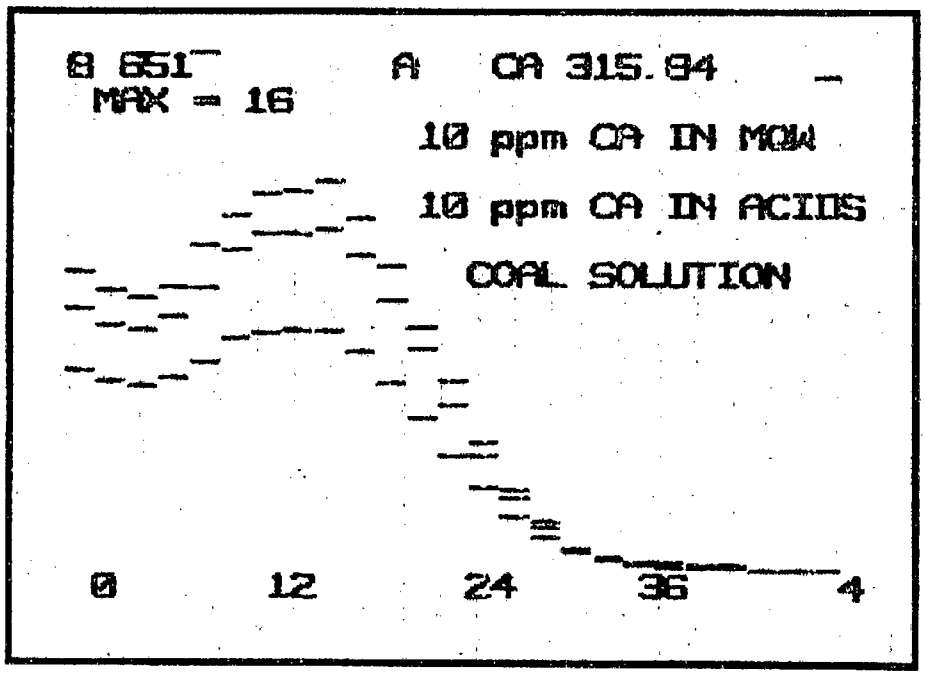


Figure 8. TPLOT routine, calcium emission.

IPLOT plots signal intensity versus time and is used primarily for making monochromator and sample introduction adjustments and to check for stability of the signal.

GPLOT is used to view the spectrum around the peak of interest. In this routine, the grating moves instead of the refractor plate so that the window is five times as large. Figure 9 shows a calcium line that causes high background on the Al 396.14 nm line.

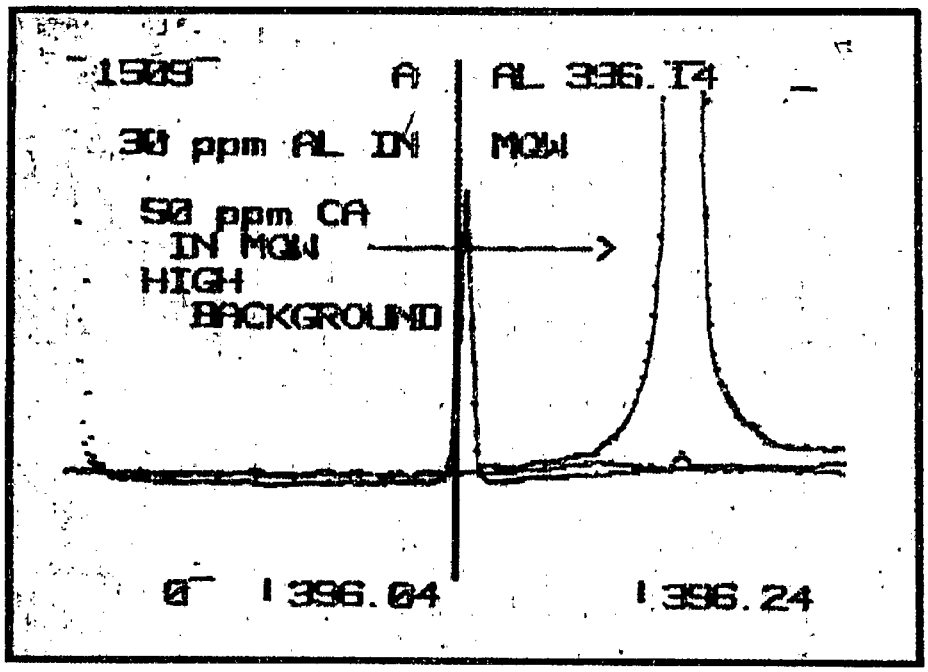


Figure 9. GPLOT routine, high background near the Al 396.14 nm due to nearby calcium line (left peak).

APPENDIX 3. Trace element spectral characteristics (chapter 4.2)

| Element | Spectral line (nm) | Obs Ht (mm) | $C_A$ (ppm) | % RSD (for $C_A$) | % RSD (for blank) | $I_N/I_B$ | $C_L$ (ppm) |
|---|---|---|---|---|---|---|---|
| Co II | 238.89 | 14 | 10 | 0.20 | 0.21 | 26.2 | 0.002 |
| II | 228.61 | | | 0.25 | 0.41 | 29.4 | 0.004 |
| II | 230.79 | | | 0.11 | 0.21 | 18.7 | 0.003 |
| II | 345.35 | | | 0.20 | 0.15 | 1.6 | 0.029 |
| Cr II | 205.55 | 14 | 10 | 0.26 | 0.64 | 48.6 | 0.004 |
| II | 206.15 | | | 0.29 | 0.68 | 37.3 | 0.006 |
| II | 267.71 | | | 0.15 | 0.18 | 22.2 | 0.002 |
| Cu I | 324.75 | 16 | 10 | 0.22 | 0.25 | 25.2 | 0.003 |
| II | 224.70 | | | 0.25 | 0.26 | 19.6 | 0.004 |
| I | 327.40 | | | 0.39 | 0.24 | 13.2 | 0.006 |
| I | 219.96 | | | 0.23 | 0.27 | 10.2 | 0.008 |
| Hg I | 253.65 | 14 | 100 | 0.30 | 0.41 | 30.8 | 0.040 |
| II | 194.23 | | | 0.18 | 1.47 | 122.7 | 0.038 |
| Mo II | 202.03 | 14 | 10 | 0.25 | 0.85 | 24.1 | 0.011 |
| II | 203.84 | | | 0.34 | 0.75 | 13.7 | 0.017 |
| II | 204.60 | | | 0.25 | 1.02 | 14.9 | 0.021 |
| Ni II | 221.65 | 16 | 10 | 0.30 | 0.46 | 30.8 | 0.005 |
| I | 232.00 | | | 0.19 | 0.18 | 9.7 | 0.006 |
| II | 331.60 | | | 0.23 | 0.27 | 20.3 | 0.006 |

| Element | Spectral line (nm) | Obs Ht (mm) | $C_A$ (ppm) | % RSD (for $C_A$) | % RSD (for blank) | $I_N/I_B$ | $C_L$ (ppm) |
|---|---|---|---|---|---|---|---|
| Pb II | 220.35 | 16 | 100 | 0.47 | 0.89 | 48.8 | 0.055 |
| I | 217.00 | | | 0.08 | 0.46 | 18.9 | 0.074 |
| I | 283.31 | | | 0.23 | 0.17 | 7.4 | 0.071 |
| I | 261.42 | | | 0.27 | 0.17 | 9.9 | 0.052 |
| Pt II | 214.42 | 14 | 100 | 0.23 | 0.48 | 59.6 | 0.024 |
| II | 203.65 | | | 0.43 | 0.99 | 44.6 | 0.067 |
| I | 306.47 | | | 0.18 | 0.07 | 11.8 | 0.017 |
| Se I | 196.03 | 14 | 100 | 0.26 | 1.03 | 38.6 | 0.081 |
| I | 203.99 | | | 0.35 | 0.60 | 17.4 | 0.100 |
| I | 206.28 | | | 0.22 | 0.84 | 5.7 | 0.440 |
| V II | 309.31 | 16 | 10 | 0.18 | 0.18 | 27.0 | 0.002 |
| II | 310.23 | | | 0.17 | 0.19 | 19.2 | 0.003 |
| II | 292.40 | | | 0.37 | 0.29 | 27.8 | 0.003 |
| W II | 207.91 | 16 | 100 | 0.33 | 0.74 | 97.1 | 0.023 |
| II | 224.88 | | | 0.32 | 0.44 | 58.0 | 0.023 |
| II | 218.94 | | | 0.25 | 0.46 | 31.7 | 0.043 |
| Zn I | 213.86 | 14 | 10 | 0.18 | 0.65 | 127.8 | 0.002 |
| II | 202.55 | | | 0.09 | 0.54 | 96.8 | 0.002 |
| II | 206.20 | | | 0.13 | 0.81 | 54.9 | 0.004 |
| Zr II | 343.82 | 16 | 10 | 0.14 | 0.14 | 22.6 | 0.002 |
| II | 339.20 | | | 0.25 | 0.15 | 27.6 | 0.002 |
| II | 349.62 | | | 0.25 | 0.22 | 17.0 | 0.004 |

APPENDIX 4. VARIATION OF ELEMENTAL CONCENTRATIONS WITH pH OF WATER SAMPLES (Chapter 8)

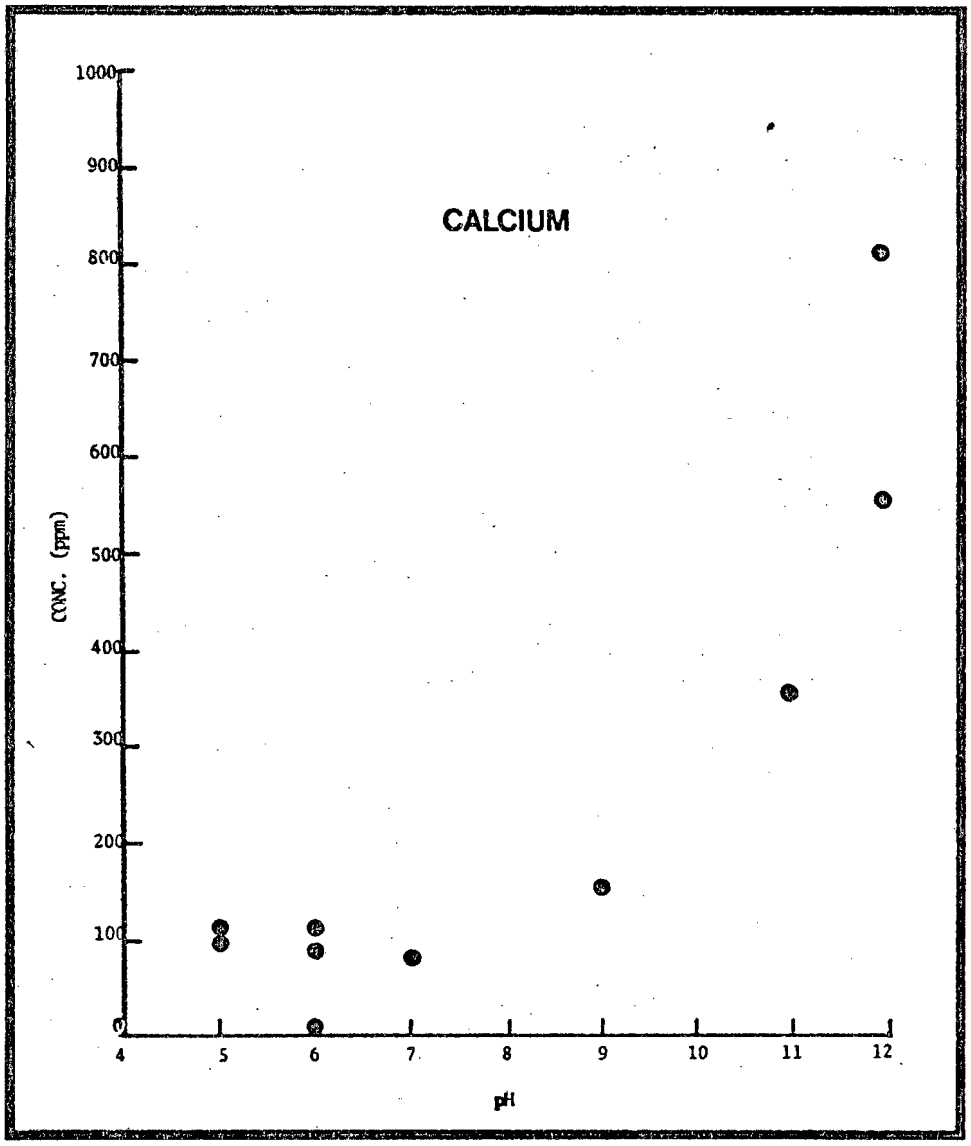

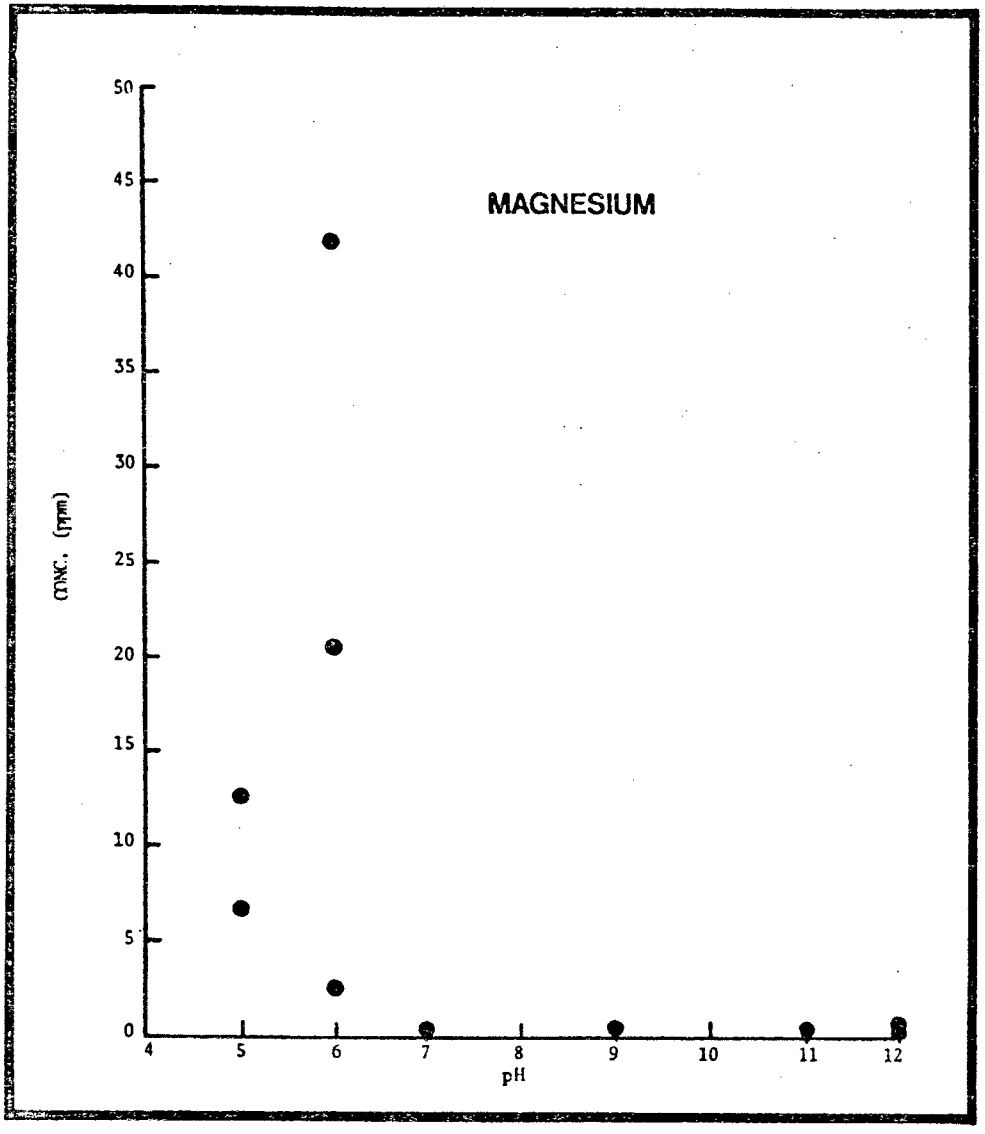
MAGNESIUM
CONC. (ppm)
50
45
40
35
30
25
20
15
10
5
0
4
5
6
7
8
9
10
11
12
pH

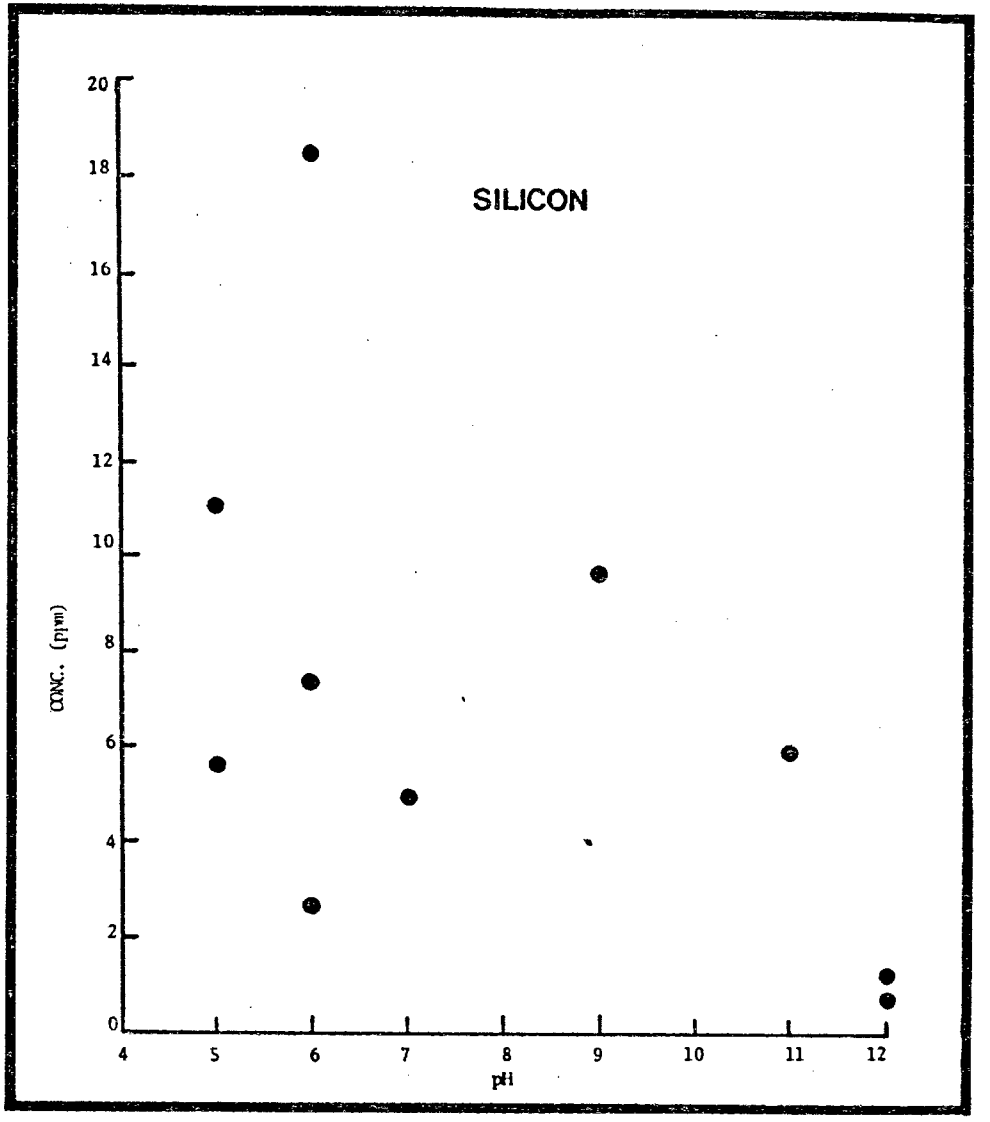
SILICON
CONC. (ppm)
20
18
16
14
12
10
8
6
4
2
0
4
5
6
7
8
9
10
11
12
pH

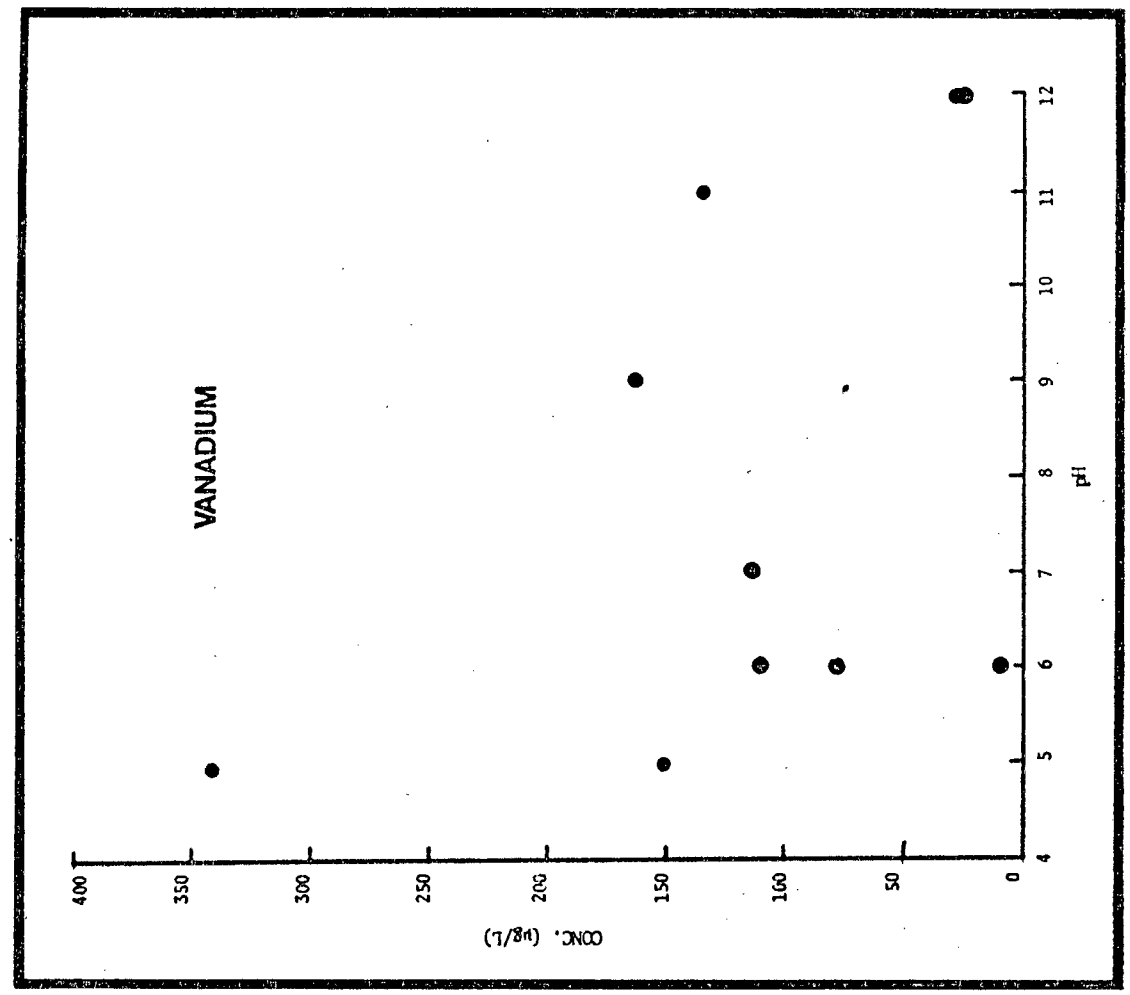
VANADIUM
CONC. (µg/L)
0
50
100
150
200
250
300
350
400
pH
4
5
6
7
8
9
10
11
12

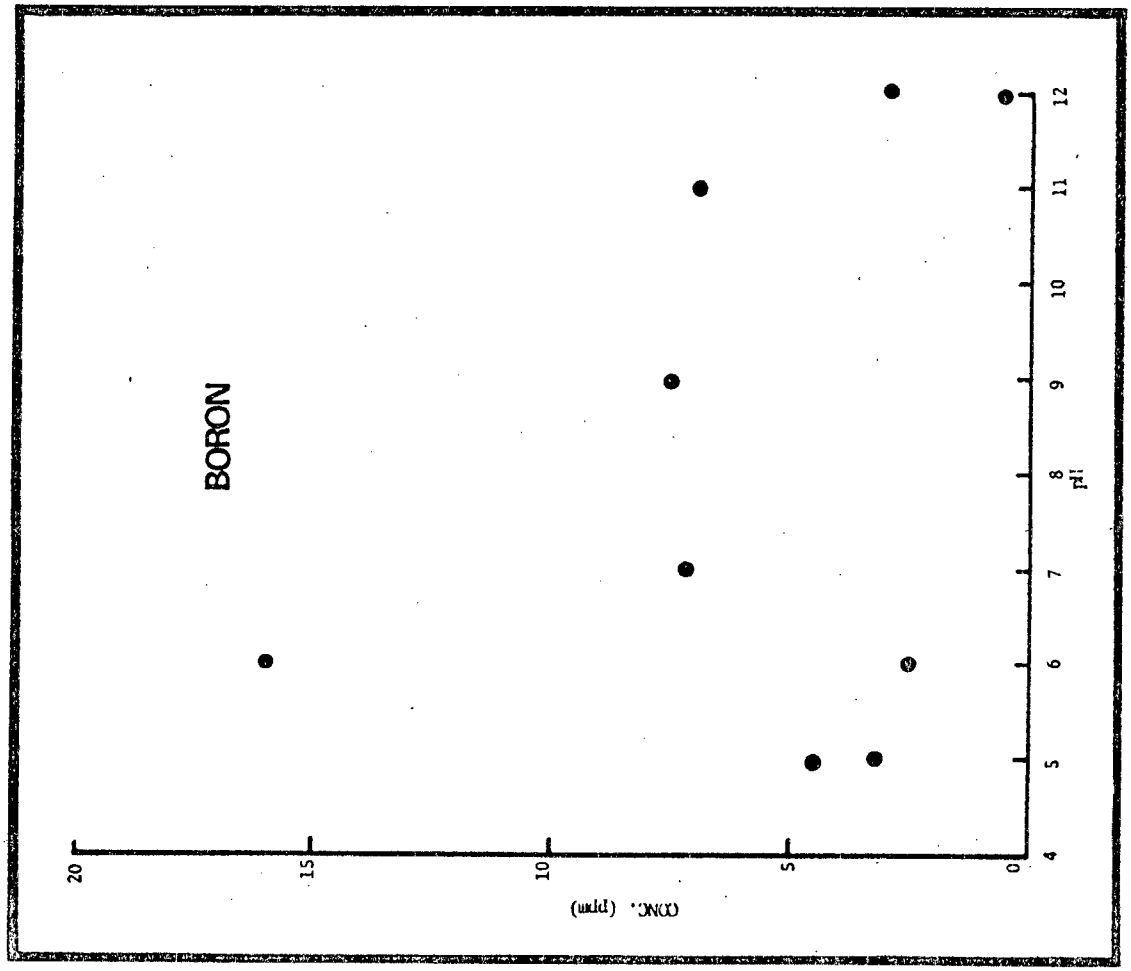
BORON
CONC. (ppm)
0
5
10
15
20
pH
4
5
6
7
8
9
10
11
12

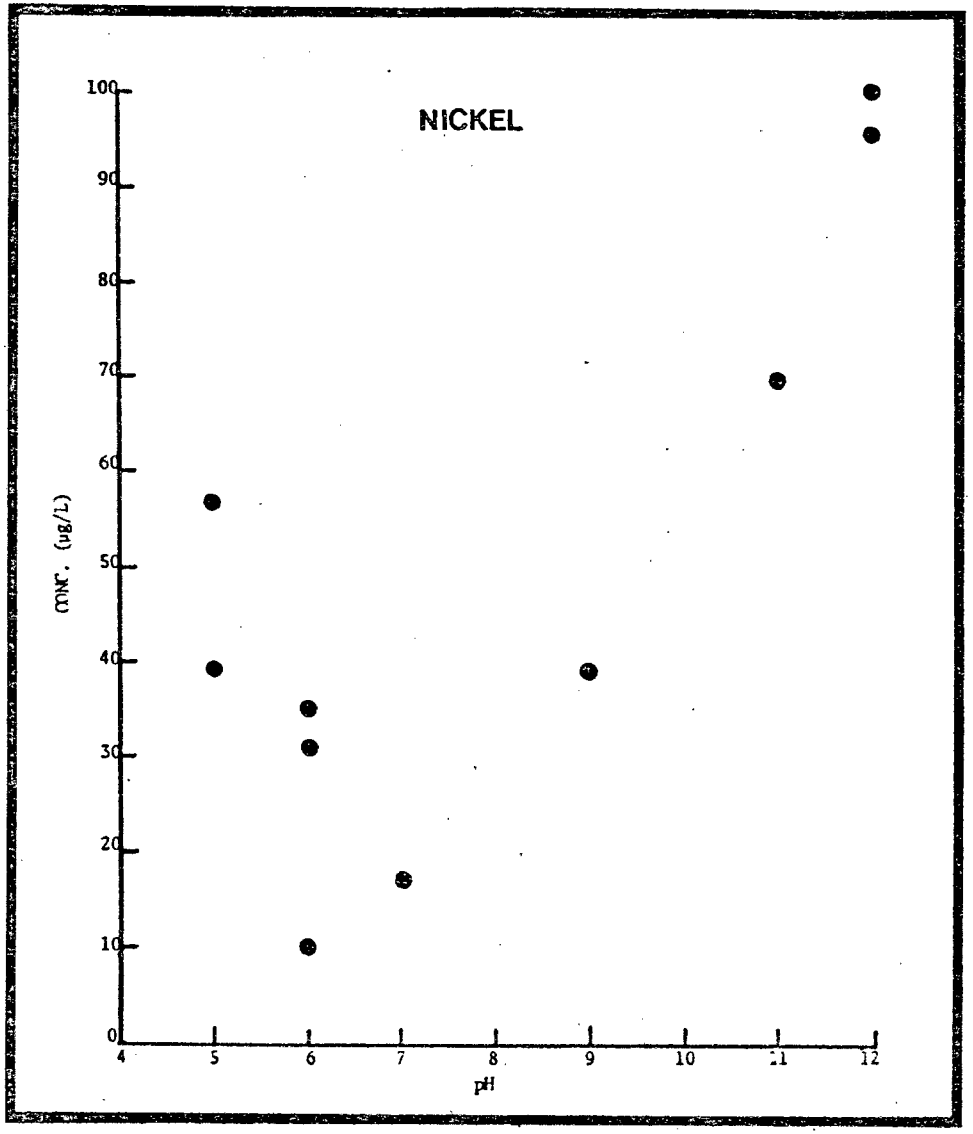
NICKEL
CONC. (µg/L)
0
10
20
30
40
50
60
70
80
90
100
4
5
6
7
8
9
10
11
12
pH

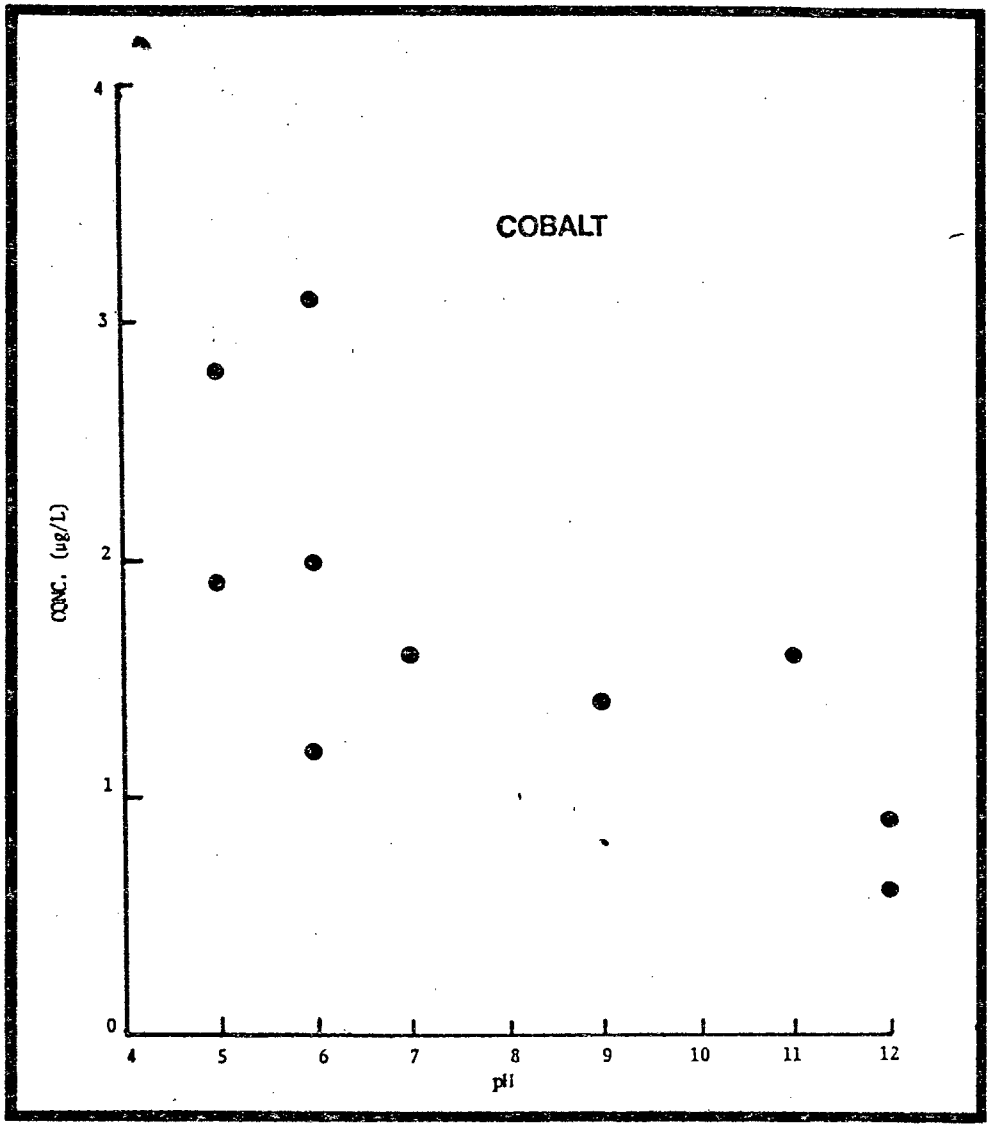
COBALT
CONC. (µg/L)
0
1
2
3
4
4
5
6
7
8
9
10
11
12
pH

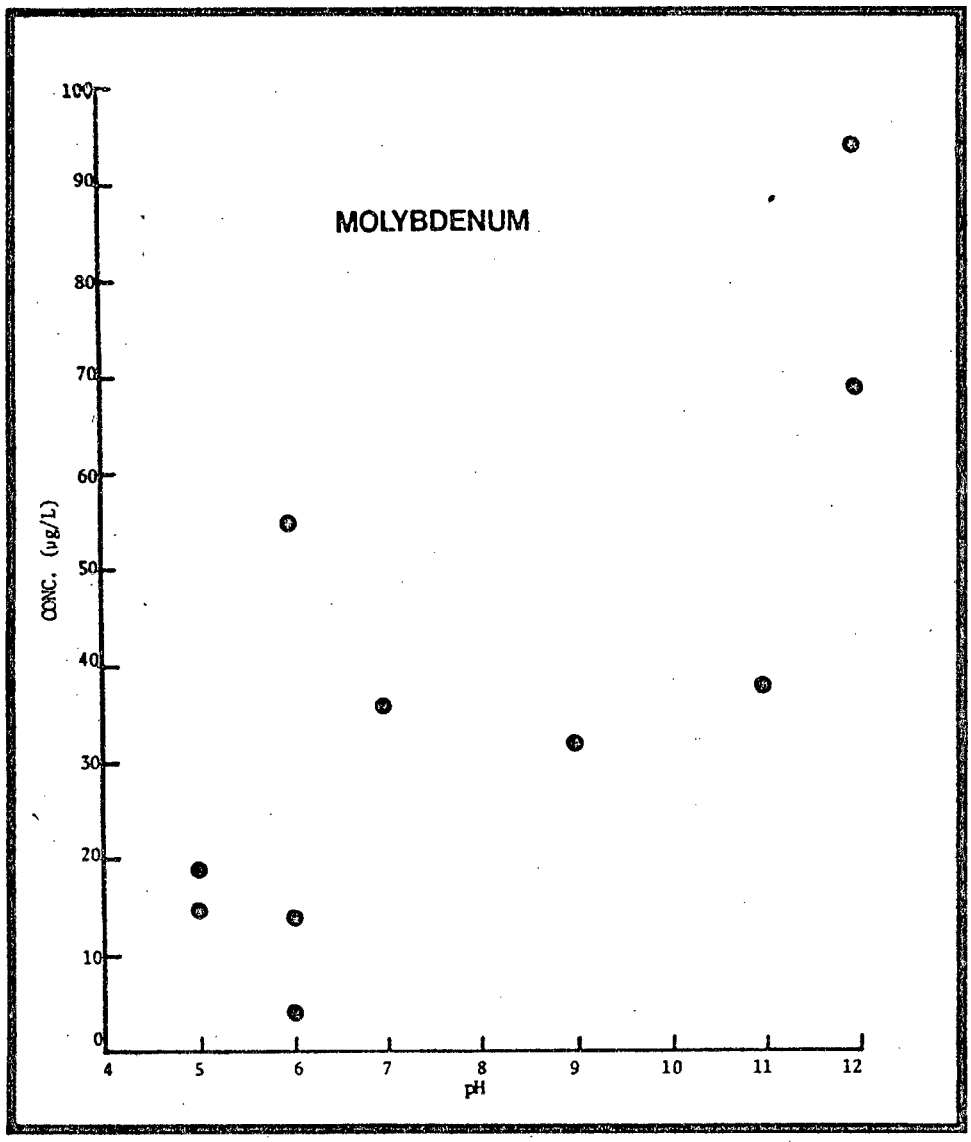
MOLYBDENUM
CONC. (µg/L)
100
90
80
70
60
50
40
30
20
10
0
4
5
6
7
8
9
10
11
12
pH